University of Stavanger

FACULTY OF SCIENCE AND TECHNOLOGY

MASTER'S THESIS

Study programme/specialisation: MSc. in Marine and Offshore Technology	Spring/ ~~Autumn semester~~, 2020 Open / ~~Confidential~~
Author: İsmail Gökay Karataş	
Programme coordinator: Prof. Muk Chen Ong Supervisor(s): Assoc. Prof Lin Li, Dr. Xinying Zhu, Prof. Muk Chen Ong	
Title of master's thesis: Dynamic analysis of lift-off operation of a subsea spool from a barge	
Credits: 30	
Keywords: Offshore lift-off operations; subsea spool; time-domain simulations; fender support; winch control system; operability analysis	Number of pages: ……143…… + supplemental material/other: ……14…… Stavanger, ……15 July 2020…… date/year

University of Stavanger

DYNAMIC ANALYSIS OF LIFT-OFF OPERATION OF A SUBSEA SPOOL FROM A BARGE

15 July 2020

Author: Ismail Gokay Karatas, 251052

Supervisors: Associate Prof. Lin Li

Dr. Xinying Zhu

Prof. Muk Chen Ong

Abstract

The lift-off operation faces great operational challenges due to the harsh environment in the North Sea. Especially, the operation becomes more susceptible to environmental conditions when the installation method involves two floating vessels. A combination of dynamic responses, such as environmental conditions, operational procedures and human error, makes lift-off operations challenging and risky. Therefore, the planning of such operation requires careful numerical studies of the installation method in order to execute the operations safely. The spool is a commonly used subsea structure in the offshore fields and is mostly installed by a lifting vessel, but there is a little work focusing on the installation method involving a transportation barge and a lifting vessel together. Thus, accurate numerical models and methods are required to predict the responses of the lifting system.

This thesis addresses the numerical analysis of the lift-off operation of a large subsea spool from a transportation barge. Numerical modelling of the lift-off is comprising a lifting vessel, a transportation barge, a spool, and coupling elements such as fender and wire couplings. Time-domain simulations are performed to capture nonlinear dynamic responses during the lift-off operations under various irregular waves. A systematic approach is used to assess allowable sea states. Based on the recommended practice, the critical events are potential snap loads, slack wire condition in slings and re-hit force between the spool and the transportation barge. Among these criteria, the dominant criterion is the re-hit force due to the large size of the spool. Therefore, it requires examining the potential increase of response-based operational limits by two methods. The first method is using different support models between the barge and the spool, and the second method is developing a new method to find best lift-off instance.

In the first method, different fender supports have been modelled, and the critical fender forces are compared to assess the potential improvement of the sea states. It has resulted in the understanding that the allowable sea state can be increased significantly by properly choosing the fender support structure. In the second method, a control method is developed to find a proper lift-off instance to start the winch. The dynamic response between the crane tip and the transportation barge plays a significant role in the initial motion of the lift-off. Therefore, the control method involves the estimation of future relative motions. Different sensitivity studies are carried out with

the control method to assess the allowable sea states. The purpose of these sensitivity studies is to define the optimum algorithm for different peak periods.

An increase sea states also indicate the significant potential of increasing the operability of lift-off operation. Therefore, the allowable sea states assessed from these methods will be used as an input of the operability analysis in order to assess of the effect of the different methods. The main objective is to define the most optimum installation method in terms of numbers of spools, and the transportation time. The sensitivity studies are concluded with increased operability by the fender models and the control method.

Acknowledgement

I would like to express my sincere gratitude to Assoc. Prof. Lin Li, Dr Xinying Zhu, and Prof. Muk Chen Ong for their patient guidance, motivation, and advice as in this project. The door to their office was always open whenever I ran into any troubles or had a question about my thesis work. I am very grateful for Assoc. Prof. Li consistently steered me in the right direction in this thesis whenever she thought that I need it. I would like to thank Dr. Zhu for her constructive comments and suggesting me to thinking more. I would like to extend my gratitude to Prof. Ong for this organizational arrangement during the spring semester and well-equipped hardware support for this thesis. It was a great and challenging experience for me to work with them.

I also want to thank my classmates and friends who created a motivating and joyful atmosphere. I appreciate all the support and knowledge we shared. By having daily activities during the long study hours, I felt the work for my thesis less stressful.

Last but not least, my warmest thank goes to my family in Turkey for their endless love and continuous support, and to my wife Ezgi, for her support, encouragement and being best companion during my master thesis.

Ismail Gökay Karataş
July, 2020
Stavanger, Norway

List of figures

List of tables

Table of Contents

Chapter 1
Introduction

1.1 Introduction

Offshore lifting operations are commonly used methods to install offshore and subsea structures. The iterations between different dynamic systems, operational procedures, environmental actions and human intervention make the operations challenging and risky. According to DNVGL, offshore lifting operations are categorized under the scope of marine operations, and these operations are exposed to the hazards of the marine environment [1].

Most of the offshore lifting operations can only be carried out in relatively low sea states to satisfy the safety requirements. Due to this reason, among other operations, offshore crane operations account for the longest downtime, which may increase the installation costs significantly. Furthermore, in order to manage unstable and harsh environmental conditions in the operation area, workable weather windows ought to be defined in advance. To increase the workable weather windows, numerical modelling and dynamic analysis for predicting the response of the lifting system in the planning phase are critical and highlighted by the recommended practice by DNVGL [2].

Most of the marine operations can only be carried out up to a certain sea state level to satisfy the safety requirements. For operations dominated by waves, operational limits are normally expressed in terms of sea state parameters, such as the significant wave height (Hs) and spectral peak period (Tp). A general methodology to express the allowable structural or motion responses in terms of Hs and Tp has been proposed by Guachamin-Acero et al [3]. The methodology includes identification of critical events of a given operation system and procedure, a corresponding numerical model for dynamic response analysis considering stochastic sea states, a comparison of the characteristic responses with their allowable limits and a backward derivation of the corresponding allowable limits of sea states [4]. Thus, the methodology provides response-based allowable limits in terms of sea states, which ensures the same safety levels as the structural capacity of structural components. This general methodology has already been applied in analyses of various marine operations by Li et al [5], Li et al [6], Guachamin-Acero et al [7] Verma et al [8]. Uncertainties on the allowable sea states from the spectral energy distribution have also been evaluated by Guachamin-Acero and Li [9].

The focus of this thesis is to assess the operational limits for the lifting operation of a large subsea spool piece. Subsea spools are often used in the subsea production systems to connect the pipe ends and the interconnecting facilities. Because of different applications, the shapes and dimensions of spool structures vary greatly. The spool can be transported to the installation site using a transportation barge. The whole installation can be divided into the following main phases

- Lift the spool off from the deck of the transportation barge by means of the main crane of the construction vessel.
- Lower the spool through the splash zone.
- Further lower the spool down to the seabed.
- Position the spool onto the target mating hubs.

The operational criteria for different installation phases are different due to the varying behaviour of the dynamic system. To evaluate the operability of the whole operation, assessment of all the critical phases are required.

1.2 State of art

In the subsea oil/gas production system (SPS), the subsea spools are often used in the subsea production systems to connect the pipe ends and subsea facilities such as subsea production facilities, subsea wells, manifolds, flowlines, and offshore platforms. Moreover, it can also provide a connection between pipe end manifold (PLEM) or a pipeline end terminator (PLETs) and riser bases. The variety of these application causes the shapes and the dimensions of the spool structures differ remarkably. A spool includes an assembly of straight pipe, bends, and two termination heads at the ends. Depends on the application, the spool can be used as rigid or flexible. For lifting purposes, there should be a reimbursement pipe installed which can be used to avoid bending of flexible spools. There are many varieties of spool shapes used in SPS for both applications. For instance, the rigid spool can be M-shaped, U-shaped or two styles used together, and horizontal Z-shaped, commonly flexible spool used in riser bases. In this article, the Z shape of the rigid spool will be used, together with the reimbursement pipe [10].

The construction vessels are used in various scopes, such as construction support vessel, dive support vessel, pipe laying support vessel, and anchor handling tug supply vessel. The vessel used in this project is a multi-purpose construction vessel that will be called as “lifting vessel” in further chapters. During the installation phase, the vessel's capabilities play a crucial role. The vessel used for this analysis is equipped with a dynamic positioning system for keeping the vessel in position and heading. This DP system processes data coming from the satellite and the vessel stability sensors to control thrusters in overcoing any changes in the location or the yaw direction as the lifting operation for the large dimensioned spool is very sensitive for any motions. Also, the rolling tanks are quite useful in keeping the vessel’s roll motion. The system operates the ballast water to achieve the even keel of the lifting vessel. This system is equipped with high-speed seawater pumps and vertically placed tanks on the port and starboard side of the vessels. Lastly but not least, the tugger lines with tugger cranes are used to keep lifted objects in position against pendulum motion. These lines are in use until the fully submerged phase, and are usually disconnected by remotely operated vehicles (ROV).

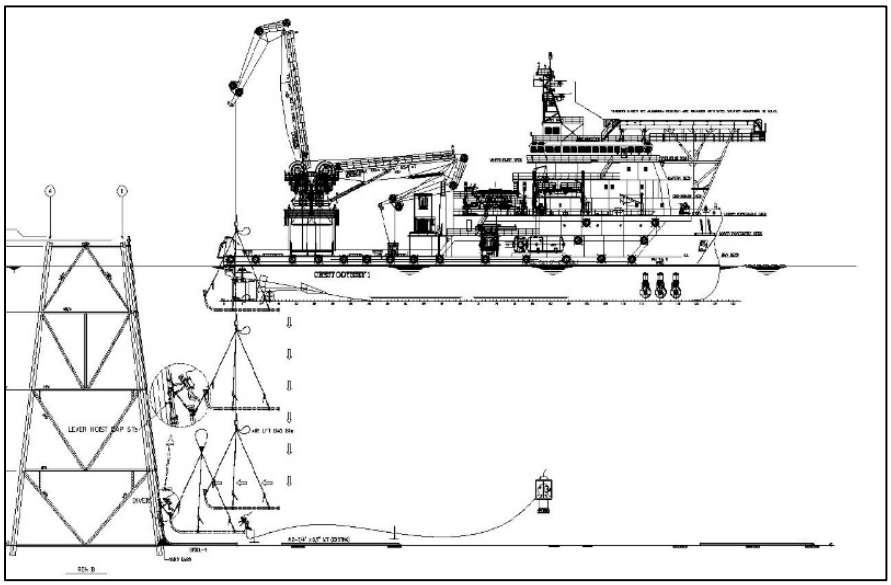

Figure 1-1: Spool installation representative drawing [11]

Because of the long dimensions, and due to many of spool installations in a particular field, it is required that the spool is transported to to the installation site by using a barge. The operational limits are not the same for all phases of the operation. The limits are affected by the result of different behaviour of the dynamic system. In order to assess the operability of the installation, evaluation of all the limiting factors are required.

1.3 Literature study

Different from lifting operation of common subsea objects, such as templates [12], suction anchors [13] and monopiles [6] the main challenge for the lifting operation of large spools comes from the large horizontal dimension of the spool. The rotational motions of the spool during the lift-off and the lowering phases can cause large relative displacements at the locations far away from the rotational centre of the structure. The large displacements will create re-hit forces during lift-off and slack slings during lowering phase, resulting in low allowable sea states. Other large dimension structures, such as wind turbine blades, also face similar challenges during the lifting operations[14]. To the authors' knowledge, limited work has been performed to study the lifting operations of spool structures. Numerical study on splash zone lowering operation of a large subsea spool has been conducted using different numerical methods, and the influences from different methods on the operability have been discussed [15]. Dreng studied limiting operational wave

criterion for the spool installation lifting; however, this study is lack of the lift-off phase and relevantly re-hit analysis [16]. Parra studied both the lowering and the lift-off phases using time-domain simulations [17]. The allowable sea states in terms of Hs and Tp have been derived. However, it was found that the allowable sea states were relatively low, especially for the lift-off operation from a barge. This was due to high re-hit forces occurring on the spool body. The low sea states resulted in low operability and high costs for the whole operation.

1.4 Aim and scope

This study focuses on the lift-off operation of a large subsea spool from a transportation barge. It is critical to improving the allowable sea states for such an operation to reduce the installation cost. The operators may focus on to proposing tailor-made mechanical equipment to avoid excessive re-hit forces to improve the sea states for such lift-off operations. As an alternative, this study proposes two methods. First method is a passive method by using fenders with different properties between the spool and the deck, and the second method is an active method by using a winch control system to define best lift-off time for the operation.

In the first method, the purpose is to absorb the impact energy and reduce the re-hit forces during lift-off. Although various fenders are often used in marine operations, their effects have not been evaluated on the deck lift-off operations for large slender structures. Because the fenders are easy to implement during the operation, this method can be more cost-efficient compared to utilizing other mechanical equipment. However, for the lift-off operation of the spool, the influences of the properties of the fender models on the allowable sea states are unknown and have not been studied in detail.

Furthermore, the lift-off operations involve different structures and equipment, and the dynamic responses of the installation system depend on many parameters, such as winch speed, lift-off instant selection, properties of the rigging system, etc. For various operations, the winch speed and the rigging properties are standard parameters that need to be considered in the analysis and the design phase. Thus, the dynamic responses in the lifting system and standard parameters are considered in the winch control system. Because of the large horizontal dimensions of the subsea spool, the operation is highly sensitive to dynamic responses and lift-off instant. Therefore,

the winch control system aims to define a favourable moment for the subsea spool. Nevertheless, the winch control system for the lift-off operation from a transportation barge is unknown and, have not been used before in the numerical analysis. Figure 1-2 presents the scope of the thesis.

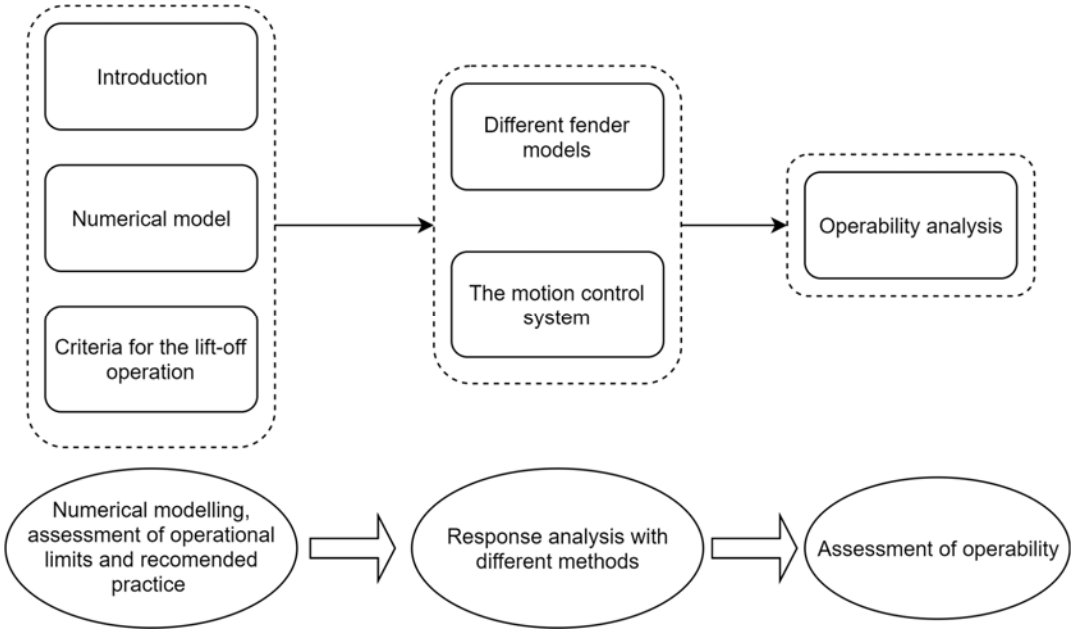

Figure 1-2: Scope of the thesis and interconnection between the chapters

The objective of this study is to evaluate the potential of improving the allowable sea states by using different support fenders for the spool on the transportation barge and the dynamic method by the winch control system.

1.5 Thesis outline

A summary of the thesis consists of seven chapters. Each chapter is briefly explained as follow:

Chapter 1: The first chapter introduces the marine operation and follows with literature study, aim and scope and outline of the thesis. State of the art in subsea spool installation, modelling and marine operations are reviewed.

Chapter 2: This chapter addresses the lifting system properties and presents the numerical modelling of the subsea spool installation operation using the transportation barge and the lifting vessel.

Chapter 3: This chapter introduces structural properties and the operational criteria recommended by DNVGL. A systematic methodology for the assessment of allowable sea states is presented. The recommended practice from DNVGL is applied in the subsea spool lifting operation, and allowable sea states for a constant winch speed is assessed [2].

Chapter 4: This chapter presents the dynamic responses using four different fender models based on the time-domain simulations. The assessment of wave seeds is examined in a fender model. Sensitivity study among the fender models is carried out.

Chapter 5: This chapter introduces the motion control system for the winch controller. Firstly, the control method is created by using the evaluation methods used in the post-process. The required algorithms are defined and compared with several methods to achieve efficient control system. Lastly, the sensitivity studies are carried out for lift-off criteria, winch speed and lift-off timing with the motion control system.

Chapter 6: In this chapter, the results assessed from the previous chapters are used in the operability study in a particular location. First part of this chapter presents a systematic methodology to assess operability for the subsea spool installation, and the latter discusses the impacts of the methods used in Chapter 4 and Chapter 5 in the operability of the subsea spool installation.

Chapter 7: In the last chapter, conclusion and recommendations for the future work is presented.

Chapter 2
Numerical model

2.1 General

In this chapter, the description of the lift-off system is presented by highlighting critical structural parameters. Set-up of the numerical model and DNVGL regulations for the lift-off system are explained. Hydrodynamic interactions between the lifting vessel and the transportation barge such as coupled motions, sheltering effect and piston mode are discussed. Time-domain simulation methods are described.

2.2 Description of the lift-off system

The system for the lift-off operation includes the lifting vessel, the transportation barge, and the spool piece. A typical offshore construction vessel is employed for the lifting operation. The construction vessel is equipped with a crane with a maximum lift capacity of 400 tonnes. The operating radius of this crane is between 10 m and 40 m. In this numerical model, the vessel is modelled at the full capacity, including the ballast water where the draft is at a maximum of 8.5m with the intention of reducing vessel motions. The modern design of the vessel does not allow for the heavier steel structure weight. Therefore the mass of the vessel is around 17 tonnes with full capacity.

The choice of barge depends on many different aspects such as cost, environmental conditions of the installation area, location, and dimensions of the lifted object. In this case, The transportation barge is a conventional barge which is capable of operations in the North Sea. It has a large deck area to transport spools with large dimensions. The main dimensions of the construction vessel and the transportation barge are given in Table 2-1. Furthermore, a conventional barge has no equipment on board, and it is only used for providing deck area for the structures. In an operational point of view, the ballast operation of the barge during lifting operation is not an option; additionally, there would be a towing vessel propelling the barge to the installation area. The towing vessel adds the capability of moving any direction after spool lifted off.

Table 2-1: Specifications of the lifting vessel and the barge

	Unit	Lifting Vessel	Transportation Barge
Length overall	m	156.7	100
Breadth	m	27	25.6
Maximum draft	m	8.5	4
Displacement	Tonnes	1.70E4	1.04E4

A large subsea spool is to be installed on the seabed, and it is composed of different sections of tubular members [17]. Figure 2-1 presents the side and top views of the spool piece, where the horizontal position of the centre of gravity (CoG) is highlighted. The total length of the spool is over 60 m, and the width is around 25 m. The large horizontal dimension of the spool makes it challenging for the lift-off operation. A small rotation of the spool will induce large vertical motions at the locations away from the CoG of the spool, which may cause re-hit between the spool and the barge. The reinforcement pipe is attached to strengthen the anti-compression capability of the spool, and thus any structural failure during the deployment can be avoided reinforcement pipe is assumed rigidly connected to the termination heads. The reinforcement pipe is connected from each end (termination heads) to strengthen anti-compressibility against the compressive forces from the tensions in the slings during the lifting operation. The total mass of

the spool and the reinforcement pipe is 45.2 tonnes. The total mass of the spool together with the reinforcement pipe is 45.2 tonnes, and contributors to the total mass are shown in Table 2-2.

Table 2-2: Specifications of the lifting vessel and the barge

	OD [cm]	Thickness [cm]	Mass [kg]
Steel pipe with coating	46,16	1.91	25826
Termination heads	35,88	1.91	4697
Reinforcement pipe	40,64	2.54	14217
Secondary Members	35,88	1,91	458
Total			45178

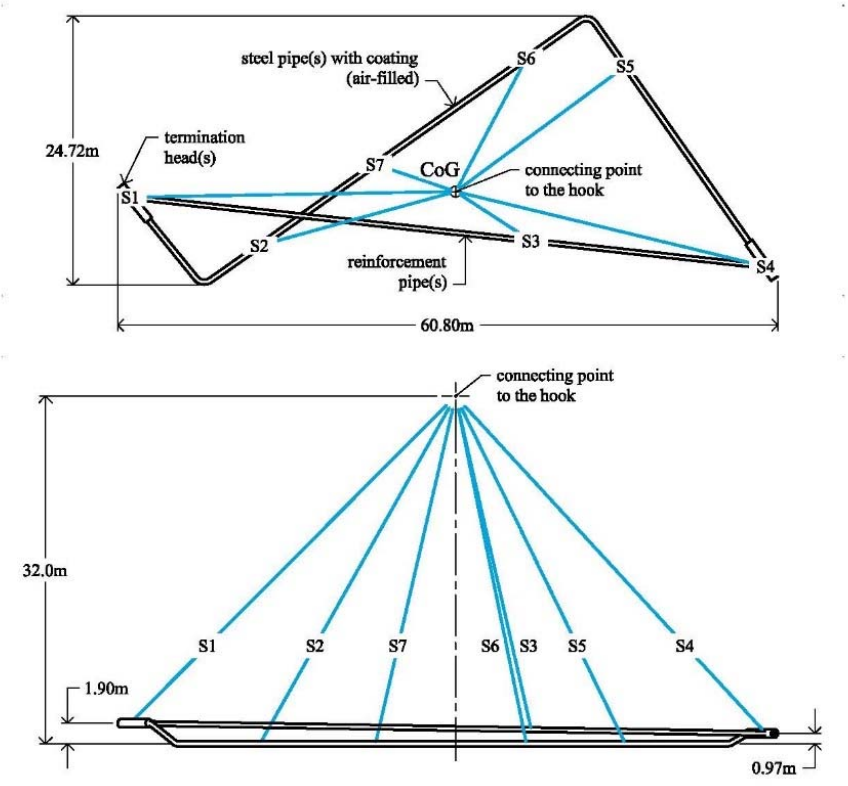

Figure 2-1: The spool side and top view with slings connection points

The spool is initially rested on the transportation barge. During lift-off, the hoisting system will lift the spool from the deck of the barge before lowering it through the splash zone. The hoisting system for the spool lifting operation includes the slings, the lift wire and the winch. The slings connect the spool to the hook of the crane block, and the lift wire is between the crane block and the crane tip. Because of the large horizontal dimension of the spool structure, seven slings are arranged to distribute the loads on the spool. The locations of the seven slings on the spool are shown in Figure 2-1. Two slings are directly attached to the termination heads, which are heavy components. Four slings are distributed along the steel pipe with the coating, while another sling is attached to the middle section of the reinforcement pipe.

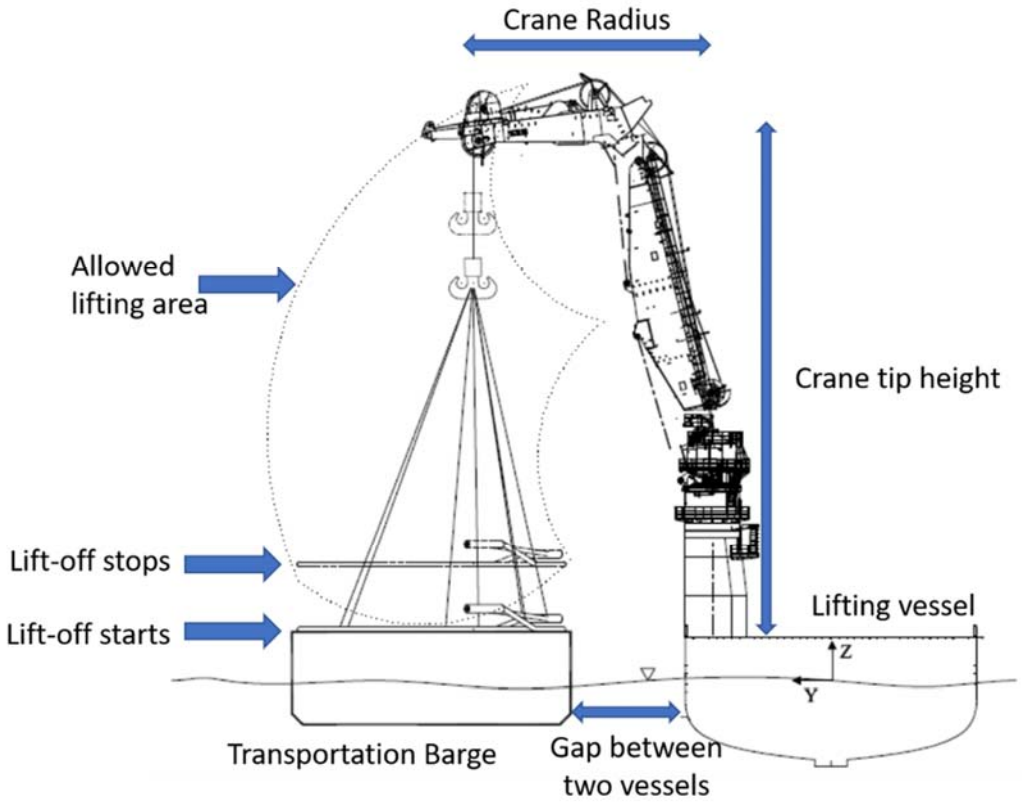

Figure 2-2: Lift-off sketch from the transportation barge

Figure 2-2 illustrates the spool lift-off. The area where the crane is able to lift or lower the objects is named allowed lifting area, and this area is defined by the crane manufacturer to guide safe operations within the crane capacity.

Based on the result of the static analysis, the spool's submerged tilting angle is lower than 2°; therefore, there is a good correlation between CoG and CoF [17]. With the aim of lift-off analysis, the hook and crane tip are placed on the CoG position of the spool. Due to the long length of the spool, lift-off operation from a barge becomes more challenging. A small rotational movement on the spool induces large vertical motions, which may cause re-hit between the spool and the deck of the barge.

2.3 Set-up of the numerical model

The numerical model is established using SIMA-SIMO program [18]. SIMA-SIMO is a time-domain analysis software developed by the research institution SINTEF Ocean (previously MARINTEK). The software was developed to perform analyses of marine operations, and most of the force effects that present in a marine operation can be modelled appropriately. The program was well-validated for a wide range of marine operations. It has been commonly used as an engineering tool in the industry with many case studies available in the literature (Reinholdtsen et al [19]; Chen et al, [20]; Valen, [21]; Næss et al, [22]; Wu et al, [23]). In the SIMO model, apart from the transportation barge and the lifting vessel, slender elements are used to build rest of the parts such as subsea spool, couplings, and fender points between the spool and the barge. Hydrodynamic coefficients of the subsea spool are not taken into account because of the analysis focused only on the lift-off of the spool from the barge.

In the current model of the lift-off operation, the construction vessel, the barge, and the spool are modelled with six degrees of freedom (DOFs), while the hook is modelled with three DOFs. The global coordinate system is a right-handed coordinate system. The origin of the global coordinate system is located on the still water surface and in the mid-ship section of the construction vessel. The X-axis points towards the bow of the construction vessel, the Y-axis points towards the port side, and the Z-axis points upwards.

The crane tip position is [-36.2 m, 33 m, 50 m] in the global coordinate when the system is at rest. The origin of the transportation barge is located at the same horizontal position as the crane tip, which at the position of [-36.2, 36.81, 0]. According to DNVGL-ST-N001[1], the minimum

distances for the lifted object in the marine operations are stated and ought to be maintained during the whole operation. These distances are given in horizontal direction and listed below,

- Between any point of the lifted object and the crane boom: 3m
- Between the lifted object and other objects on the same vessel, without tugger lines and bumpers: 5m
- Between lifted object and any other structures such as lifting vessel without using bumpers or guides: 3m

Hence, these regulations from DNVGL are taken into account for the modelling of the lift-off operation. In the lift-off instant, the crane beam is extended by 10m on the port side of the lifting vessel. This distance together with the weight of the subsea spool leads to roll motion towards the port side of the lifting vessel. On the other hand, the manoeuvring of transportation barge is easier after the spool is lifted because of the distance between the transportation barge and the lifting vessel. The numerical model in SIMA-SIMO is shown in Figure 2-3.The spool is rested on the deck of the transportation barge and supported by fenders. The locations of fender points are highlighted with yellow circles in Figure 2-3. The name of the fender points is linked to the position relative to the barge body and is listed below.

- PortFwd(Port Forward); fender point on the port and forward side of the barge
- MidFwd(Middle Forward); fender point on the midsection and forward side of the barge
- StbdFwd (Starboard Forward); fender point on the starboard and forward side of the barge
- PortAft (Port Aft); fender point on the port and aft side of the barge
- MidAft (Mid Aft); fender point on the port and forward side of the barge
- StbdAft (Starboard Aft); fender point on the port and forward side of the barge

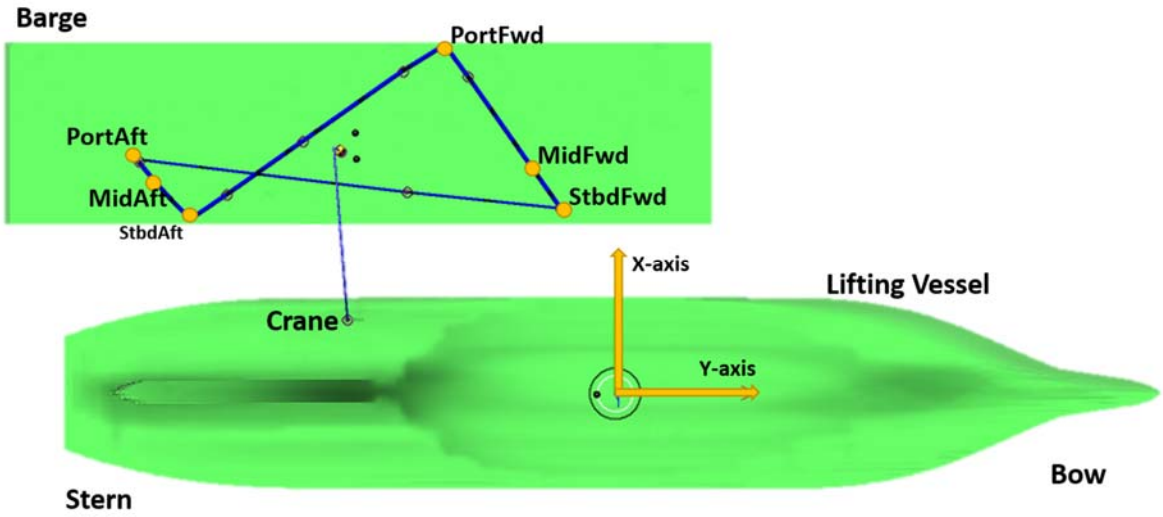

Figure 2-3: Lift-off model top view on SIMA software

The locations of fender points are representing the possible hit points on the spool body. Fenders are coupled with the spool body to analyze re-hit force as black spheres in Figure 2-4. In this method, any possibility of the spool hits other points on the deck other than the fenders is avoided.

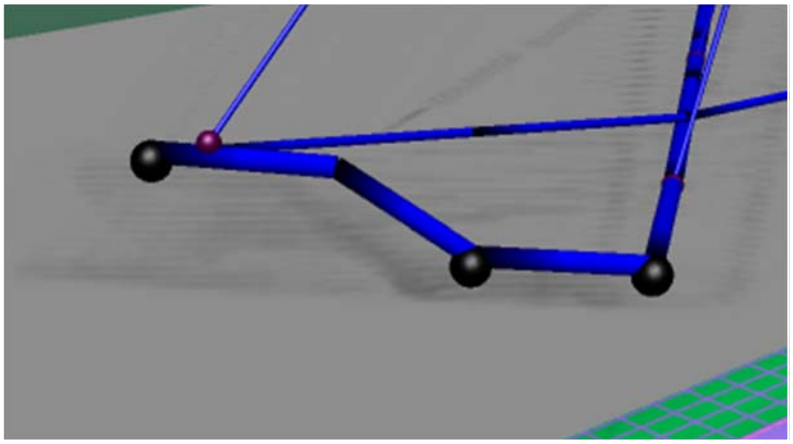

Figure 2-4: Fender points on the spool body on the aft side

In the model, the spool is considered as the rigid structure, and the spool's flexibility is kept in the stiffness module of slings. The wire couplings through seven slings and the lift wire are

modeled as linear springs. That is achieved by the constant flexibility $k_{0,}$ which is also unique for each coupling element. The effective axial stiffness can be expressed as:

$$\frac{1}{k} = \frac{1}{EA} + \frac{1}{k_0} + \frac{1}{k_s} \qquad \text{Eq. 2-1}$$

Where E is the modulus of elasticity, A is the cross-sectional area of the wire, $1/k_0$ and $1/k_s$ are the crane and spool flexibility, respectively. l is the total length of the lift wire. During the lift-off operation, l decreases as the winch run. As mentioned, the spool has deflections due to its flexibility, which will influence the dynamic tensions in the slings. The flexibility of the spool is added and distributed in the flexibility of the seven slings. It is realized by adjusting the flexibility parameter in the sling property until the tension in each sling under static condition matches that from the structural model, where the spool is modelled as a flexible structure. Moreover, tugger lines are often used in the spool lifting operation to constrain the horizontal motions of the spool. In the current model, yaw stiffness has been added to the spool for simplicity, to represent the restoring forces from tugger lines.

2.4 Hydrodynamic interactions between the construction vessel and the barge

The hydrodynamic analysis of the lifting vessel and the barge is required to obtain the hydrodynamic properties on both vessels. For the lift-off operation, the hydrodynamic interactions between the vessel and the barge should be considered because the two structures are in close vicinity and the hydrodynamic properties are coupled. Thus, two-panel models of the vessel and the barge have been built, and the hydrodynamic interaction problems are solved using the panel method program WADAM in the frequency domain. The frequency-dependent hydrodynamic coefficients, including excitation forces, added mass and damping is generated from the hydrodynamic analysis. It has been observed that compared to single body case, the interactions influence the hydrodynamic properties of the body, mainly in the transverse direction, namely in sway, roll and yaw [17]. This is a result of the side by side arrangement of the two floating bodies. Two body panel model in WADAM software is shown in Figure 2-5.

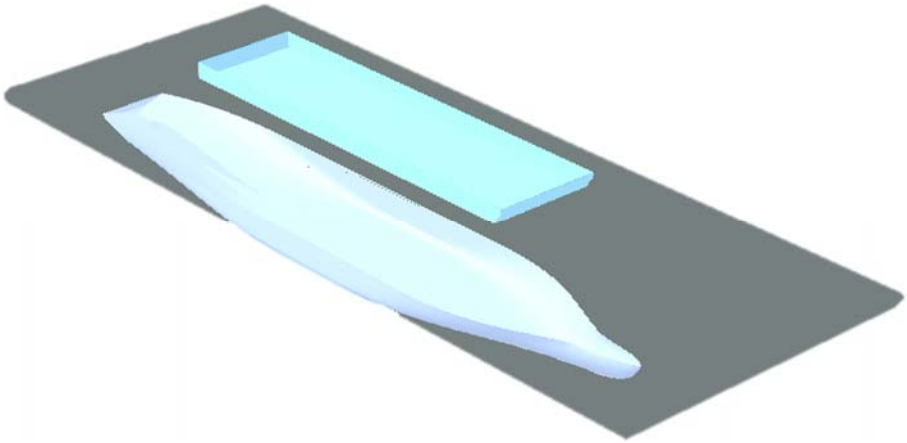

Figure 2-5: Multibody model on WADAM software

In the case that the lifting vessel and the barge are placed side by side, the hydrodynamic responses are different because of the sheltering factor where the lifting vessel body absorbs most of the wave energy. This is because of the wave propagation from the direction of the lifting vessel. The responses amplitude operator (RAO) is calculated for the lifting vessel in unrestricted water not applied for lifting operations.

When analyzing hydrodynamic interactions between multiple floaters, another significant factor is the resonance of the trapped water between the floaters that may amplify the roll and sway motions. The eigenfrequency w_0 of the piston mode is given in the frequency range in Eq. 2-2 [2].

$$1 + \frac{2}{\pi} * \frac{G}{D} < w_0^2 * \frac{D}{g} < 1 + \frac{\pi}{2} * \frac{G}{D} \qquad \text{Eq. 2-2}$$

where

D = draft of the transportation barge [m]

G = width of the gap [m]

g = acceleration of gravity [m/s^2]

Generally, this equation applies to a narrow gap between floating structures. Based on the current lifting arrangement between the construction vessel and transportation barge, the natural

period of the piston mode is found to be around 3s, which is away from the dominant wave periods. Thus, this effect is neglected in the current numerical analysis.

The alignment of the transportation barge and the lifting vessel provides a sheltering effect, which results in smaller motions on the lee side than on the weather side. So, positioning of the barge respect to lifting vessel and dynamic position against the waves is a crucial fact in the vessel behaviours. Usually, the transportation barge is moored or positioned in a suitable place for the crane, and the sheltering effect is applied by rotating floating bodies together in the yaw direction. The vessels are facing the waves in 180° ($\pm$15°) in order to diminish the transportation barge motions on the lee side. The sensitivity analysis of this model for the vessel position angle against the waves conducted by Parra [17], and as a result, 165° is found feasible to carry out this lifting operation.

2.5 Time-domain simulations

Because of the high nonlinearity and the transient effects during lift-off operation, time-domain simulation is required to directly solve the motions of the system. The coupled lifting system composes of 21 DOFs of rigid body motions, including 6 DOFs for the lifting vessel, transportation barge and spool, respectively, and 3 DOFs for the hook. The equation motion is expressed as in Eq. 2-3[1] [18].

$$\big(M + A(\infty)\big).\ddot{x} + D_1\dot{x} + D_2 f(\ddot{x}) + Kx + \int_0^t h(t-\tau)\dot{x}\,(\tau)d\tau = q(t, x, \dot{x}) \qquad \text{Eq. 2-3}$$

where M refers to the mass matrix; x is the rigid body motion vector for all bodies in 21 DOFs; A(∞) is the infinite frequency added mass matrix; D is the damping matrix, 1 and 2 denotes to linear and quadratic terms, respectively; K is the hydrostatic stiffness matrix; h is the retardation function calculated by the frequency-dependent added mass; q(t,x, $\dot{x}$) is the force vector, including the all wave excitation forces shown in Eq. 2-4.

$$q(t, x, \dot{x}) = q_{WA}^{(1)} + q_{WA}^{(2)} + q_{ext} \qquad \text{Eq. 2-4}$$

where $q_{WA}^{(1)}$ is denoted for first-order wave excitation, $q_{WA}^{(2)}$ is the second-order wave excitation and q_{ext} is the external forces from the positioning system of the lifting vessel and the barge.

Step-by-step integration method is applied to solve the coupled equations of motion for the lift-off system using an iterative routine. The equations of motion are solved by Newmark-beta numerical integration with a time step of 0.02 s. In a case of any structure containing a group or series masses supported by a deformable structure, the Newark-beta numerical method is applicable [24].

The wave excitation forces on the construction vessel and the transportation barge are pre-generated from the transfer functions obtained from the frequency-domain analysis at their mean positions using Fast Fourier Transformation (FFT). The radiation effects on frequency-dependent added mass and damping forces are included in terms of coupled retardation functions in the time domain. The coupling forces including the wire and fender couplings are directly calculated for each time step based on the relative motions between the bodies.

Chapter 3
Criteria for the lift-off operation

3.1 Overview

This study focuses on the lift-off phase of the spool installation. Besides, the assessment method of the allowable sea states is explained, and a systematic methodology is presented. Impact of the evaluation method is discussed in the conventional model. Based on the recommended practice from DNVGL [2], the critical events which limit the operation are discussed in this chapter, and the re-hit probability is calculated. Based on the re-hit probability and given exceedance limit, preliminary assessment of allowable sea states carried out as a reference.

3.2 Operational criteria

When searching for allowable sea states for the lift-off operation, the subsea spool's material properties play a significant role in defining limits for the coupling. The coupling elements such as lift wire and slings have specific maximum tension loads with the safety factor which is described as a safe working load in a practical way. This load will be used to describe snap tension value for each sling element in the post-processing phase.

Table 3-1: Material Specifications for lift wire & slings

	Units	Lift wire	Slings
Diameter	[mm]	128	40
Minimum breaking load	[kN]	13290	1116
Safe working limit	[kN]		159.43
Elastic Modulus	[kN/mm²]	130	103.7
Effective cross section area	[mm²]	9260	
Stiffness	[N]	1.204E+9	2.0361E+8
Weight in air	[kg/m]	77.8	6.6
Damping	[Ns]	1.0E+07	1.0E+06
Flexibility	[m/N]	1.30E-07	

Therefore, safe working load (SWL) of slings is calculated by dividing the minimum breaking load (MBL) to the safety factor (SF) . In Table 3-1, MBL is 1116kN for the sling elements and safety factors considered as 7.

$$SWL = \frac{MBL}{SF} = \frac{1116kN}{7} = 159.43kN \qquad \text{Eq. 3-1}$$

Since the SWL is defined under static conditions, the dynamic amplification factor (DAF) contributes to the effect of the global dynamic load caused by the static loads. In the offshore lifting operations, DAF should be indicated for the dynamic analysis to base on a comprehensive argument [1]. DAF is taken as two, which is the same value used in the STAAD analysis for the spool lift-off operation.

$$DLC = SWL * DAF = 159.43kN * 2 = 318.86kN \qquad \text{Eq. 3-2}$$

Consequently, the snap force in the other name characteristic total force for each sling connected to the spool is shown in Equation 3-2 as 318.86kN.

Re-hit of the subsea spool to the deck of transportation barge is considered a critical event during lift-off operation [17]. In the numerical model, the spool is rested on the barge by the support of fender elements. For the re-hit force on the fender points, the static weight of the spool is considered on each fender point as the re-hit criteria for evaluation. The highest force acting on the fender points in the static phase is taken as re-hit, which is 145.2kN.

3.3 Method to assess allowable sea states

Allowable sea states are obtained by evaluating the responses from different wave seeds following two steps.

The first criterion is the increasing relative distance between the crane tip and the barge. This criterion is inspired by the re-hit probability calculation recommended by DNVGL [2]. The proper lift-off scenarios are selected by checking the relative motion between the crane tip and the deck of the barge shortly after lift-off. During this step, the relative motion should have a continuous increase during 1 s after the activation of the winch (55th second). The wave seeds that fulfil such requirement are selected as proper seeds. The purpose of the first step is to exclude the unreasonable wave seeds that do not fulfil the judgement of the crane operators in the real operation. Then, these proper seeds are further used, and the critical responses are evaluated against the lift-off criteria, including the sling tensions and re-hit forces on the fenders. The first criterion is observed in the numerical analysis in Chapter 4.4.1.

Before the second step of the evaluation method, it is required to define actual lift-off time for different sections of the subsea spool due to the large horizontal dimensions and flexibility in the sling couplings. The separation of the subsea spool from the deck occurs at different time steps. This focus relies on the basic principle of signal filtering. By taken time step into consideration, every motion and the force is calculated in the 0.02s intervals. At the time of lift-off, coupling forces start to oscillate excessively wherein some of the cases these force values even pass over the structural limits. These values in the other name as noise should be ignored to proceed further of wave seeds. Besides, these values do not represent the actual state on the fender points, provided

that an interval of three seconds applied to the available seeds. After the lift-off time for each fender point is defined, the second criterion is considered from this time o the end of the simulation.

Secondly, the structural limitations of coupling elements and the subsea spool, as well as re-hit criteria, are applied to the time steps of available seeds from the lift-off instance until the end. The structural limits include potential snap loads, slack wire condition of slings, and re-hit forces acting on the fender points[17]. The structural properties are introduced in the previous chapter. Application of these limits is summarized in the following list.

(i) Re-hit of the spool against the supporting fender. During an offshore lift-off operation, re-hit of the object against the supporting deck is identified as a critical event. Here, re-hit shall mean the event in which the object hits the supporting deck after any attempt to be lifted. The static fender force on the spool is 145.2 kN, which is calculated based on the initial static condition when the spool is rested on the fenders. Thus, after the spool is lifted from the fender, the following criterion should be fulfilled:

$$F_{fender} < 145.2kN \qquad \text{Eq. 3-3}$$

(ii) Potential snap loads in the slings. The dynamic load capacity (DLC) of the sling should not be exceeded. In the current case, the DLC of the sling is 318.8 kN. The following criterion should, therefore, be satisfied to avoid potential snap load:

$$F_{sling} < 318.8kN \qquad \text{Eq. 3-4}$$

(iii) Slack wire condition for slings. The slack-sling condition occurs when the dynamic tension becomes zero. Hence, the criterion regarding the slack-wire condition of slings follows:

$$F_{sling} > 0 \qquad \text{Eq. 3-5}$$

A safe lift operation requires the contribution of all criteria of lifting operation simultaneously. The seeds with proper lift-off scenario are evaluated against the aforementioned three criteria during the period when the spool is lifted off until the end of the simulation. The

seeds that fulfil all the lift-off criteria are defined as “safe seeds’, indicating the operation can be conducted safely under these wave realizations. For a given Hs and Tp condition, the ratio between the number of the ‘safe seeds’ and the number of the seeds with the proper scenario is calculated. If the ratio is higher than 90%, this sea state is considered as allowable sea state. On the other hand, if the ratio is lower than 90%, the sea states are not considered allowable. The 90% threshold for the ratio is to ensure a high rate of ‘safe seeds’ for the operation to fulfil the criteria under the allowable sea state conditions, and the value is chosen based on the experiences and the risks from similar operations.

This evaluation is handled by a post-processing code written in MATLAB software. MATLAB is an interactive software for numerical calculation and analysis [25]. There are three loops involved in the post process code shown below,

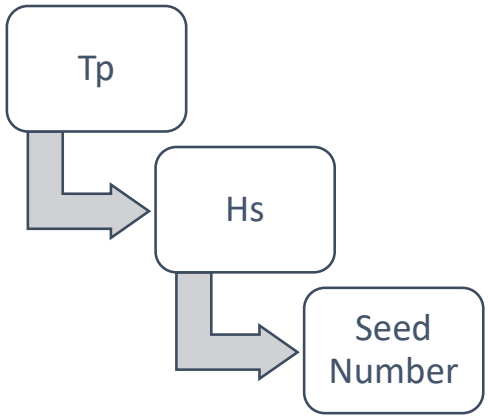

Figure 3-1: Loops in the post-processing code

Hence, the evaluation method proceeds for each seed number in a Hs. After completion of all Hs for one Tp, the process continues with the next Tp. Besides, only one wave direction is used in this model; alternatively, the loops can be extended with the range of wave directions or different fender models properties by creating another loop on the top of the Tp loop function. After the loop for the seed numbers is completed, the amount of proper and the safe seeds are evaluated within the 90% rule for the allowable sea states. If 90% rule is satisfied for the Hs, the process continues with a higher Hs until the rule is not satisfied. The post-processing code's methodology is described in detail in Figure 3-2.

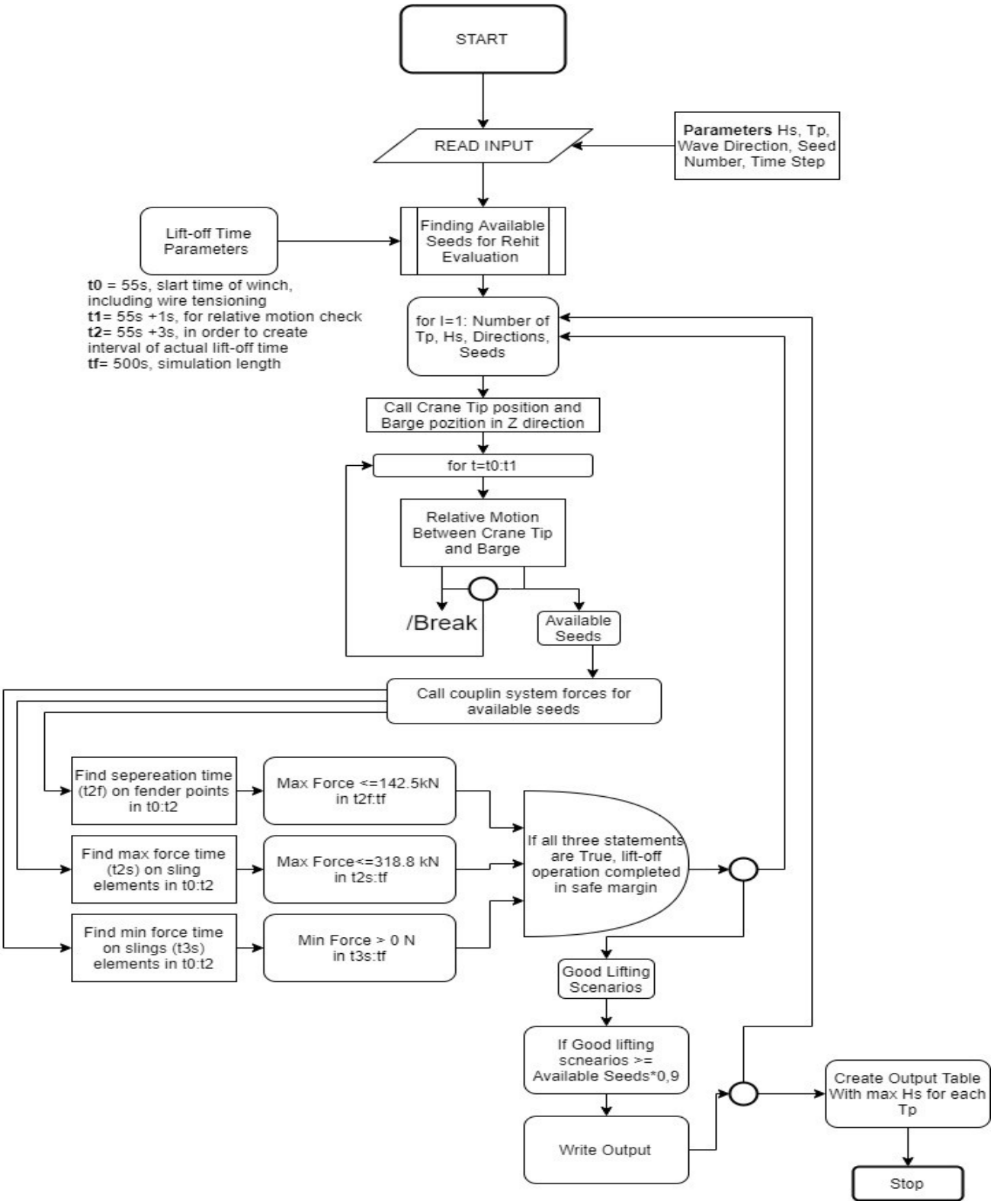

Figure 3-2: Post-process of wave seeds

3.4 Recommended practice for lifting operation

This practice is a very preliminary method of the lift-off operation before time-domain simulation to provide preliminary allowable sea states. This method does not include any coupling of wires, slings, fenders. According to DNVGL guidelines, the motions of the barge and the lifting vessel are assumed Gaussian distribution obtained from linear wave theory [2]. The most critical parameter of the lift-off operation is relative motion between the crane tip and barge, which determines the probability of re-hit. Following assumptions and the equations in order to calculate re-hit probability are followed from DNVGL guidelines [2].

- The hoisting speed of 0.25m/s is constant.
- The motion responses of the barge and the vessel is narrow banded.
- The probability of spool hitting barge more than once lift-off is zero.
- The lift-off instance of the spool is when relative vertical (z) motion between crane tip and barge is maximum

The re-hit probability has resulted from the below equation [2].

$$P(\tau) = \frac{1}{2} * \exp\left(-\frac{\tau^2}{2}\right) * \left(1 - \frac{\tau * \sqrt{\pi}}{2} * \exp\left(\frac{\tau^2}{4}\right) erfc\left(\frac{\tau}{2}\right)\right) \qquad \text{Eq. 3-6}$$

where τ is,

$$\tau = \frac{U * T}{\sigma} \qquad \text{Eq. 3-7}$$

U is hoisting speed, T is zero up-crossing periods, and finally, yet importantly, σ is taken from the standard deviation of relative motion between the crane tip and the barge. The total acceptable probability in a series of 10 lifting operations is 0.01 that results that the probability of each operation should be less than 0.001. Also, the probability of 0.01 can be achieved by having τ bigger than 2.9. Furthermore, 'erfc' stands for error function which is

$$erfc(x) = \frac{2}{\sqrt{\pi}} \int_{x}^{\infty} e^{-t^2} \mathrm{dt} \qquad \text{Eq. 3-8}$$

As seen from the formula of the probability, the re-hit probability function is not related to the size of the object lifted, neither mass of the object. Therefore, the re-hit probability function would not be covering all the aspects of this spool lifting case. With that in mind, given assumptions provide distinct allowed sea states from the results of the numerical analysis. The allowed sea states are assessed by having a constant speed and using the probability equation. The results are given in Chapter 3.4.2.

3.4.1 Method to estimate the re-hit probability

In the time domain simulations, the lift-off model has four bodies, such as vessel, barge, spool, and hook. The probability function requires using only relative heave motion between crane tip and the barge, and the lift-off model is modified into two main bodies, i.e. the lifting vessel and the barge, as it is shown in Figure 3-3. The spool is a slender element on the barge body with the same specifications, and the hook is defined as a slender element in the same position respect to the vessel body. The reason behind not modelling coupling for this case is probability relies on the standard deviation of the relative distance between the hook and the barge. Indeed, the relative motion is the dominant factor in the re-hit probability.

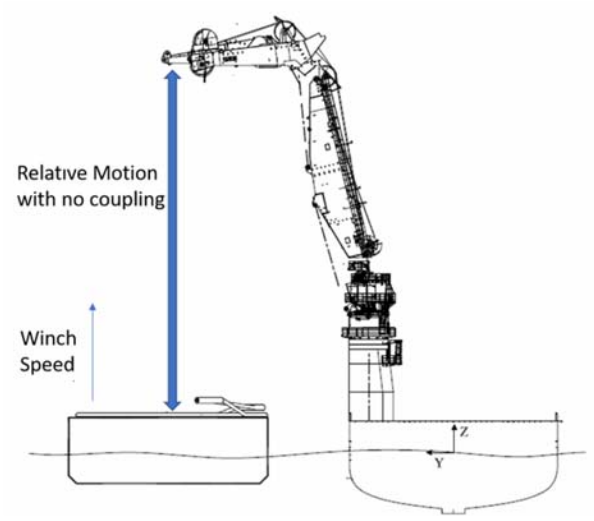

Figure 3-3: The lift-off model for re-hit criteria

There is only one wave seed run for each case of Hs and Tp. Each seed has three hours of simulation to comply with standard deviation and 3 hours probability.

3.4.2 Re-hit probability result

According to DNVGL-RP-N103, the probability graph is created by assuming that the relative motion is proportional to the wave motion; therefore, the standard deviation values are proportional to the Hs values. The plot is shown in Figure 3-4. It is generated for only one Tp, and the hoisting speed is assumed as 0.3m/s.

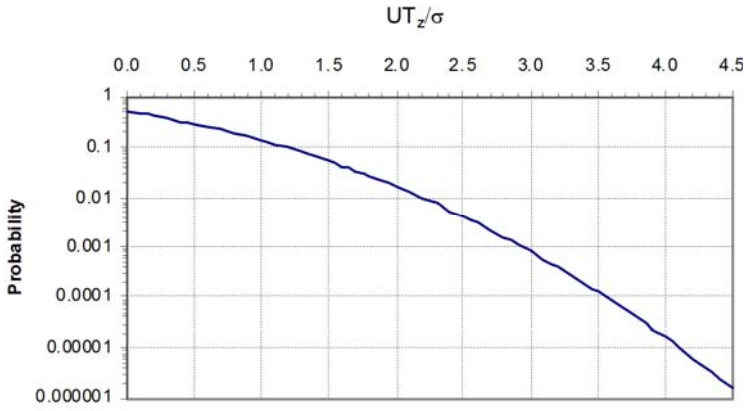

Figure 3-4: Probability of barge hitting to a lifted object [2]

In this work, the results will be shown respect to each Hs and Tp. The standard deviation of the relative motion between the crane tip and the deck of the transportation barge is shown in Figure 3-5. The value is increased gradually by the increase of Hs and Tp. However, at the Tp of 6s and 11s, the standard deviation decreases. This is because of the natural period of heave motion in the crane tip, which equals 5.5s.

As mentioned before, τ shown in Eq. 3-7 is the main criteria for this probability equation. The standard deviation, in the planning phase, can be considered as proportional to the Hs. Since the availability of the time simulations, the standard deviation of the motion is taken into account. τ for the probability function is plotted in Figure 3-6. The dominant factor in this equation is the zero up crossing periods for the relative motion.

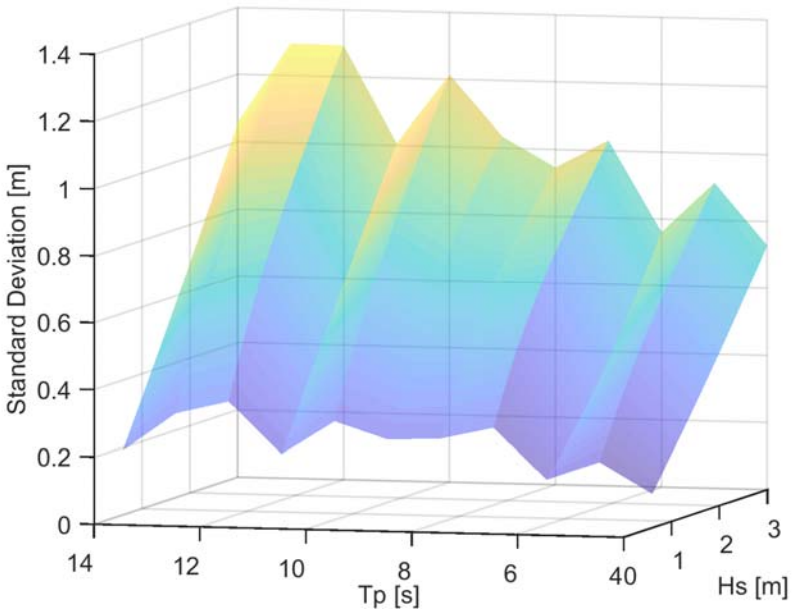

Figure 3-5: Standard deviation of relative motion between the barge and the crane tip

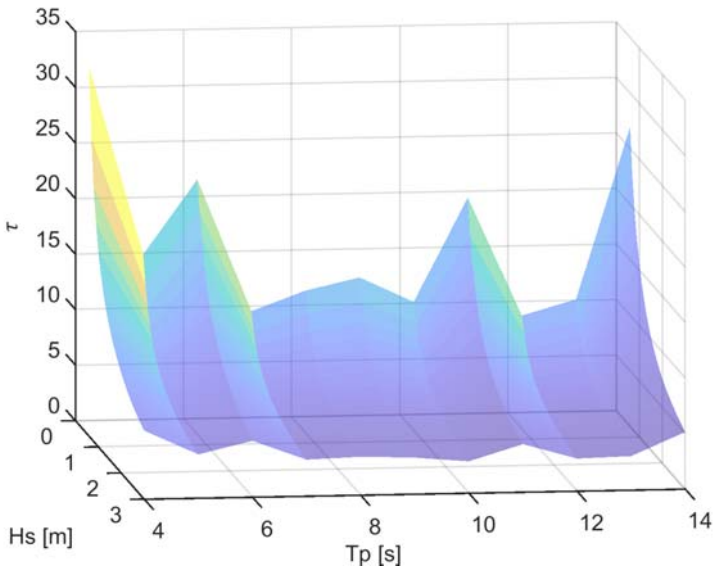

Figure 3-6: Plot of τ for each Hs and Tp

The probability of the re-hit is plotted in Figure 3-7. According to DNVGL-RP-N103, the probability ought not to exceed 0.01 for each operation in a total of ten operations[2] . This probability is considered as the one time with the maximum limit of 1% of failure. The red plot shows the limit of 0.01, and the white line shows the merge points between two plots. On Tp equals to 6 and 11, the probability of re-hit is decreased. This condition can be explained by considering the natural period of the lifting system as its also shown in the standard deviation Figure 3-5. This re-hit probability is used as a winch speed criterion for the sensitivity study in Chapter 5.4.4

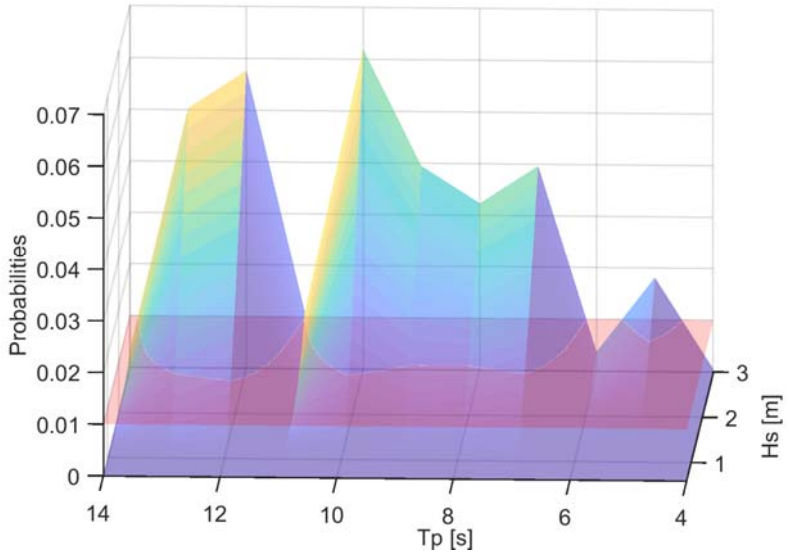

Figure 3-7: Probability figure of re-hit

Allowable sea states for re-hit probability from DNVGL

As a preliminary estimation of the allowable sea states is referenced from DNVGL to present an initial view for the allowable sea states of the lift-off operation from a barge. Allowable sea states are assessed by using constant hoisting speed for the lifting operation. According to DNVGL-RP-N103, the probability value of re-hit is defined as the probability for each lifting operation is 0.01 in a series of ten lifting operations[2]. Hence, the probability should be less than 0.001. Regarding the probability calculations of re-hit, the results on the allowable sea states are shown in Table 3-2 with the limit probability of 0.001.

Table 3-2: Allowable sea states for re-hit criteria

Tp [s]	4	5	6	7	8	9	10	11	12	13	14
Hs [m]	>3.00	1.70	2.50	1.10	1.30	1.40	1.20	2.10	1.00	1.20	2.60

Since there will be only one spool lifting operation will be conducted in this case, the allowable sea states with the limiting probability of 0.01 shown in Table 3-3.

Table 3-3: Allowable sea states for re-hit criteria

Tp [s]	4	5	6	7	8	9	10	11	12	13	14
Hs [m]	>3.00	2.50	>3.00	1.70	1.90	1.90	1.70	2.10	1.50	1.70	>3.00

Allowable sea states are compared in Figure 3-8. The maximum Hs is the same for the 11s Tp. This is because of the standard deviation for the 11s Tp is low as shown in Figure 3-5. This leads to a high Hs for different probability limits.

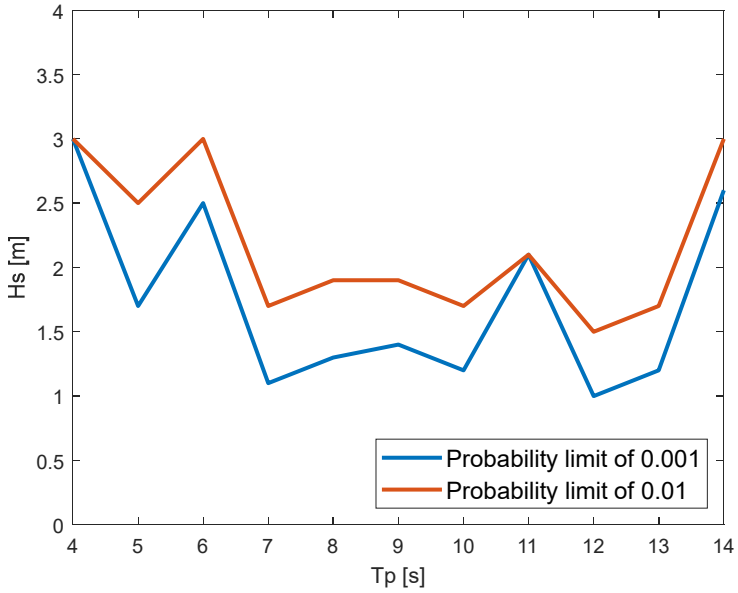

Figure 3-8: Allowable sea states for re-hit probabilities

Chapter 4
Allowable sea states using different fender[1]

4.1 Overview

In the marine industry, fenders are used as bumpers to absorb collision energy during contacts by converting kinetic energy to the fenders' elastic energy. The design and analysis of marine fenders have been studied in various applications, such as in mooring systems [26], vessel berthing structures [27], inflatable offshore barrier systems [28], offshore wind turbine berthing system [29], bridge protection models [30], and pile support fender systems [31]. Optimization analysis on the geometry and energy absorption of marine fenders can also be found in previous studies [32]. In this thesis work, the fender models are applied between the barge and the spool to decrease the re-hit force during lift-off to ensure the structural integrity of the spool. The main

[1] Part of this chapter's result and work is accepted in ISOPE 2020. Conference Paper No. 2020-TPC-1132

factors that influence the behaviour of the fenders during the transformation of kinetic energy to elastic deformation are the magnitude of loads, transmission rates of the energy and material properties of the fenders [33].

The operational limits of the lift-off operation from a barge are dominant by the re-hit criterion. The limiting parameter is the re-hit force at the fender points after the spool being lifted off from the deck of the barge. The value of the re-hit force should be less than the limiting value, which is taken as the static compression force on the fender before lift-off. Different material properties for the fender will result in different re-hit forces under the same environmental conditions. Therefore, it is important to study different material properties for the fender and compare their influences on the allowable sea states.

4.2 Significant parameters in fender models

The selection of the fender models is based on different material behaviours and their applications. The material behaviours, as referenced in stiffness and damping properties, need to be specified appropriately to obtain the forces from the fender couplings. The impact between the subsea spool and the fender generally analyses in the following concepts to enhance understanding of the fender properties.

- Energy balance
- Force equilibrium
- Impact area and damping coefficient

4.2.1 Energy balance

According to the law of conversation of energy, energy can neither be created nor destroyed. Indeed, it can be explained as in a closed system, energy input (external) minus energy output (internal) from a system is always in balance with the energy gained by the system. In the model, the spool rested on the fender points but, under the harmonic effect of wave loads. The impulse load is the re-hit force of the subsea spool to the deck of the barge in the lift-off model. The impulse load transmits the energy to the fenders called $W_{external}$ .The external energy that is added to the system of the fenders is equal to the internal energy change of the fender model plus the energy

damped and plus the energy that flows out of the fenders shown in Figure *4-1*. The capacity of dissipating energy is generally referred to as damping. Following methodology of identification of energy dissipation is introduced by Gómez [34].

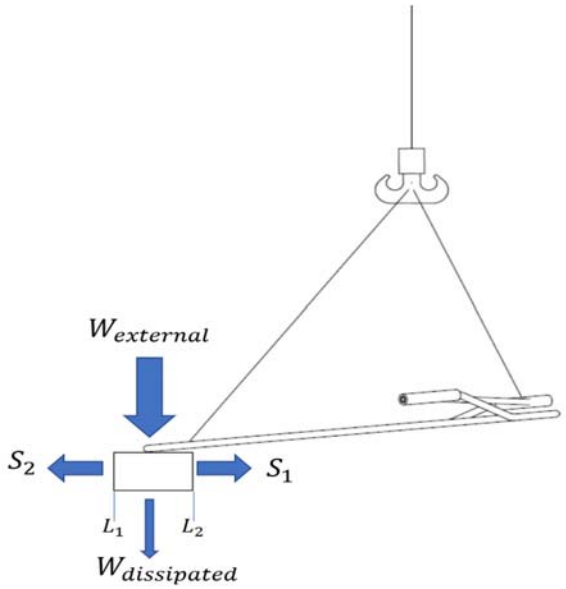

Figure 4-1: Energy balance on the fender models

In the following Equation 4-1, E(t) is the energy of the fender point comprising the kinetic energy and the elastic energy stored in the fender structure and the springs. S(x,t) is the energy flux that crosses the boundaries of this fender point located at fender points with ΔL, which is the length of the impact area. The energy balance is expressed in the following equation,

$$W_{external} = \frac{dE(t)}{dt} \mp S(x,t)|_{L_1}^{L_2} + W_{dissipated}(t) \quad \text{Eq. 4-1}$$

$$S(x,t) = 2(M * \frac{d\varphi(x,t)}{dt} + Q * \frac{dw(x,t)}{dt}) \quad \text{Eq. 4-2}$$

where Q is the shear force, and M is the bending moment. Hence, energy flux is computed by the shear force multiplied with the velocity plus the bending moment multiplied by the time rate of the rotation. In order to accumulate energy formulation for the maximum dissipated energy, the above equations can be written in the following way,

$$\frac{dE(t)}{dt} + S(x,t)\Big|_{x_j-\Delta L}^{x_j+\Delta L} = W_{dissipated}(t) \qquad \text{Eq. 4-3}$$

where,

$$E(t) = \int_{x_j-\Delta L}^{x_j+\Delta L} \frac{1}{2}\left[2\rho A\left(\frac{\partial w(x,t)}{\partial t}\right)^2 + 2EI\left(\frac{\partial^2 w(x,t)}{\partial x^2}\right)^2\right] dx \qquad \text{Eq. 4-4}$$

E(t) is the elastic energy stored in the fender by comprising the kinetic energy. Damping coefficient of a material, related to $W_{dissipated}(t)$ restored elastic energy in the material is found from the below formula as a result of computing cumulative dissipated energy within a specified period. This equation can be obtained by Eq. 4-5.

$$W_{Diss.}(t) = 2Ct\left[\dot{w}^2(x_j+\Delta L) - \dot{w}(x_j+\Delta L)\dot{w}(x_j) + \dot{w}^2(x_j-\Delta L) - \dot{w}(x_j-\Delta L)\dot{w}(x_j)\right] \qquad \text{Eq. 4-5}$$

4.2.2 Force equilibrium

In the SIMA-SIMO software, the coupling forces are calculated by the Newton's third law. The energy conversation law is founded on Newton's third law, where bodies are in equilibrium. The force equilibrium is depicted in Figure 4-2.

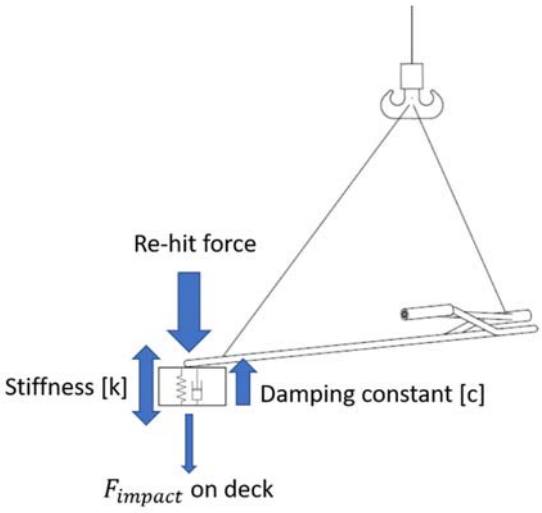

Figure 4-2: Force equilibrium diagram

In the numerical model, a fender coupling includes a fender point and a fender plane. It provides friction forces along the fender plane to prevent sliding between the bodies, as well as compression forces perpendicular to the fender plane when the two bodies have a contact at the fender point[18].

The normal compressive force is found by interpolating the distance to the force from the specified internal damping from a specified relation [18]. The distance between the fixed points and the fender plane listed in the below table, projected into the sliding plane's normal vector is used. The vertical compressive force is found from linear interpolation from the relationship between force and distance, as well as the corresponding damping coefficient [18].

Table 4-1: Fender coupling points

Fender attached to	**Barge**	**Spool**	**Coupling**
Attachment Point	X_{FB}	X_{FS}	X_{FB1}
Fender Plane Point	X_{PB}	X_{PS}	X_{PB1}
Normal Vector	X_{NB}	X_{NS}	X_{NB1}

The distance [r] is found from, subtracting fender plane location from the fixed point on the spool body.

$$r = \begin{bmatrix} \boldsymbol{X_F(1) - X_P(1)} \\ \boldsymbol{X_F(2) - X_P(2)} \\ \boldsymbol{X_F(3) - X_P(3)} \end{bmatrix} \quad \text{Eq. 4-6}$$

Normal vector 'n' for each fender point is in Z-direction only, and the plane parallel vector is in X components. Hence, projected distance 'R' is expressed as,

$$R = r.n \quad \text{Eq. 4-7}$$

Ignoring shear deformation 'S' of the fender, the new contact point on the sliding plane, S is given as

$$S = r - R \quad \text{Eq. 4-8}$$

Finally, the compressive fender force. 'F_n' found from,

$$F_n = -\left(f(R) + c\left|\dot{R}\right|^e . \frac{\dot{R}}{\left|\dot{R}\right|} \right) . n \quad \text{Eq. 4-9}$$

where,

c damping coefficient

f(R) fender characteristics

$\dot{R}$ deformation velocity

e exponential value

Therefore, specifics of different fender models are applied to this equation by fender characteristics' f(R)' along with corresponding damping coefficients. In the numerical model, fender characteristics are defined in the table of three statements, such as Distance, Force, and Damping. The force on the fender point proportional to displacement, which is correlated to the damping coefficient. Furthermore, Equation. 4-9 results in fender force acting on the connection points between fender and spool. For instance, the less stiff element which has the same height results in more displacement and higher damping coefficient than the stiffer element, and a higher damping coefficient corresponds to lower fender force on the spool.

4.2.3 Impact area and damping coefficient

Regarding implementing impact absorption and elastic energy values on the technical sheets to the numerical model, the impact area between two bodies is crucial for the calculation of actual energy absorption and therefore, the damping coefficient. While the spool is merging into the fender body, the impact area increases because of the circular shape of the spool as it shown in Figure 4-3. Therefore, the damping capacity of the material also increases. Usually, in the technical datasheets, the impact absorption energy is given as pressure or absorption energy, which is related to the impact area between the fender and the spool.

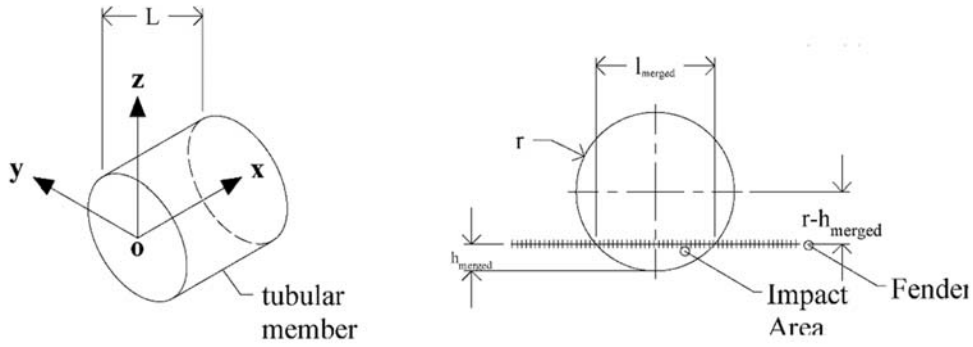

Figure 4-3: Tubular member section for the fender and spool merging points

The impact area can be found from merged length (l_{merged}) multiplied with L of the tubular member. l_{merged} can be found from hypotenuse (r^2-h_{merged}^2.) In this thesis work, to simplify the impact and fender models, L is taken as the unit length, and the fender is considered as a fender point, so the damping coefficient defined as a linear function.

4.3 Fender models

Four fender models are used in the numerical analysis to assess the allowable limits of the lift-off operation. The selection of the fender models is based on different material behaviours and their applications. The fender types are defined as listed below,

- DeckFender: Regular model
- SoftFender1: Material mixed-celled PU elastomer
- SoftFender2: EPS model
- SoftFender3: Shore 70 model

DeckFender model

DeckFender model consists of regular structural steel contact on the barge deck (Steel-steel contact).

Table 4-2 shows the features of the deck fender model. The properties of this fender model, including friction coefficients and shear stiffness, are based on the standard steel to steel contact model.

Table 4-2: DeckFender specifications

Friction Coefficient		**Shear Stiffness**
Static	Dynamic	[N/m]
0.42	0.78	$4.68X10^7$

SoftFender1 model

The material for SoftFender1 is mixed-celled Polyurethane elastomers [35]. It has less stiffness but higher damping than the rubber fenders used for marine applications. This fender model is generally used in the production lines to avoid damage on the products. The higher damping coefficient of this material is provided by the larger grain size [36]. According to the datasheet, the material has a shape of 1.5m wide, 1.0m long and 25mm thick. The pressure range of such material is up to 50 bar, and the damping coefficient can be as high as 84000 Ns/m [35]. However, these values are taken for the fender when it stays in the elastic phase; thus, the material can perform slightly different damping behaviour for the second or more hits. If the material cannot damp the force within the specified thickness, the spool is facing reaction forces from the deck. So, the fender forces reach higher points. Damping coefficient is also optimized using different dimensions of the material.

SoftFender2 model

SoftFender2 applies the Expanded Polystyrene (EPS) material, which is commonly used during the transportation of equipment or structures to offshore fields[37]. EPS' material structure is a polymer blends material. EPS' properties are well known for impact absorption, lightweight, self-resistance, water resistance, insulation [38]. EPS' main structure is a polymer blends material. It has a wide range of material properties, and it is also quick and easy to mold. This enables a great variety of EPS products in order to be used in various applications. This model has a capacity with impact pressure of 4 bar with 10% deflection. The stiffness of SoftFender2 is quite close to that used in SoftFender1, but the damping coefficient of this material is much lower. The EPS

material has a relatively less damping coefficient with a maximum value of 7860 Ns/m (Sundolitt, 2020).

SoftFender3 model

SoftFender3 is the regular rubber fender used around the vessel to protect from collisions with 'M'-shaped model [39]. The fender system is placed around the vessel in order to absorb the impact energy by converting kinetic energy to strain energy [40]. These fender models are commonly applied to almost every marine project at various dimensions and qualities, such as from small boats to massive offshore structures. Comparing to the SoftFender2, this model behaves relatively less stiff and has less damping coefficient. These types of fenders are typically used for lower energy transmissions, corresponding to impacts with high mass and low relative velocity. However, in order to provide higher elastic energy and less stiff behaviour for the fender, this fender is modelled with an extended height.

Above all, bilinear stiffness and damping models are used in SIMA for the four fenders. The relation between the force with respect to the distance is shown in Figure 4-4, where the slopes of the curves represent the stiffness. The first slope of the curves represents the stiffness K_1 of the fender materials. The height of the soft fenders equals to the X-values at the turning points in Figure 4-4 for different models.

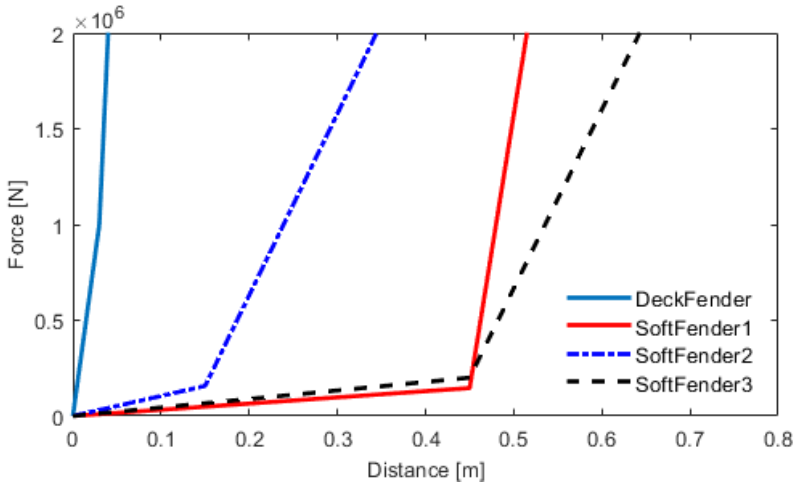

Figure 4-4: Stiffness values for the four fender models

The larger height indicates the larger compression displacement the fenders are capable of withstanding. When the distance is larger than the turning point, a higher stiffness K2 will apply, representing a hard contact between the fully compressed material with the spool. The stiffness K1 and K2 for the bilinear stiffness and corresponding damping coefficients (B1 and B2) for the four fender models are given in Table 4-3.

Table 4-3: Fender model specifications

Fender Models	**Stiffness [kN/m]**		**Damping Coefficient [Ns/m]**	
	K1	*K2*	*B1*	*B2*
DeckFender	6000	150000	20000	60000
SoftFender1	324.4	30000	84000	60000
SoftFender2	1046.6	10000	7800	60000
SoftFender3	444.4	10000	4000	60000

4.4 Result and discussions

As discussed in the methodology to assess allowable sea states in Chapter 3.3, the first criterion is examined in this subchapter. The first criterion is used with the DeckFender model. After proper lift-off scenarios, the responses from the different fender models are discussed.

4.4.1 Proper lift-off scenarios

In practice, given the appropriate wave condition, the instant when the winch is activated to lift an object is usually determined by the crane operator on board. The decision is made by monitoring the critical responses in the real-time. In this case, the spool is rested on a transportation barge before being lifted. The critical response that influences the activation of the winch is the relative vertical motion between the crane hook and the corresponding location on the deck of the barge[2]. The ideal period to start the winch of the crane is when this relative vertical motion starts to increase.

Unlike the real operation, in the numerical simulation in SIMA-SIMO, a fixed time to start the winch is pre-defined. Due to the stochastic nature of irregular waves, this fixed time may not represent a favourable time instant for the lift-off for different wave realizations. Under the same sea state, if the winch is activated at an improper time instant for a given wave realization, the operation will be unsuccessful. On the other hand, if the winch is activated at a proper time when the relative motion increases, the operation may be successful without violating the operational criteria. Thus, those wave realizations with an improper winch activation instant should not be taken into consideration when assessing the allowable sea states.

According to the recommendation, the spool should be lifted from the deck of the barge when the vessel is rolling away from the transportation barge. This will increase the relative vertical motion between the crane tip and the deck of the barge and will consequently decrease the chance of re-hit of the spool after being lifted off. Thus, the proper lift-off scenario corresponds to the case when this relative motion increases while the lift-off initiates. Figure 4-5 shows the time histories of the responses of the lift-off system under two random wave realizations for the same sea state. The responses in the figure include the roll motion of the vessel, the relative motion between the crane tip and the barge, the impact force on Port-forward and Starboard-aft fenders, and the tensions in S1, and S2 slings. The winch is activated at 55 s. As shown, Figure 4-5 (a) displays the proper lift-off scenario, where the roll motion and the relative vertical motion keep increasing from lift-off starts and the increase lasts for Δt of 1 s. On the other hand, these motions start to decrease right after the lift-off instant in Figure 4-5 (b), representing an improper lift-off scenario.

Because of the improper lift-off instant, re-hit occurs many times afterwards during lift-off operation with a higher tension in the slings compared to those in Figure 4-5 (a). Based on this comparison, we define the proper lift-off scenario as the cases where the relative vertical motion between the crane tip and the deck of the barge keeps increasing between 55-56 s in the response time history. Therefore, during the time-domain simulations in SIMA-SIMO, 100 stochastic wave realizations are simulated for each Hs and Tp combination using different seed numbers. Among these 100 seeds, only the proper lift-off scenarios based on the above requirement are used to

assess the allowable sea states. The purpose of this selection is to accurately represent the judgement from the crane operator onboard during the real operation.

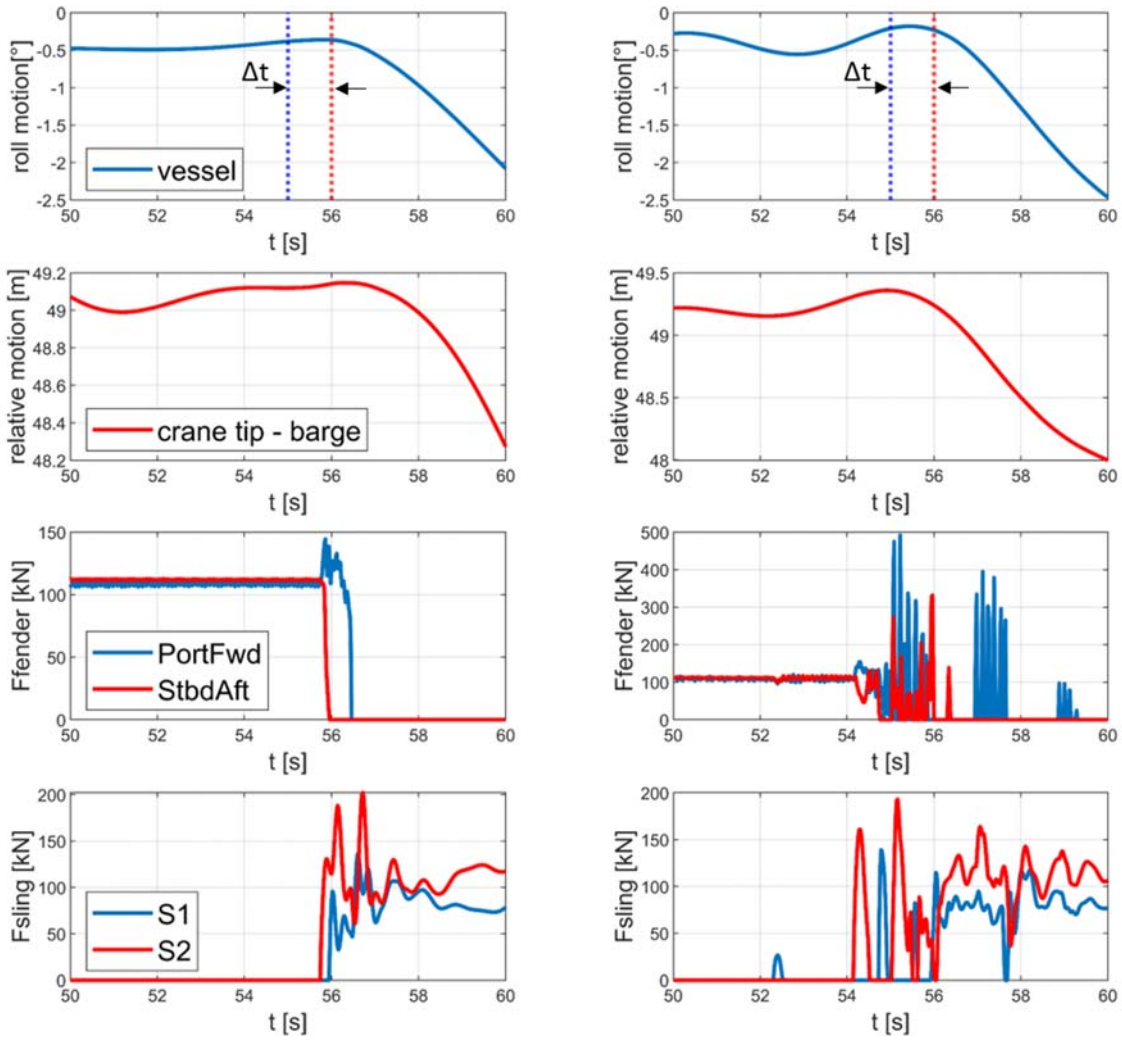

(a) The proper scenario for the lift-off (b) The improper scenario for the lift-off

Figure 4-5: Comparison of scenarios

Therefore, one hundred wave seeds are simulated for each Hs and Tp to show the effect of the first criterion. The wave seeds which is compatible with this criterion are named proper seeds. Figure 4-6 shows the proper seed numbers for a different Hs in a particular Tp. The proper seed number ranges between 20 and 38 out of 100 seeds. For example, there are 39 proper seeds which

are considered further for the operational limits in the environmental conditions that Hs is 1.4m and Tp is 10s.

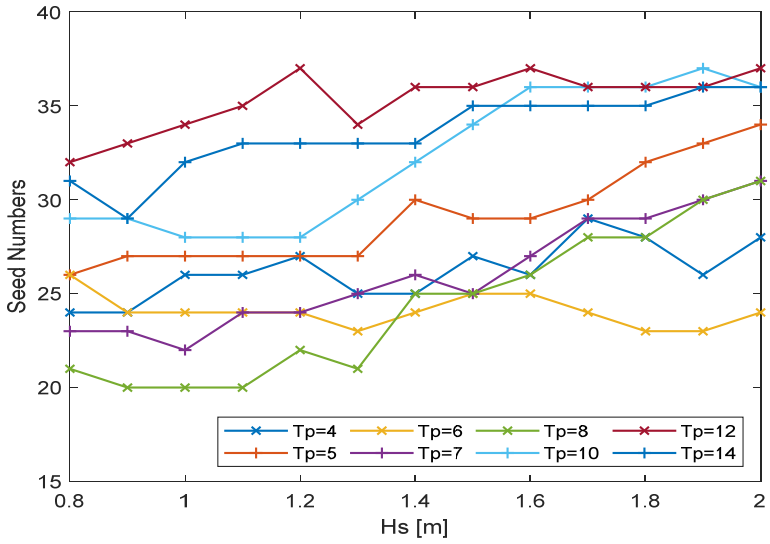

Figure 4-6: Proper seed numbers for the evaluation method

Figure 4-7 shows a preliminary comparison of the operational criteria used after the proper seeds. The same environmental conditions are used in Figure 4-6.

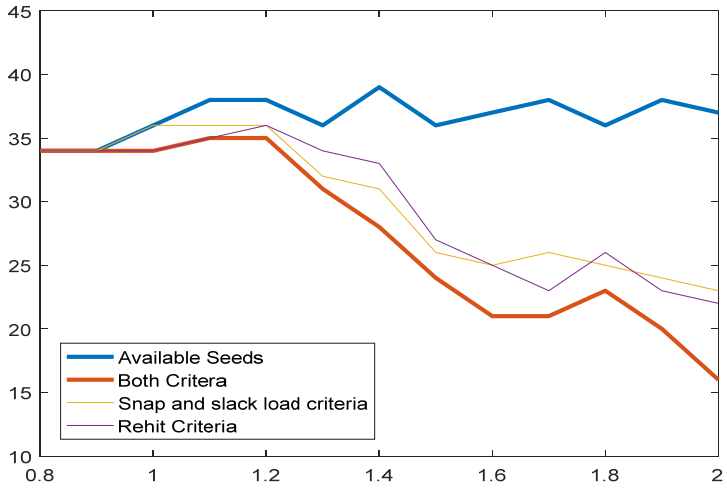

Figure 4-7: Seed evaluation plot for Tp=10s

The orange plot shows both criteria are in use for the proper seeds while the yellow plot shows safe seeds with the snap and slack loads on the slings. Furthermore, the purple one is safe seeds with only re-hit criterion. As shown in the figure, the re-hit criterion is dominant in assessing the proper seeds of the lift-off simulation. The seeds and processed seeds are shown in the below Figure 4-8 for two different Tp's.

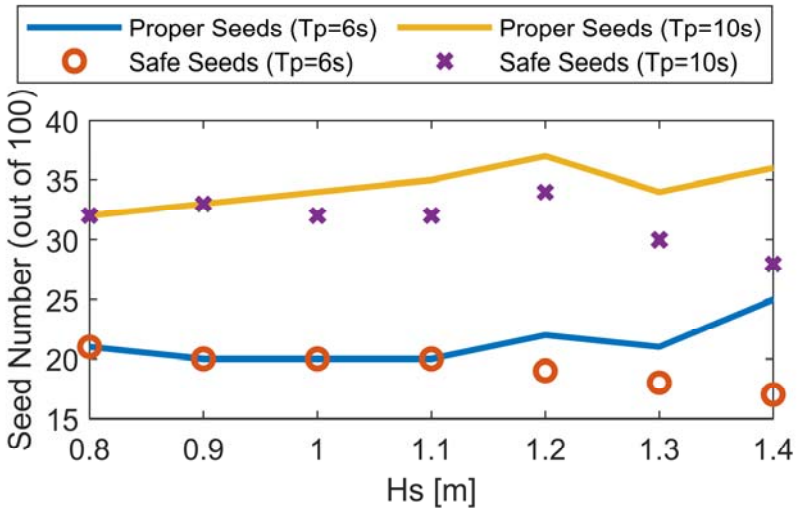

Figure 4-8: Proper and safe seed seeds numbers

As mentioned, 100 wave seeds are used for each simulation. Figure 4-8 shows the numbers of the proper seeds and 'safe seeds' extracted from the simulations using 100 wave seeds for two conditions. DeckFender model is used in this figure. It can be observed that the proper seed numbers are different for the two Tp conditions, and higher numbers are obtained for Tp = 10 s compared to Tp = 6 s. Because of the stochastic nature of the irregular waves, among 100 seeds, more than half of the seeds are considered improper seeds for the chosen examples. In Figure 4-8, when Hs = 1.2 m and Tp = 10 s, the numerical simulations provide 37 seeds with proper winch activation time, and among them, 34 seeds provide a safe lift-off operation by fulfilling all the criteria. So, the number of 'safe seeds' are higher than the 90% of the number of the proper seeds. Thus, this sea state is considered allowable to carry out the operation. It is also clear that with increasing Hs, the ratio between the safe seeds and the proper seeds are decreasing, indicating the decreasing success rate of the operation due to increased risk to violate the operational criteria. For

example, for Tp = 10 s and Hs = 1.4 m, and the ratio between the number of safe seed and the proper seed is 67%. Consequently, the failure of the operation under this condition is as high as 33%, and the sea state is not allowable.

4.4.2 Responses using different fender models

In the numerical model, fender characteristics are defined in terms of stiffness and damping coefficients. The re-hit force on the fender point causes compressions on the fender body, and the corresponding re-hit force is calculated based on the inputs such as stiffness and damping coefficients (see Figure 4-4 and Table 4-3). The re-hit force results in the reaction force to the spool structure. In Figure 5, the fender forces acting on the PortFwd fender point using four fender models are compared under the same condition with Hs = 1.6 m and Tp = 6 s together with the vessel roll motion, the spool roll motion, and the relative vertical motion between the crane tip and the barge. The same seed is used for all the four fender models. From the time histories of the fender forces, unfavourable re-hit forces on the fender point are observed using all fender models under this condition. The lowest force occurs using the SoftFender1 model, followed by SoftFender3 and SoftFender2.

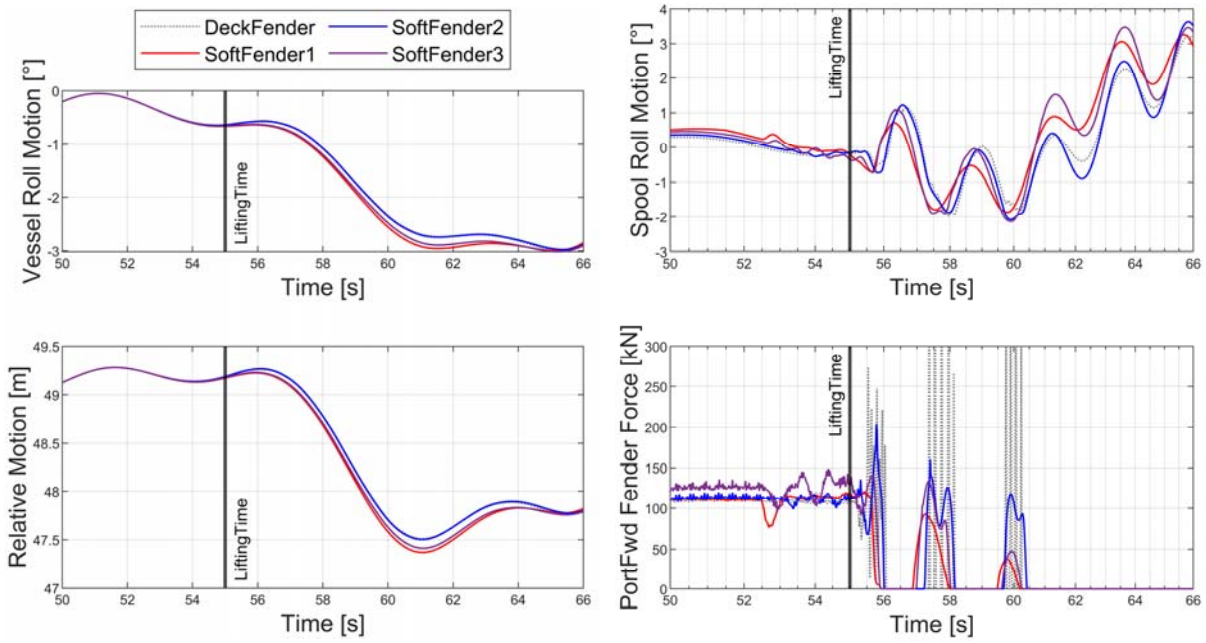

Figure 4-9: Forces on Port fender point

The higher damping behaviour of the material in SofterFender1 dissipates the impact energy between the spool and the transportation barge, and this leads to lower fender force. The re-hit force is highest using the DeckFender due to the high stiffness and low damping of the steel to steel contact model. Based on this fact, by using SoftFender1 model, the lifting operation can be conducted in the sea states where the forces using other fender models may exceed the required re-hit criterion.

Although the fender forces are significantly different using the four fenders, the differences in the global responses of the lifting system are minor. As shown in Figure 4-9, the vessel roll motion and the relative vertical displacement between the crane tip and the barge follow the same trend using the four fenders and the differences are relatively small. This is because the duration of the impact force on the fenders is too short to cause large changes in the global responses of the vessel and the barge. On the other hand, the influences of the fender models on the spool roll motions are more visible. As shown in Figure 4-9, the roll motion of the spool changes rapidly with the impact forces and the differences of the instantaneous roll motions are visible using different fender models.

During lift-off, the system experience lots of non-linearities with interactions between different structures in the system. The re-hit forces from the fenders can introduce rotation motions of the spool in different directions. Because of the large horizontal dimension and the low mass of the spool structure, a small re-hit force on the fender may create a noticeable rotation at the fender point locations. Correspondingly, the rotational motions of the spool will also cause high re-hit forces on the fenders located far away from the spool CoG. The spool roll motion can large vertical relative displacement at the fenders located away from the spool CoG in the Y direction, causing higher re-hit forces at the PortFwd Fender. As shown in Figure 4-9, the peaks of the spool roll motions in the time history coincide with the re-hit forces occurred at the PortFwd fender after lift-off. For example, the roll declines rapidly from 1 deg to -2 deg between 56.5 s to 57.5 s, causing a 0.62 m vertical displacement at the spool point moving towards the PortFwd Fender. This transition in a short time leads to a high velocity, and consequently, high impact forces occur between 57 s to 58 s. Due to these re-hit forces, the spool becomes less stable and roll motion increases to around 4 deg in the following few seconds. Similarly, if the pitch motion is dominant,

the high re-hit forces may occur on the MidFwd fender, which is located away from the spool CoG in the X-direction. However, because of the high non-linearities involved in a short time, it is difficult to predict the relative motions between the spool and the barge, and the dominant fender points. Thus, many wave seeds are needed in the time-domain simulations for one sea state, and all the fender points should be considered when assessing the operational criteria.

By using the same wave realization as in Figure 4-9, the maximum re-hit forces experienced by various fender points during the whole lift-off operation are summarized in Table 4-4. The forces on StbdFwd and PortAft fender points are not shown in this table because no re-hit occurs on these two fender points. The spool has a three-dimensional shape, and there is a distance between the termination heads and the deck of the transportation barge when it is rested on the deck. These two fender points are placed on the spool body to observe extreme conditions if any re-hit occurs. As shown, the highest fender forces using different models occur at different fender locations. For example, for this condition, the highest force occurs at PortFwd using DeckFender, while it occurs at MidFwd using SoftFender1.

Table 4-4:Maximum forces occurred on fender points

Types	**PortFwd**	**MidFwd**	**MidAft**	**StbdAft**
DeckFender	575.55	195.31	469.60	114.57
SoftFender1	121.30	182.04	106.015	116.020
SoftFender2	204.37	158.96	117.73	112.15
SoftFender3	151.58	158.45	188.53	296.51

To further illustrate the forces at different fender points, Figure 6 presents the forces acting on different fender points. The results in Figure 6 are generated by using the same condition as shown in Figure 5. As expected, SoftFender1 results in lower impact forces between the spool and

the fender point for different locations of the fender points because of its comparatively higher damping capacity.

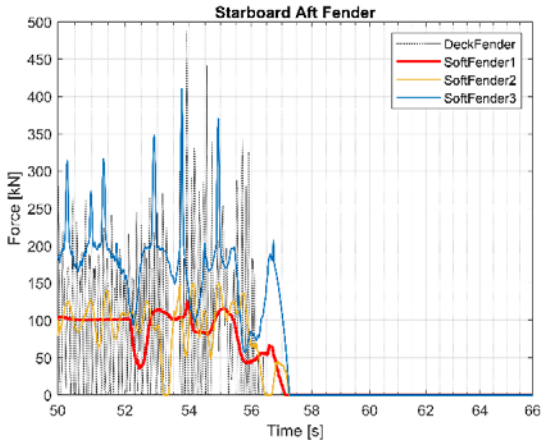

(a) Starboard Aft Fender

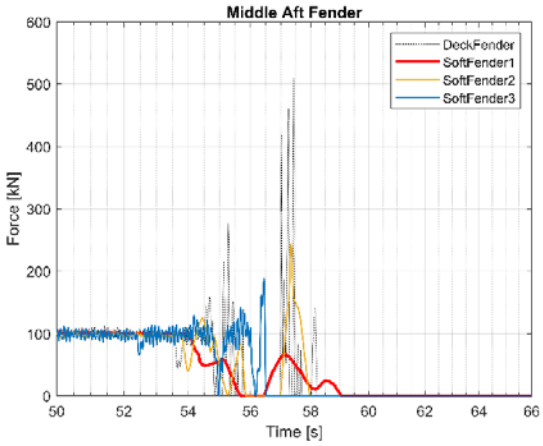

(b) Middle Aft Fender

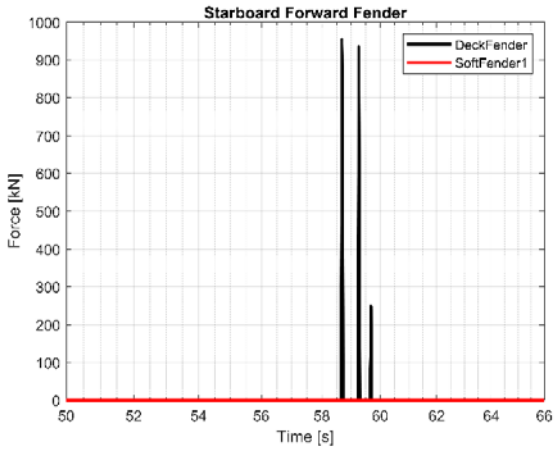

(c) Starboard Forward Fender*

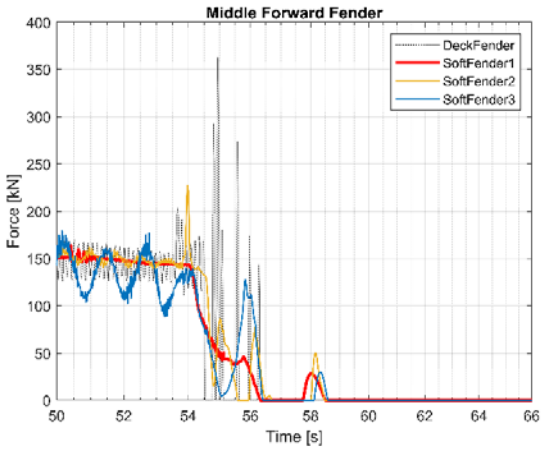

(d) Middle Forward Fender

Figure 4-10: Forces acting on other fender points

Despite the fact that StbdFwd has zero force on the fender point statically due to the structural shape of the spool, there is a possibility for a re-hit on the endpoints of the spool (starboard forward & port aft, terminations) during lift-off. For instance, it is shown in Figure 4-10 (c). Besides, these fender points provide relatively more conservative results for re-hit criterion.

In Figure 4-11, deck fender is used to present how Hs affects in a similar wave seed. After the lift-off, re-hit occurs at 61s for the case with Hs of 1.2m, and therefore, this seed is not counted as feasible for the lift-off operation.

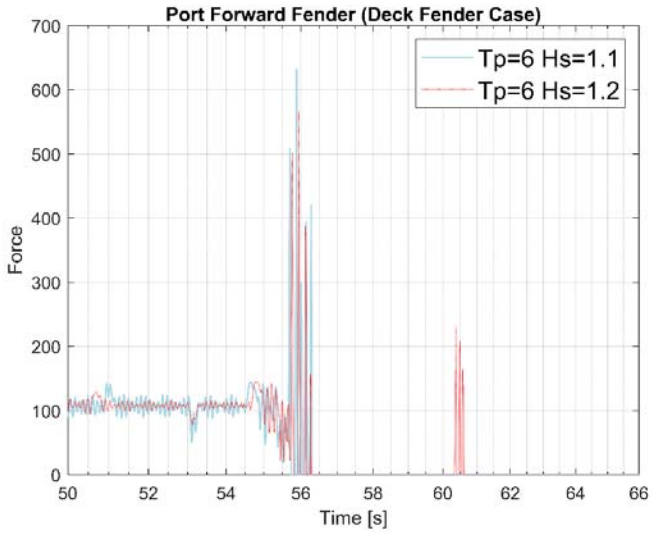

Figure 4-11: Port forward fender different Hs

4.4.3 Allowable sea states

Following the assessment procedure mentioned in Chapter 3.3, the allowable sea states for different Tp values using the four fender models is assessed, and results are presented in Figure *4-12*. As the lift-off operation is dominant by the re-hit criterion on the fenders, the numerical model using the DeckFender model always results in the lowest Hs values for all Tp conditions, due to its high stiffness and low damping feature. Softfender2 has the 2nd largest stiffness among the four models. When using Softfender2 model, the limiting Hs values for different Tp are on average 0.4 m higher than those using the DeckFender model. SoftFender3 model further improves the sea states for the lift-off operation with an average Hs value of 1.5 m. The best model in terms of allowable sea states based on the comparison is the SoftFender1 model because it has both a relatively low stiffness and a high damping coefficient among all the fender models. This fender model increases the Hs to an average of 2 m for Tp ranging from 4 s to 14 s. Thus, SoftFender1 model enables the lift-off operation to be conducted in relatively higher sea states than using the other models.

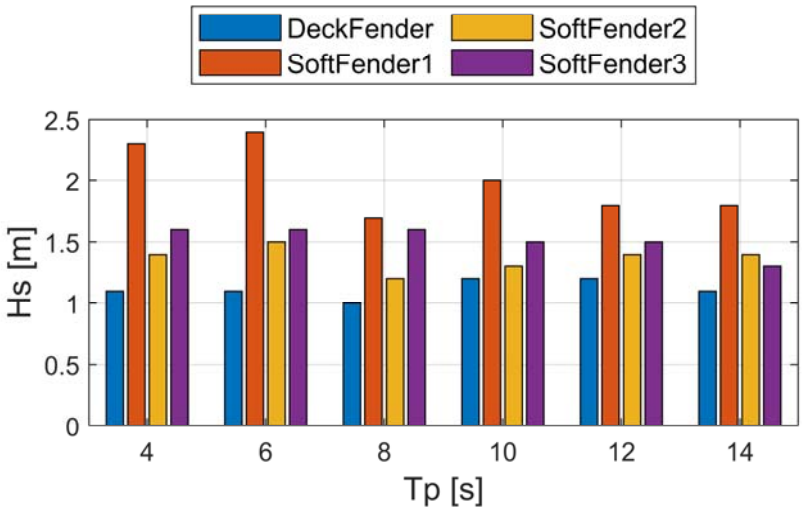

Figure 4-12: Comparison of fender models

Furthermore, the differences in the allowable sea states also indicate the potential differences in the operability for the operation. For example, when Tp = 6 s, the allowable Hs is highest using SoftFender1 with 2.6 m, but the values are below 1.5 m using DeckFender and Softfender2. In the North Sea, the wave conditions are dominant with peak periods between 5 s to 8 s. Thus, these differences in the allowable Hs values will greatly affect the operability. Therefore, by properly choosing the fender models, the allowable sea states, and the operability of critical lift-off operations can be significantly increased.

Chapter 5
Application and analysis of motion control system

5.1 Overview

The objective in this chapter is to create a winch control system to define the optimum instant for the subsea spool lift-off. Due to the large dimensions of the spool body, the lifting operation is susceptible to specific instants when the spool and the crane are in a favourable position. This relative vessel motion is evaluated for different wave seeds, which are mentioned earlier in Chapter 3. In this chapter, the winch control system is implemented in the time domain simulations to define the winch starting time. The effect of the approaches will be discussed and compared for different wave conditions of the lifting operation. The improved approach will be implemented in the motion control algorithms for SIMA-SIMO Model.

5.2 Lift-off criterion

In Chapter 3, the importance of choosing proper lift-off instant positive relative vertical motion between the crane tip and the barge is discussed. In the relative motion criterion used in the post process, increase in the distance between the crane tip and the barge is used as the first

criterion to define proper seeds which have the favourable motion at the start time of the winch. However, if there were no filtering method implied to wave seeds, the results are not so different. The results are shown in Table 5-1 for the DeckFender model. Since there is no filtering criterion applied, all seeds are considered as proper seeds, and evaluation method is applied to a hundred wave realizations to describe safe seeds for the results below.

Table 5-1: Allowable sea states for DeckFender (without criteria)

Tp [s]	4	5	7	8	10	12	14
Hs [m]	1.3	1.1	0.9	0.9	0.9	0.7	0.7
Safe Seeds	90	94	90	91	90	92	92

The allowable Hs for Tp in the range of 4s to 7s are increasing compared to the results achieved in Chapter 4.4.3 for DeckFender model, and Hs is decreased for higher peak periods. Although the increasing relative distance helps the winch with an additional heave motion on the crane tip to achieve higher sea states, it does not cover all the motions in the proper lift-off timing.

When the relative distance between crane tip and the barge is considered only in the Z-direction, an initial increment in this motion from the zero position (static position) leads to higher tension on the lifting wire and consequently higher acceleration on the spool body. Therefore, the spool lifts off from the deck faster than the same winch operation without roll motion. For instance, if the roll motion (+) of the lifting vessel favourably provokes crane tip with 0.2m/s in the positive z-direction, this motion together with the winch pulling speed of 0.2m/s up to 0.4m/s on the spool. Therefore, the spool will be lifted faster, and re-hit possibility will be lower. Nevertheless, the roll motion of the lifting vessel does not contribute to the crane tip motions also in the y-direction. The crane tip is rigidly connected to the lifting vessel; therefore, it alters the location of the crane tip position in y and z-direction. This shift in crane tip position might result in an unbalanced lifting of the spool where the spool is dragged on the deck in the y-direction at the lift-off instance.

Figure 5-1 shows lift-off instant where both vessel and the transportation barge are in the positive roll motion. The mapping colour is based on the time history of the lifting analysis. It is elaborated with the aim of a better understanding of the lifting instance.

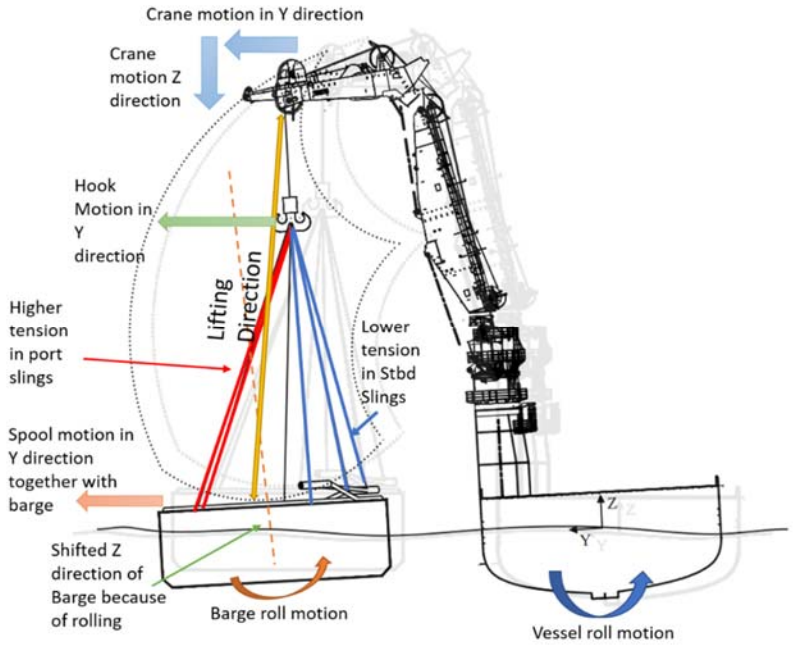

Figure 5-1: Lift-off instant when the lifting vessel and the transportation barge

The darker lines show the lifting vessel and the transportation barge after the negative roll motion while the lighter lines show the static (original) position. In this lifting operation shown in Figure 5-1, the facts listed below can be observed.

- Crane tip position moves in Y and Z direction
- Hook position moves in Y-direction until the slings tensioned reached to a specific limit.
- Higher tensions occur on port slings
- Lower tensions occur on the starboard slings
- Lifting directions is tilted.

As a result, it is observed that further consideration required to be implemented in winch control concept. Therefore, the misalignment criterion is introduced to the lift-off criteria. The relative distance criterion is discussed further in Chapter 5.4.3.

5.2.1 Misalignment criterion

In this criterion, the distance in the X and Y-direction between the crane tip and the transportation barge is the main criterion used for the evaluation. The evaluation relies on comparing actual distance in the time domain to the designed distance for the lifting model. This criterion aims to help the lift-off operation by dissipating the horizontal forces occurred due to misalignment of the crane tip with the subsea spool at the lift-off instance. Therefore, the spool will be lifted in more stable condition with less rotational motion. If the rotational motions of the spool body are reduced enough, the barge motions will be dominant for the re-hit case. The wave seeds are filtered out with misalignment criterion. The seeds are complied with this criterion are named as "aligned seeds". Two cases are defined for further explanation. The first case is using only the relative motion criterion, and the second case is using two of the lifting criteria. Although the sea state is allowable for the second case, the same sea state does not provide safe operating conditions for the first case. Furthermore, the second case is named as aligned seeds, and the crane tip motion is depicted in Figure 5-2.

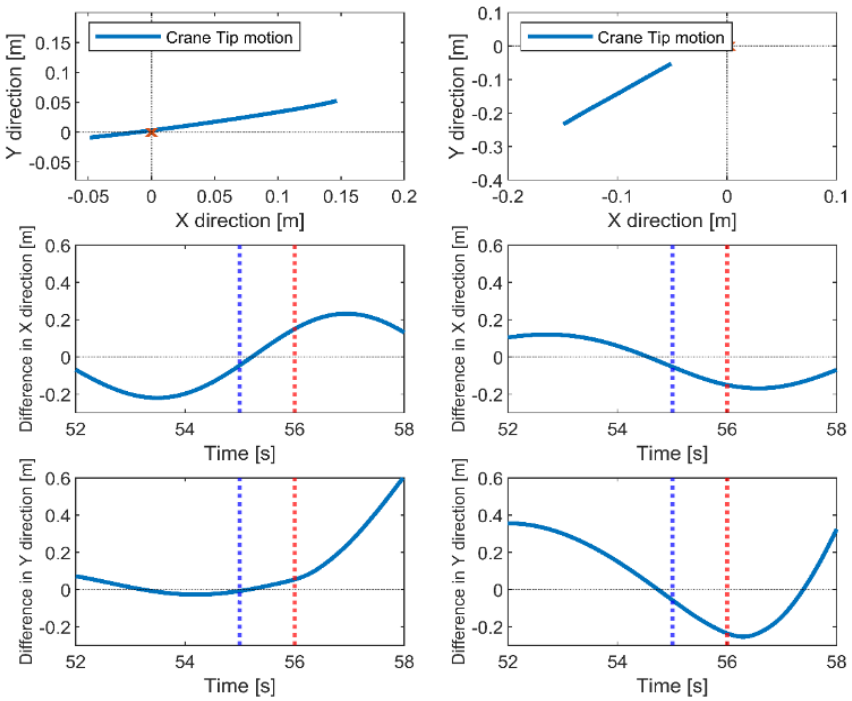

(a) Aligned seed (b) Misaligned scenario

Figure 5-2: Crane tip motions between in DeckFender model (Hs=1.1m Tp=8s)

In Figure 5-2, in the aligned case, the crane tip position in the limits of 0.1 m to its original position for 1s. However, in the misaligned scenario, the crane tip is located away from its designated position, which leads to an unbalanced motion of the spool. In Figure 5-3, two long time histories are shown to explain the directional motions in each directions respect to the winch start time. The crane tip shift from the designated position is shown in Figure 5-3.

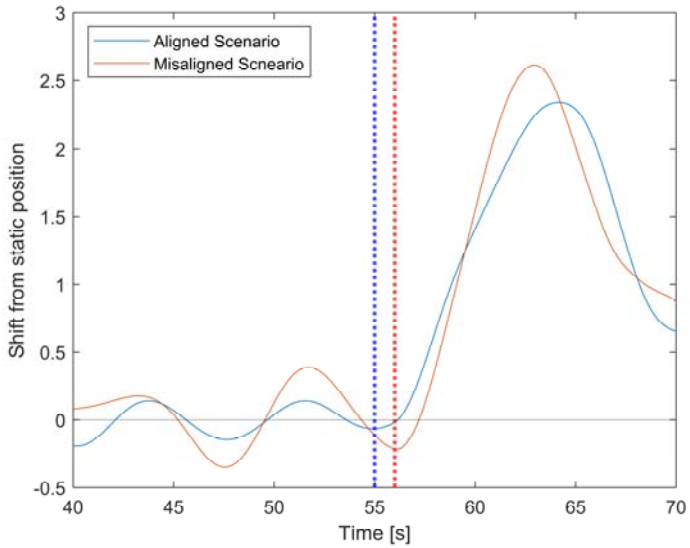

(a) X and Y-direction

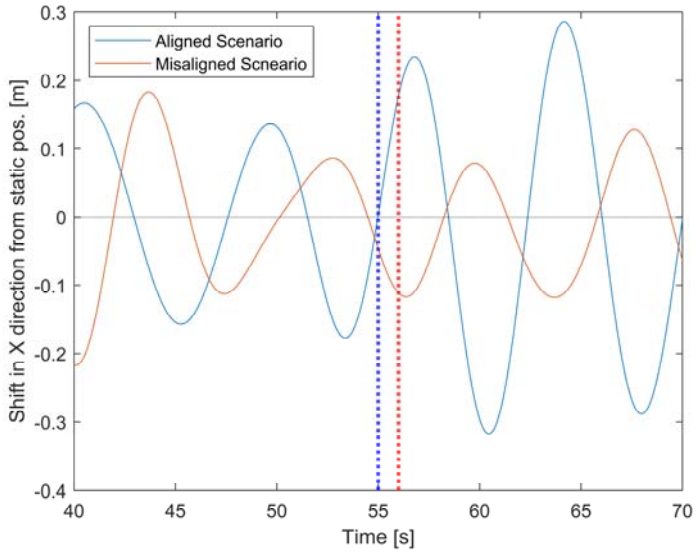

(b) X-direction

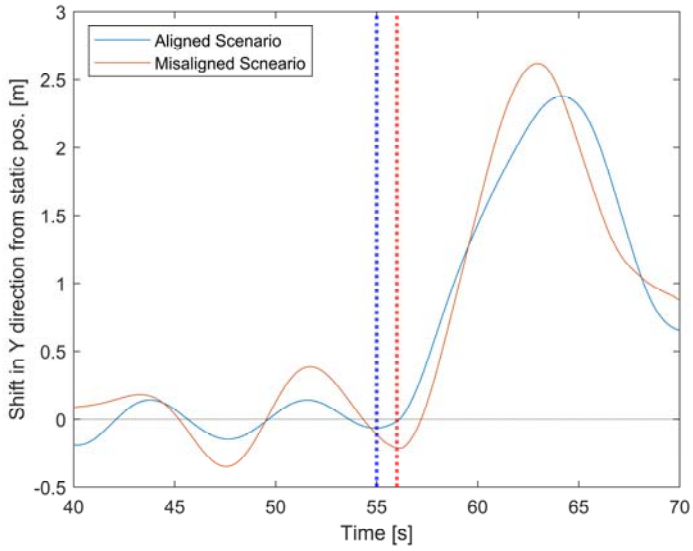

(c) Y-direction

Figure 5-3: Shift in crane tip position in DeckFender Model (Hs=1.1m, Tp=8s)

Based on these time histories depicted for the shift in crane tip motion, it is observed that the dominant contributor to the misalignment criterion is in the y-direction which is mainly triggered by the roll motion of the vessel. After the spool is lifted, the vessel is on the rolling motion towards transportation barge due to the moment in z-direction occurred during lifting. If the operation considered as statically stable to simplify the process, this rolling motion continues until the point that buoyancy force in the port side of the vessel multiplied by the distance to the vessel roll centre equals this moment. In dynamic analysis, the hydrodynamic loads involve in the stability of the operation and vary in each time step. This rolling of the vessel can be controlled by the ballast water operation on the starboard side; however, the lift-off operation completes in a maximum time of 15s. Therefore, the ballasting system operational capacity would not be enough to balance the lifting force occurring on the crane tip in the limited time.

In Figure 5-4, the operational effect of the alignment criterion is depicted. The misaligned scenario and aligned scenario follow the same trend in the relative motion and the vessel roll motion as its shown in Figure 5-4. The unique fact is the crane alignment to the transportation barge in each scenarios. The misalignment causes the unbalanced lifting in the sling couplings.

While the unbalanced lifting of the spool results in different tensions among the seven slings, it is seen that the high tension is in one sling S1 in the early phases of the lift-off. This high tension does not only affect its position but also increases the spool's roll and pitching motions where the next steps of the lifting operation are in more challenging condition.

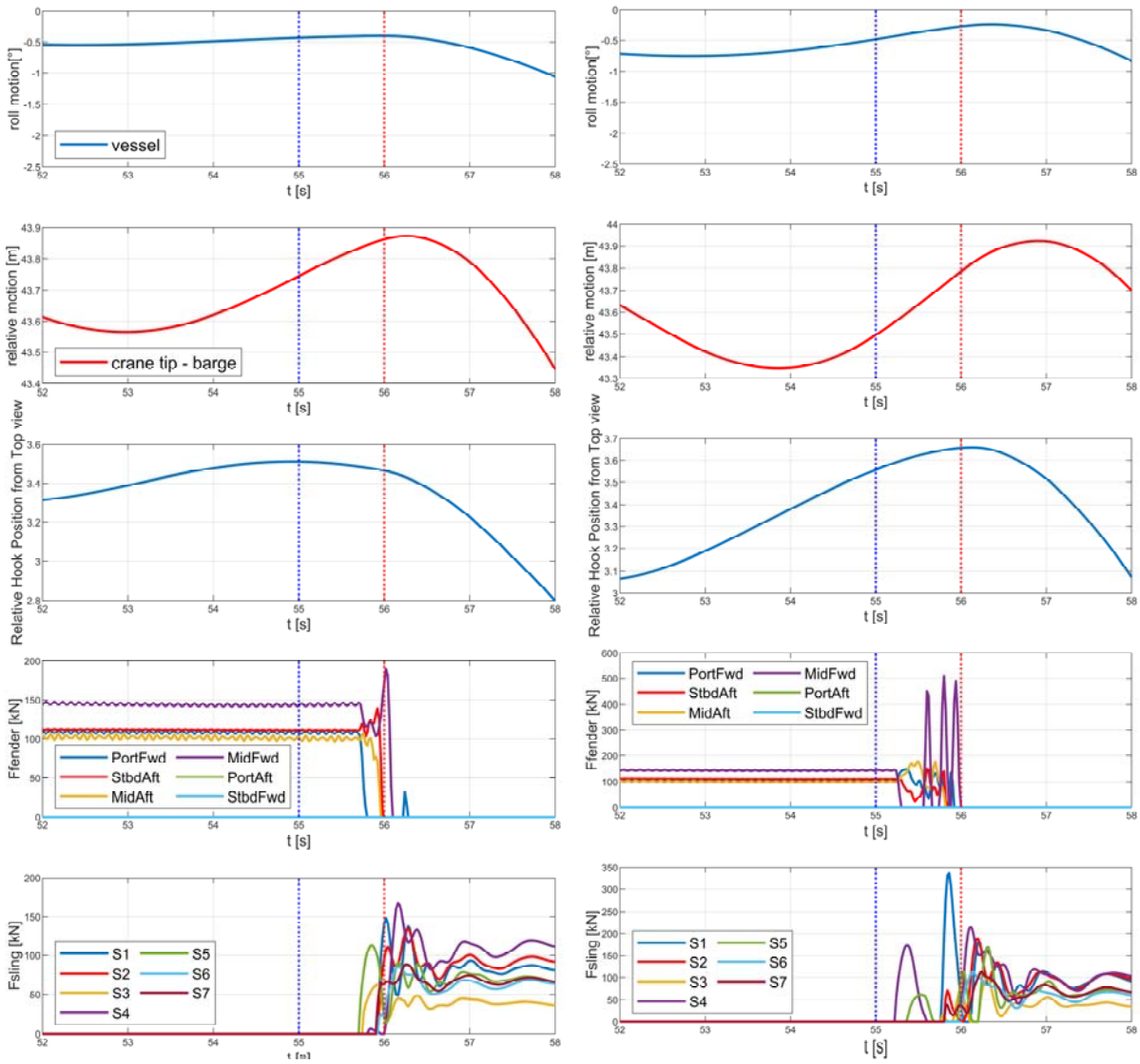

(a) Aligned scenario (b) Misaligned scenario

Figure 5-4: Misalignment scenario comparison in DeckFender model

In Figure 5-4, higher tensions are observed in S4 and S1 slings, which is the spool termination heads connected to each side. These sling connection points are supported respectively

with MidFwd and MidAft fender points on the deck. In the misaligned scenario, high impact forces are also observed on the MidFwd fender around 500 kN for three times.

Time histories of these sling S1 and S4, together with the crane tip position are shown in Figure 5-5.

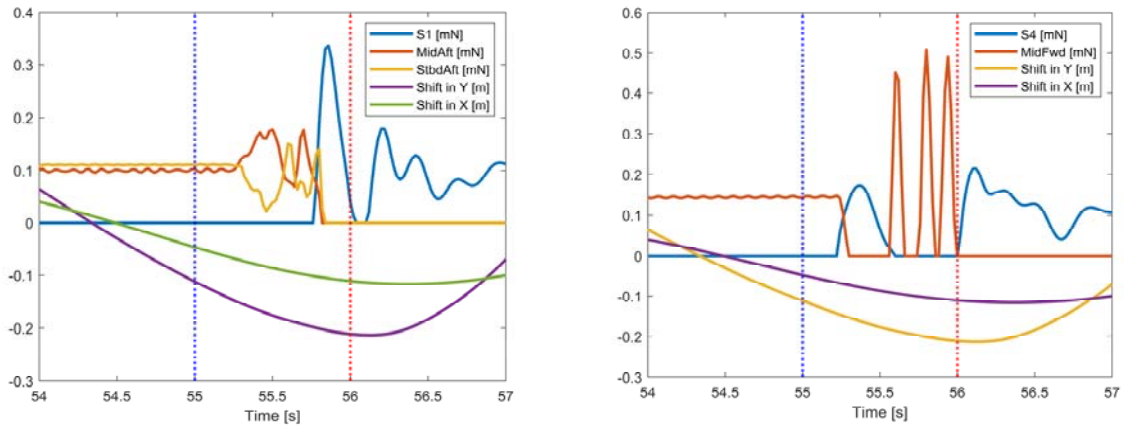

a. Sling S1 b. Sling S4

Figure 5-5: Sling and fender forces comparison in misaligned seed

In Figure 5-5, the shift in the crane tip position is shown together with sling forces and fender forces in the corresponding location. The units of the fender forces and sling tensions are in mN and shift in the crane tip position is in meter to combine them in one figure. Two plots going under the zero are the crane tip position in the misaligned scenario, which is the same in Figure 5-5 (a) and (b). It is observed that while the tension in the sling S4 is increasing, the fender force in MidFwd decreases. This instant can be illustrated as the starboard forward side of the spool is lifted before the rest of the spool body. As it is shown in Figure 5-5 (b), relatively higher fender forces occur in the MidAft and StbdAft fenders which are placed on the aft side of the spool. Related to the higher fender forces, the tension in the sling S1 reaches a higher magnitude as a result of the unbalanced lifting of the spool.

Misalignment Criterion Results

Post-process analysis is carried out with the misalignment criterion for the DeckFender model in order to define new allowable sea states. The criterion is based on an absolute distance between the crane tip and the barge. If the actual absolute distance in the time domain is higher than the designed distance, this condition is measured as a misaligned case. Therefore, the actual distance should be less than the designed distance to have the lift-off operation in a favourable state. The allowable sea states are shown below in Table 5-2. Although the significant wave height increases relative to the previous models, the confidence of these sea states is quite low since the seed numbers are lower than ten out of a hundred wave seeds. Thus, this criterion might be too strict for finding suitable instant in the lifting operation. Therefore, the lift-off criteria are evaluated in the appearance of favourable conditions in three hours of simulation in Chapter 5.2.2.

Table 5-2: Allowable sea states by using two criteria

Tp [s]	4	5	7	8	10	12	14
Hs [m]	1.8	1.3	1.1	1	1.5	1.6	1.7
Safe Seeds	8	10	9	7	12	15	7
Proper Seeds	8	11	10	7	13	15	7

5.2.2 Lift-off instant appearance

In Chapter 5.2.1, it is discussed that the lifting criterion can be updated to seek for more precise motions to start the lifting operation. However, precise motion criteria are not promising in terms of supporting allowable sea states with the number of seeds. It might conclude the post-processing analysis with higher sea state limits, on the other hand, not having enough confidence in making the scenario operational. Therefore, the lifting criteria are observed in the time-domain simulations. The objective is to find out possible suitable instance with these criteria in 3-hours.

The time-domain simulations consist of time steps of 0.01s that provide a smooth transition between the time steps. Therefore, there will not be a considerable difference between the values in each step. A suitable lift-off moment can appear at any time step, but the criteria should be valid for a second, which equals to 100-time steps. These appropriate moments will be called a lift-off moment in further explanations. The same method is used in this analysis with the evaluation of proper seeds explained in Chapter 3.3. The only difference is that evaluation continues throughout the whole simulation, and the result is in the ratio of lift-off moments to the length of the simulation. The same uncoupled model, which is designed for the re-hit probability calculation, is used to analyze lift-off moment in 3-hours. The subsea spool installation is a short term operation [1]; therefore, the maximum amount of 3 hours is enough to analyse the overall picture. The uncoupled model includes the lifting vessel, the transportation barge and lastly the spool placed on the barge. There is no coupling element modelled between bodies. The environmental condition ranges between 0.6m to 3m for Hs and 4s to 14s for Tp. There is only one seed representative of each sea states.

Firstly, the relative motion criterion has been tested for the lift-off moment. This criterion includes increasing motion between the crane tip and the barge. It has resulted in an average of 35.17% for all sea states. The detailed table for each Hs and Tp can be found in Appendix A. Secondly; the relative motion criterion is combined with the misalignment criterion. The misalignment criterion is used with 0.1m allowance. Since this criterion has a narrower window than the relative motion criterion, the average of lift-off moment results in a small average, such as 2.47%. A table for all Hs and Tp is shown in Appendix B. This criterion can be improved by defining an allowance limit to its position where the criterion dictates that the actual position should be in limits with the designed position to initiate the operation. Hence the average appearances are low in the previous criteria; this allowance limit (difference in the actual X and Y-direction from static X and Y-direction) is increased to 0.2m and then 0.5m. The average appearance is respectively 6.79% and 18.76% (Appendix C & Appendix D). While the effect of the crane tip position criterion decreases, the amount of appearance is increased. However, the allowable sea states are remarkably lower as it is shown in Table 5-3 and Table 5-4.

Table 5-3: Allowable sea states for misalignment criterion with the limit of 0.2m

Tp [s]	4	5	7	8	10	12	14
Hs [m]	1.1	1.4	0.8	1.3	1.2	1.2	1.1
Safe Seeds	22	18	22	18	19	15	8
Proper Seeds	23	20	24	20	21	16	8

Table 5-4: Allowable sea states for misalignment criterion with allowance limit of 0.5m

Tp [s]	4	5	7	8	10	12	14
Hs [m]	1.1	1	0.8	1	1.2	1	1.2
Safe Seeds	23	21	22	26	34	29	20
Proper Seeds	24	22	24	28	37	32	22

This criterion will be included in the definition of the suitable lift-off time in the motion control system with 0.5m allowance limit. The misalignment function works as only in the current time. Alternatively, it does not need any data from the past or future. On the other hand, the relative motion criterion entails the information of the future steps to check whether the relative distance increases or decreases for a second. Therefore, the estimation of future motions from the past data is required in the winch control algorithm.

5.3 Estimation of future motion

In the post-processing analysis, time-histories of the lifting operations are analyzed with the advantage of knowing the information of the future steps. Indeed, when the post-process is at a time step, the further steps are known; thus, the lift-off criteria can be applied easily to seek for suitable conditions. Besides, the lifting operation cannot be completed in a one-time step. Therefore the suitable motions for the lift-off criteria are influenced not only by the current step but also includes the essence of the future steps. Lift-off operation, coupled with a precise criterion improves the allowable sea states for the operation. In the real approach of lift-off analysis, the

knowledge is limited on the only present time. The decision of starting the operation is made by the knowledge earned until the present time. Therefore, the working method of the control system is similar to that is in real practice. The confidence comes from the estimation of future steps. With these facts in mind, the estimation of the future motion is required to define in the motion control system to satisfy the lifting criteria. Thus, the post-process analysis is used to define the optimum estimation method for the lift-off operation. The optimum method for the estimation is based on confidence in the estimations and process speed. Preliminary estimation method is briefly seeking for regular waves in the irregular wave, is defined and compared with two main estimation methods to evaluate success.

In this chapter, three different data estimation tools are studied in the post-process in the lift-off model. Data estimation tools are listed below.

- Preliminary Approach
- Machine Learning
- Markov Chains

5.3.1 Preliminary estimation method

In this approach, the symmetric response in the vessel motions is the thruster of this method. Indeed, this estimation method depends on the similarity between the lifting vessel's roll motion in the starboard and the port side. In the relative distance criteria, the dominant factor is the roll motion of the lifting vessel. That is why assumptions are mainly relying on the lifting vessel's roll motion. Although the waves are considered as a stochastic process, the vessel response against the hydrodynamic loads is a chaotic function addressed by stiffness and damping matrices. The chaotic function enables the vessel motion results in a smoother curve than the wave motions. For instance, these chaotic conditions can be visualized by a ship in heavy seas which follows less nonlinear motions than the waves. This concept helps most of the stabilizing systems, such as the pumping system for anti-rolling tanks based on accurately defined assumptions such as offsets and intervals [41]. Including the similarity in these motions, the estimation method can be specified in a preliminary way where the results may lead to a higher success rate.

This method starts with getting necessary insights in the relative distance between the crane tip and the transportation barge. Firstly, zero up crossing period of the relative motion is analyzed by taking the whole simulation into account. Alternatively, the zero up crossing period can be considered as a time window that includes only two turning points in the motion, which are a crest and a trough. The zero-up crossing period is also a representative input from the vessel's response to the environmental condition. So, this parameter will help the estimation method to estimate favourable lift-off moments to start the operation.

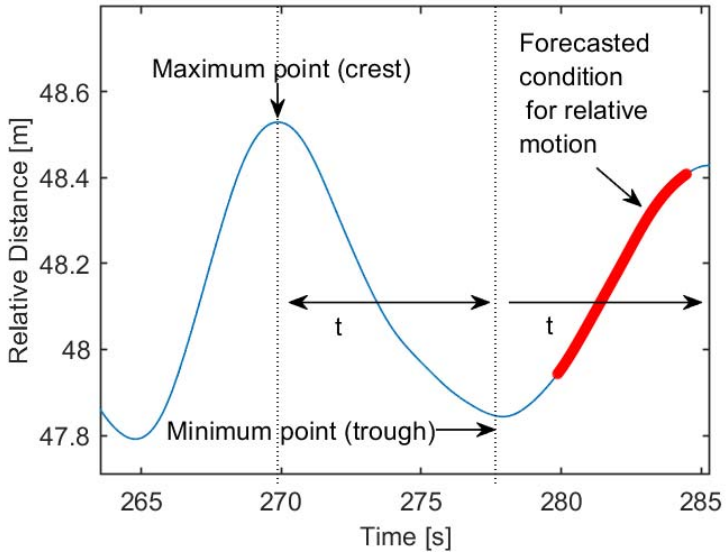

Figure 5-6: Preliminary estimation method description

After the zero up crossing period is found, the method for the estimation can be set. The procedure includes several steps. The first step is to find the crest point. Once there is a crest found in the relative motion time history, the relative motion would start decreasing. However, it is a stochastic process, and this decrement could be for a shorter time or a longer time. Therefore, this decreasing motion should be checked in a precise time criterion that will affects the motions after the trough. For instance, when the trough comes earlier than its calculated time in a regular waves theory, at that moment, the motions of the two vessels are induced by a higher frequency wave. Thus, these moments cannot be considered as a good lift-off instance, and these moments should be avoided because of the wave is highly unpredictable.

The method is defined in the following steps.

- Wave crest is found in the relative motion between the crane tip and the transportation barge.
- After crest, there should be a decreasing relative motion for a quarter of the zero up crossing period.
- If the previous criterion is satisfied, after the wave trough, increasing relative motion is expected for a second.

This method is tested in 3 hours of simulation in the range of Hs from 0.6m to 3m and Tp from 4s to 14s. The success rate for the estimation is found as an average of 95.60% for all sea states. The results for each environmental conditions are presented in Appendix E.

In conclusion, the preliminary estimation results as a sufficient and correct estimation for the relative motion. Due to lower CPU usage, it concludes in a shorter time. Since the objective is to find a suitable moment for increasing relative motion for one second, this method works sufficiently. However, this method will be compared to the other well-known methods to see the difference.

5.3.2 Deep learning method

Deep learning method includes the learning period from the past data and uses the network knowledge to estimate the future motions. The central process depends on the networking system. The networking system is defined by learning the relationship of values along the time in the past. Alternatively, the relations create an algorithm which is called as the network. This algorithm is the rule to estimate the future steps in our analysis. The network type used for time series is long-short term memory where the data in the current step is analyzed together with entire sequences of the data [42].

Deep learning method starts after the clutch time. The training data is the past data used to teach the network. The training data is chosen as 20s between 40s to 60s. In this phase, the adaptive moment estimation method (ADAM) performs network training with 150 iterations. "Adam" has an optimized algorithm for stochastic gradients to train deep learning networks. It uses the root

mean square properties and optimized learning rate by "AdaGrad" [42]. Therefore, the process can handle noisy time histories toward to future node estimation at the optimized speed.

In this DeckModel, data in the only one wave seed is examined. High-frequency model is taken into consideration with a peak period of 4 seconds with 1.1m Hs. Thus, in a small period of training, the training is relatively more accessible since there are more waves available in a short time. The relative motion between the crane tip and the transportation deck is used from 40 seconds to 60 seconds. This data is plotted in Figure 5-7. The x-axis is arranged in a time intervals of 0.02 seconds when the origin at X-axis shows 40 s, and the 1000th step corresponds to 60s.

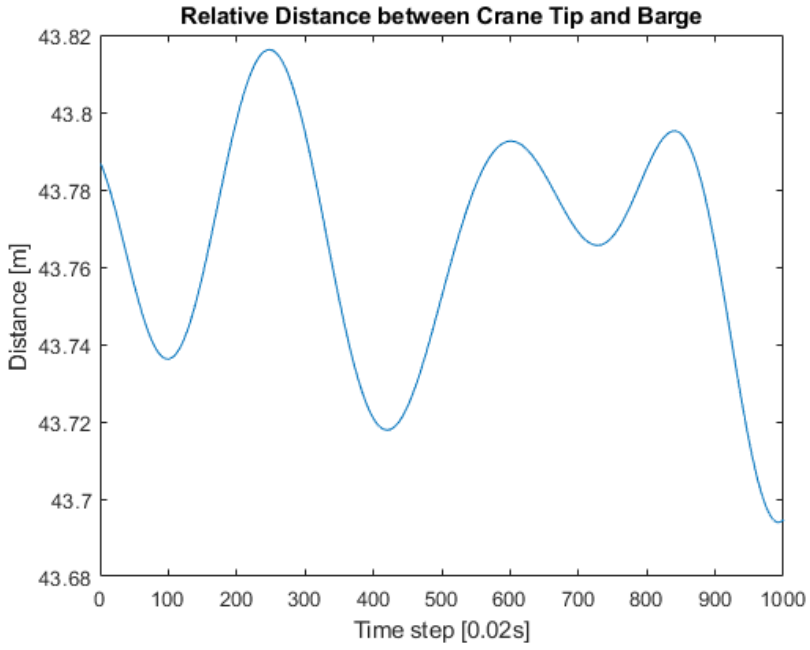

Figure 5-7: Actual data from relative motion from the 40s to 60s (Hs=0.6m, Tp=4s)

Furthermore, in this 20 s of data, the first 19 s are used the train network with 150 iterations. This network is used to estimate the next 1 second (50-time steps). Predicted motion for 1s is plotted in Figure 5-8.

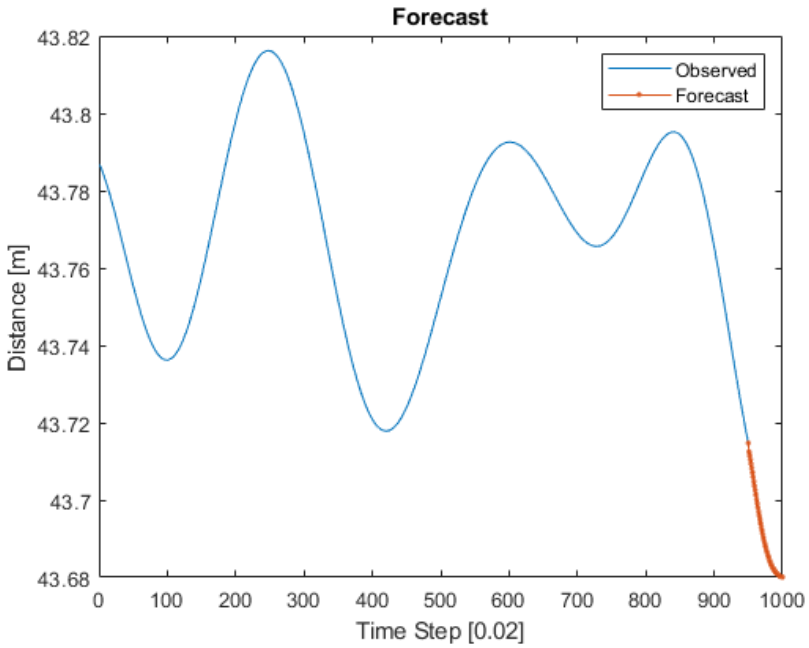

Figure 5-8: Observed data and forecasted data

In a detailed comparison between the forecasted and actual data, it is seen that the turning point in the relative motion is not similar. Nevertheless, it is a successful estimation when it comes to predicting the condition of the relative motion in the way of increasing or decreasing. In Figure 5-9, the close look at the observed and forecasted data is plotted for 1 second, which is equal to 50-time steps. Further, as a result of the trained data; the error increases as in Root Mean Square Error (RMSE). The manipulation in the lifting vessel's motion triggers this error having more discrepancy from the actual values by the time. This manipulation is induced by the tensioning of the lift-wire. The weight of the subsea spool is transferred to the lift wire, and this weight is acting in the negative z-direction at the crane tip. This force affects the lifting vessel to roll on the barge side where relative distance criterion reduces. Since there was no effect of winch work involved in the training data, the deep network does not have any knowledge before lift-off is started. Alternatively, there is no defined algorithm to describe this manipulation. Therefore, while the winch disrupts the vessel motions, the error will be increased by using this method.

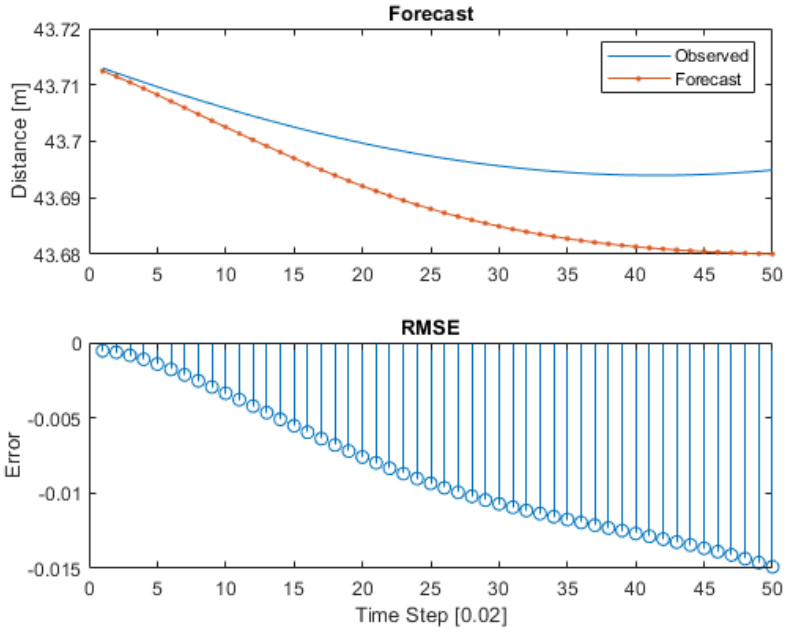

Figure 5-9: Comparision of observed and forecast data

On the other hand, this method allows us to have the foreseen motion of the two vessels , and it is estimated with the average error of 0.02%. This method is tested for the continuous learning of the deep learning method. With the purpose of having a signal processing of the future motions, this method is applied continuously to each step in a second to estimate a further 1 second. So in total, two seconds will be estimated continuously using this method. The table with errors can be found in Appendix F.

However, it is a vast time-consuming approach when it comes to predicting further second and also it requires powerful hardware. For example, to predict further one second from the training of 19s long data, the whole process takes around 50s. If we consider a situation where we need to use it continuously until we found the favourable moment to carry out the operation, there would be a need for expensive hardware. Besides, if this method has to take in practice, each time step has 0.01s difference, so the method is required to complete the estimation before the next time step. The run signal can be sent to the winch to initiate the operation in the following time step. Above all, it concludes the estimation with lower errors for the further relative motions than the preliminary estimation method. However, the processing time is significantly higher. That is why

the preliminary estimation method has an advantage over the deep learning method in the motion control system.

5.3.3 Markov chain

As the last model for estimating the future coupled motions, Markov chains model is used. Markov chain has stationary transition probabilities for the conditional distributions [43]. Since the aim of this estimation is to find the relative motion's condition, the simplified Markov chain model is generated. The simplified model involves a probability matrix which only considers the distance between the crane tip and the transportation barge. For the probability matrix, 1 and 0 values are assigned for each condition in the relative distance. These conditions listed below are presented in Figure 5-10.

- An increment in relative motion is 1.
- A decrement in the relative motion is 0.
- Going from the decreasing motion to increasing motion is 1.
- Proceeding from the increasing motion to decreasing motion is 0.

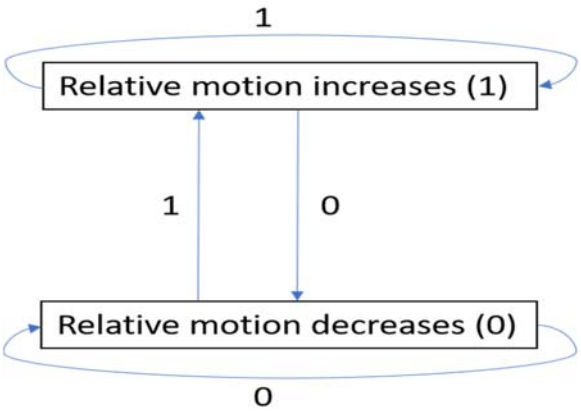

Figure 5-10: Markov chain model for the relative motion

Firstly, the probability matrix is based on past data. Indeed, the past data from the current step is used within two objectives.

- More extended past data used to define the zero up crossing period.
- Zero up crossing period before the current step is used to create a probability matrix in a way to define the intention of the relative motion for the next step.

In conclusion, the Markov chain approach gives us a correct prediction with the confidence of 51.40% for the one step further from the current step. Further, we have considered it for 1s, which equals to 50-time steps; the correction rate decreases remarkably. Therefore, regarding the stochastic process of the lifting operation, this method is not successful to estimate coupled motion for the future one second.

In a comparison of all the estimation methods, the Markov Chain estimation method processes the old data and gives the estimation in a short time, but the correctness is relatively low, especially for the further time steps. Among the estimation methods, the most effective one is the preliminary estimation method. Therefore, It concludes that the preliminary estimation will be used in the motion control system for the estimation of the relative motion.

5.4 Motion control system

Motion Control System (MCS) is the winch controller algorithm written in Java for the lifting operation, includes a motion estimation mechanism as well. MCS provides control over the two body motions to define the lifting operation in the desired moment. This system works on the two main parts;

- Generic External Control System
- Motion Control System Java Code

5.4.1 Generic external control system

MCS is working through a Generic External Control System with SIMA-SIMO software. Generic External Control System is an interface that transfers the data from the simulation to the MCS and receives the feedbacks for the winch control. This data includes the control parameters for the lifting operation and the measurements from the simulation. The measurements are a complete signal package of the couplings, as well as the bodies in position, direction, acceleration

and velocity. Besides, the control parameters for the lifting operation are sent to java code in the signal package.

The interface in the SIMA Software includes 3 sections as follows:

- Control system setup
- Feedback and measurement entities
- Control system parameters

Control system setup

The jar file includes the Motion Control Java Code and is merged to model from this section in the SIMA software. A jar file can include more than one class, and a class contains only one motion control algorithm. Therefore, there is also a class section in this part to select different cases from the same jar file.

Feedback and measurement entities

Measurements and feedback are signal packages transferred between SIMO and the Motion Control Java code in every time-step of the simulation. Since the MCS relies on object-oriented programming (OOP), the objects are chosen in the General External Control System interface. MCS Java code is executed for each object. Indeed, MCS Java code uses specifications of the objects, which are the bodies in this case for the measurements. Therefore, if a particular property needed in each step to calculate further with the lifting algorithm, this property should be taken from the object defined in the measurement entities. MCS is conditional to relative motion and, spool movements, so consequently, the lifting vessel, the transportation barge and the spool are selected in this field. If the object is not selected in Measurement Entities, no specification of that object is sent to the Java code. By contrast, after the java code is executed based on the values taken as measurements, the resulting signal is sent to the winches defined in the feedback entities section. The feedback signal is not only capable of controlling one winch; there might be more winches for tugger lines or cranes in the model. So, all these winches operate efficiently using by

checking the motions of the lifted object. In this model, there is one winch for the main crane, and hence, "winch1" is defined in the feedback entities.

Control System Parameters

Control system parameters are a set of parameters including integers, numbers and strings (words) that are passed to Java Code. These parameters provide easy modifications for sensitivity studies without editing the java code. All parameters are either user-defined values or constant values taken directly from the SIMA model.

Firstly, integer parameters are for time-sets in the lifting model due to the positions in the time-arrays are integer parameters. The integer parameter list is shown below.

- logInterval is for the logging interval for output of selected variables.
- logValues sets the initial time to log values.
- TensionTime alters the time to give tensioning speed feedback to the winch.
- MinTension is the minimum time required for tensioning the slings.
- MaxTension is the maximum time for tensioning the slings. This value takes a role in MCS if lifting speed criterion does not meet before the MaxTension time.
- LiftTime adjusts the lifting speed time. Thus, lifting speed can be sent to simulation before or after the specified moment.

In the interface, number parameters are in the name of "Real Parameters". These parameters could be referred to any values in the initial of the SIMA model. Accordingly, the crane tip and the transportation barge position in three directions are taken from the model to assess the dynamic values in the simulation. Notably, the tensioning and the lifting speeds are set in the Real Parameters section.

The string parameters are words needed to execute the Java code properly. The required words are related to the body names in the model and also the output file name. This word parameters help to call objects in the measurement entities in order to have measured values sent

in the Java code. Instead of the actual names of the bodies, these are called by the string parameters. Thus, any change in the naming of the bodies does not cause any error in the code.

5.4.2 Motion control system Java code

Motion control system (MCS) Java code is a signal processing code containing the estimation of the future steps for the vessel's motions. The primary purpose of MCS is to delineate the favourable moment for the lifting operation of the spool from the transportation barge. With this in mind, the future motion estimation and the lifting criteria are utilized in the Java code.

Constitutively, the structure of the java code ought to be compatible with the Generic External Control to execute the code successfully. Due to this reason, an interface called IController is provided by SINTEF in order to ensure compatibility[44]. It is added to the Eclipse program (Java editor) and implemented in the class description. IController builds three required methods in the class. These three methods are shown in the below list.

- The INIT-method
- The STEP-method
- The FINISH-method

These three methods are related to the dynamic simulation of SIMO so that each process can be interpreted by using the java code. Nevertheless, this interpretation should be in the limits of Generic External Control interface.

The INIT-method

The init method is the initial method in the MCS Java code. Before the dynamic mode, the init method is executed. Java code receives all the parameters in the Generic External Control System as well as properties of the dynamic mode such as the time-step. Similar to initial mode in SIMO, the init-method makes the java code ready to be executed together with dynamic mode.

The STEP-method

After the init-method, the step-method is executed at every time-step of the SIMO simulation. Indeed in every step of the dynamic mode, the current time, signal-measurements and

signal-feedbacks are passed between SIMO and the java code. The time value from the simulation is the hearth of the MCS Java code. This step-method iterates until the dynamic mode completes in the SIMO simulation.

The FINISH-method

The finish-method is the last executed part of the Java code. This method runs after the completion of the dynamic simulation in SIMA-SIMO software. This method only runs once at the end. The primary objective of this method is to close the logs and to carry out post-process of the SIMO model results. This method does not require any signal communication with the generic external control system. Therefore, the finish-method is an open section of the java code, so that any calculation for post-processing, statistical analysis or commands can be processed in the model. This method can be used to define the allowable sea states automatically for SIMA-SIMO models.

Algorithm and Functions

The Motion Control System Java code starts with introducing all the class variables used in all methods to the Java code. There are sixty class variables inserted in the java code. Those variables can be categorized in the below list.

- Integers are used for step timing.
- Double arrays with different dimensions are for data-storage.
- Double array with 1 row is for live-data such as current time checking and feedback.
- Boolean is for predefined if conditions.

After the variables are generated, Java code runs with the init-method. In the init-method, it calls all the controlling parameters from the SIMA software, time step as well as creates the log file in CSV format for the winch speed. In this init-method, calling parameter functions is reinforced with if-contains function. Accordingly, rather than hard-coding, any controller coefficient can be deactivated by crossing out just in the SIMA model.

The MCS Java code is capable of motion estimation and checking for the lift-off criteria. In order to have this feature in the decision algorithm; the following functions are built prior to the

step-method. Firstly, the preliminary estimation is taken into account for the estimation method in the control system. This estimation is based on the relative distance between the crane tip and the transportation barge. Thus, the relative distance function is constructed first. As mentioned before in the measurement entities, the transportation barge is a body in the SIMO model so actual positions can be passed to Java code. However, the crane tip is a rigid body point in the lifting vessel body. Then, the actual positions of the crane tip are calculated through the coordinate transformation from the lifting vessel's positions. The equation for the coordinate transformation is shown below.

$$x^{(G)} = \Delta x^{(B)} \qquad \text{Eq. 5-1}$$

where $x^{(G)}$ is the point in the global system, $x^{(B)}$ is the vector in the body system and Δ is the rotational matrix. Then, the rotational matrix is shown in the below equation.

$$\Delta = \begin{bmatrix} cos\psi cos\theta & -sin\psi cos\varphi + \cos\psi \sin\theta sin\varphi & sin\phi sin\psi + cos\psi sin\theta cos\phi \\ sin\psi cos\theta & cos\psi cos\phi + sin\psi sin\theta sin\phi & -cos\psi sin\phi + sin\psi sin\theta cos\phi \\ -sin\theta & cos\theta sin\phi & cos\theta cos\phi \end{bmatrix} \qquad \text{Eq. 5-2}$$

The T matrix is not in the 3x3 format as in Eq. 5-2. It is sent in array format, which is 1x9 matrix as in the below equation. A key thing to remember, arrays in the java syntax starts from 0 so if T_{33} is called into the equation; it is in the name of T[8].

$$T = [T_{11}, T_{21}, T_{31}, T_{12}, T_{22}, T_{32}, T_{13}, T_{23}, T_{33}] \qquad \text{Eq. 5-3}$$

T matrix is called for the lifting vessel and coupled with the crane tip position in respect to the vessel body. The crane tip positions are passed to Java code in the init method as x_0, y_0, z_0. GetEntity is a method to call actual values in the dynamic simulation of the bodies listed in Measurement Entities. These arguments are in the scope of position, velocity, acceleration, force, and the rotational matrix. This method is used to get actual transportation barge and the lifting vessel positions. So, the current crane tip position in the z-direction is found from the below equation.

$$\text{cranetip.z} = \text{vesselposition}[2] + \text{T}[2] * \text{x0} + \text{T}[5] * \text{y0} + \text{T}[8] * \text{z0} \qquad \text{Eq. 5-4}$$

After the actual crane tip position is resulted, the actual barge position is subtracted from the crane tip position to find the relative distance, which is the return from this function. In addition to the relative distance criterion, the misalignment criterion is studied in the time-history analysis. Therefore, it is added as the second function before the step-method. In the misalignment criterion, the principle relies on the position of the crane tip and the transportation barge in x and y directions. This criterion analyzes the alignment in the X and Y-direction; in other words, an absolute difference in the X and Y- direction. The actual position of the transportation barge in x and y directions is called in with the GetEntity method. Similar to the relative distance function, the crane tip in the x and y direction is calculated together with the T matrix. The equations for crane tip in x and y directions are shown as follows.

$$\begin{aligned} \text{cranetip.x} &= \text{vesselposition}[0] + \text{T}[0] * \text{x0} + \text{T}[3] * \text{y0} + \text{T}[6] * \text{z0} \\ \text{cranetip.y} &= \text{vesselposition}[1] + \text{T}[1] * \text{x0} + \text{T}[4] * \text{y0} + \text{T}[7] * \text{z0} \end{aligned} \qquad \text{Eq. 5-5}$$

Hence, positions of the transportation barge and the crane tip in the X and Y-direction is found from the Pythagorean Theorem. This function returned as the difference between the crane tip position and the transportation barge position in X and Y-direction.

The next step in the MCS Java code is the step-method. In the dynamic simulation of the SIMO model, there should be only one lifting operation. So, the step-method starts with If-statement conditional to lift criteria (Boolean) equal to false. Since the lifting operation is irreversible, the winch ought to run once and continues until the lift-off operation completes. When the feedback signal returns to the SIMO as the lifting speed at the last step of the lifting operation, this if-statement will be true, and the motion of the vessels will not be evaluated anymore to find a suitable time window to run the winch.

In the first step (t=0), the results of the static mode can be found. So, the misalignment function's static condition is taken to compare the alignment in the further steps. The misalignment criterion would be demanding the values only in the current signal time. The difference will be checked with the values in the static model. Besides, the MCS Java code starts to insert zero values in the corresponding columns in the feedback arrays. Following twenty seconds is the clutch time of the dynamic simulation. Therefore, these two thousand steps are ignored by the MCS.

The next step in the MCS Java code is to obtain insights from the environmental conditions. This step is named the insight interval and longs for two thousand steps in the simulation after the clutch time. The most significant insight is the period between the crest and the trough in the relative distance function. Therefore, MCS Java code retrieves time-steps of the troughs and the crests by looking for turning points of the relative motion in this interval. These retrieved time-steps are written in separate two arrays. As a result, two new arrays are generated respectively with the trough time steps and the crests time steps. These arrays do include not only the time steps but also zero values for the steps which do not indicate a turning point. The calculation of the period between the crest and the trough is held in the one-step after the insight interval. In this step, firstly, zeros are taken out from the arrays. Then, the new modified arrays are deducted from each other and placed in "the result array" as a positive value always. The last step in order to find the period is the sum of the result array divided by the length of the result array. In conclusion, the insight into the period between the crest and the trough is available in the following steps.

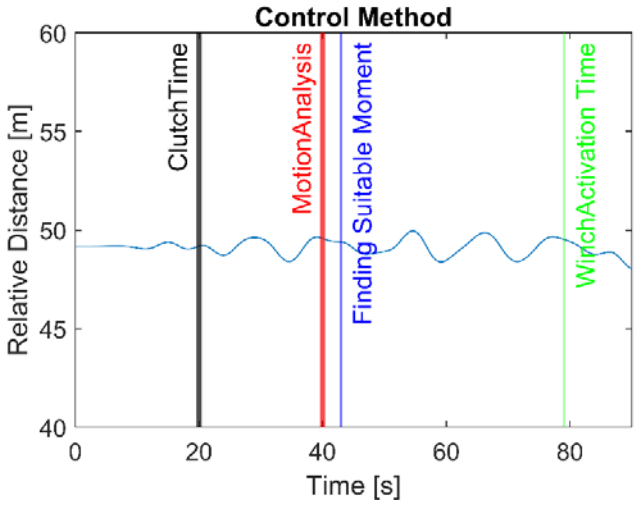

Figure 5-11: The MCS methodology intervals

Afterwards, the lifting criteria began to check the motions of the lifting vessel and the transportation barge. As mentioned before, MCS is a live process with dynamic simulation. Therefore, the lifting criteria are checked in the current and the past steps, unlike the time-history analysis. After motion analysis completes, the required calculations are conducted for 3-time steps to use in lift-off criteria. After the time step of 4003 (40,03s), the misalignment function begins to collect data into a double array with 1 row, and the winch speed is logged in an external file. The

argument of the lifting criteria starts with finding the crest before the current step. The crest should be in a fixed time before the current step. This time is formed with the period attained in the previous steps. Indeed, it is described in half of the period plus the tension time input from the SIMO-SIMA model. In this time interval, the relative motion ought always to be decreasing. Furthermore, the same method is also applied before the crest in the relative motion. The interval is half of the period is checked before the crest. The relative motion in this interval ought always to be increasing. So, it can be assumed that there is a noise-free and less non-linear relative motion where the relative motion does not alter in short times. Moreover, if the result of misalignment function is in the limits with the misalignment calculated in the first step, the tensioning speed of 0.2 m is sent back to simulation. The misalignment limit and the tensioning speed also can be changed directly from the SIMA-SIMO model. The tensioning speed is sent back to SIMA at least for minimum tensioning time. Furthermore, in the interval of the minimum and the maximum tensioning time, the lifting criteria are checked for the preliminary estimation where the current step is found as increasing for the next 1 second. Thus, if the preliminary estimation is carried out for the current step, the winch speed increases to lifting speed of 0.5m. If the current step condition does not satisfy the lifting criterion, the maximum tensioning time is taken in the control method and runs the winch with the lifting speed. The preliminary estimated time can be shifted forward or backwards by using the lifting time parameter in the Generic External Control System. The MCS sends the lifting speed to SIMA for ten seconds or until the spool body reaches up to eleven meters in the z-direction. At the last feedback signal, the lift criteria (Boolean) is turned to be true; after the operation completes, the feedback signal can not be sent to SIMA for winch speed other than zero. The step method ends together with the dynamic simulation in SIMA. Figure 5-2 shows the general methodology of MCS algorithm.

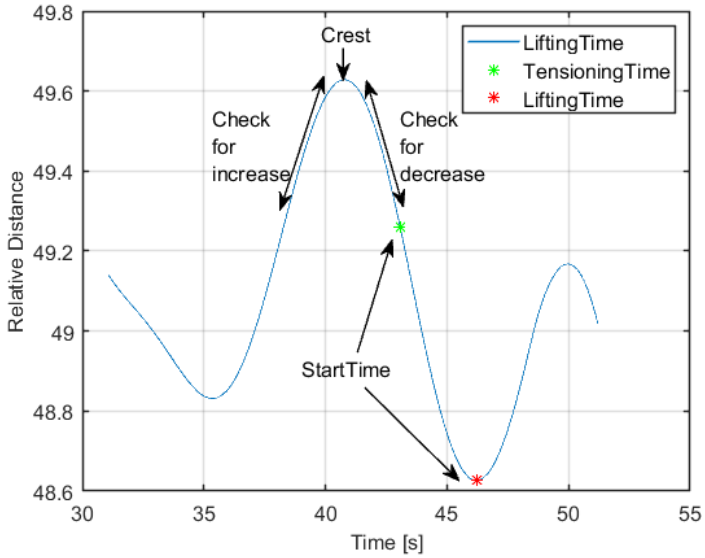

Figure 5-12: The MCS algorithm for the feedback signal

The finish-method is executed after the step method. Since the post-processing is done by the Matlab, as mentioned in Chapter 3.3, the finish method is only used for closing the winch speed log. Moreover, the post-processing codes are updated with the functions to define the dynamic winch speed times and to start the analyses after this moment. These updates will be discussed in the following chapters.

5.4.3 Lift-off criteria study

The lift-off instant analysis has been conducted over the wave realizations in the post-processing phase in the numerical analysis. The whole objective is to define better operational timing to initiate the lift-off for the spool body from the transportation barge. These criteria are working as a filtering method of the whole seeds. Therefore, the number of remaining seeds labelled as proper seeds are relatively lower than the whole amount of wave realizations. Based on this reason, in the continuous process, the impact of these operational time criteria might not provide the whole picture of the objectives clearly. With this in mind, these timing criteria are applied in the MCS with the following objectives listed below.

- To check the impact of the operational criteria in the continuous motion monitoring systems.

- To see the consequences of more proper seeds in the evaluation of the allowable sea states.
- To see how the MCS can reflect the actual purpose of the decision methods on the launch of the operation.
- To evaluate the criteria mentioned in the lift-off analysis.

In light of the objectives, the relative motion criterion is applied in the MCS. This criterion involves the increment in the relative motion after the tensioning speed applies. Therefore, it requires an estimation of the following relative motion for the next second. The preliminary estimation method is used in this analysis.

Secondly, the alignment criterion is applied in the MCS algorithm. Based on this method, the crane tip and the transportation barge should be aligned with the statical position designed for the lifting operation in X and Y directions, that the rotational motions of the subsea spool can be minimized. These rotational motions are mostly triggered by the initial acceleration of the spool body. When the acceleration is not equal on each side, the spool experiences forces with a different magnitude. This condition leads to high degree rolls, and consequently, re-hits occur in the lift-off operation. This criterion is applied in the MCS. Unlike the relative motion criterion, this method does not need a further estimation of the motions. The current time step is compared with the static position in X and Y directions between the crane tip and the transportation barge.

The roll motion-defined with the relative distance criterion in this study is more dominant than the misalignment criterion since the transportation vessel is aligned to the lifting vessel on the port side. Lastly, the two criteria are applied to the MCS. The results have been shown in the figure below.

The DeckFender model is used in this sensitivity study with the edits in the MCS algorithm. The modifications include the decision criteria for starting the winch. The allowable sea states from the DeckFender model will be compared to these criteria to evaluate the methodology.

Although all these criteria are examined in the lift-off analysis in the post-processing section, a comparative figure will be presented between the scenarios using both criteria and only alignment criterion in order to show the criteria's effect in the MCS. The same seeds are used to

illustrate this figure in the environmental conditions of 6s Tp and 1m Hs. Due to the dynamic winch control system, the figures are plotted in the reference of tensioning time and lifting times. Therefore, y-axis does not represent the actual time but relative operational time to start time of the winch. As can be seen from the figure, the relative distance increases after the winch gears up to lifting speed in both criteria scenario while it stays stable and goes down in the scenario used for only misalignment criterion.

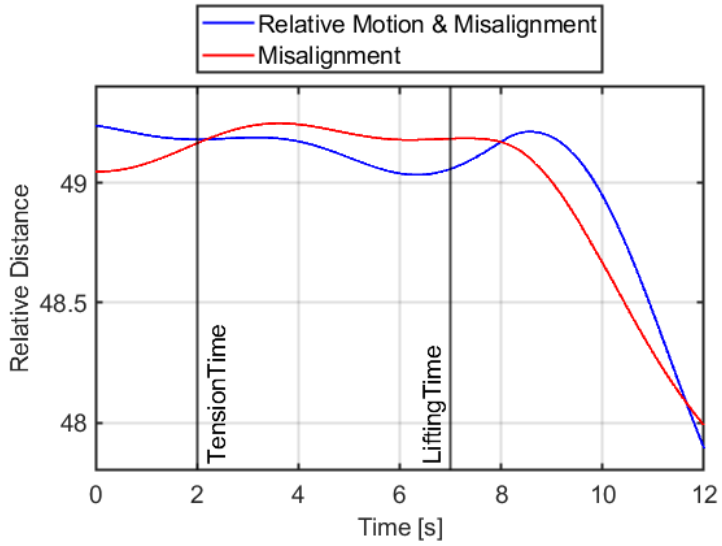

Figure 5-13: Comparison of relative distance for lift-off criteria

Figure 5-4 represents the forces that occurred in the coupling points in the scenarios described above. The misalignment scenario represents a not safe operation due to the re-hit forces occurred after the lifting time. This re-hit between the deck and the subsea spool causes high fluctuations in the sling tensions. However, on the other side, the scenario using both criteria results in safe operation. In this realization, there is no re-hit observed, and the load transaction is handled smoothly, where fewer oscillations observed in the tension figures.

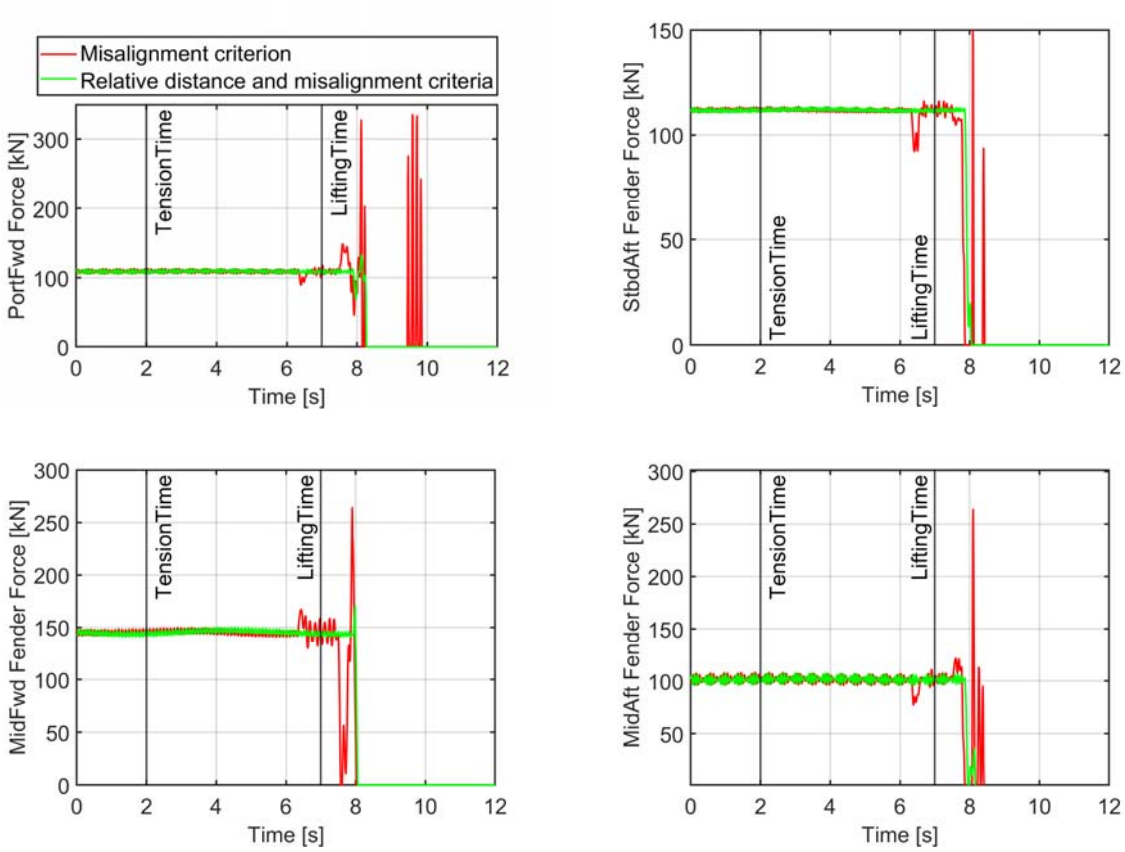

(a) Fender force

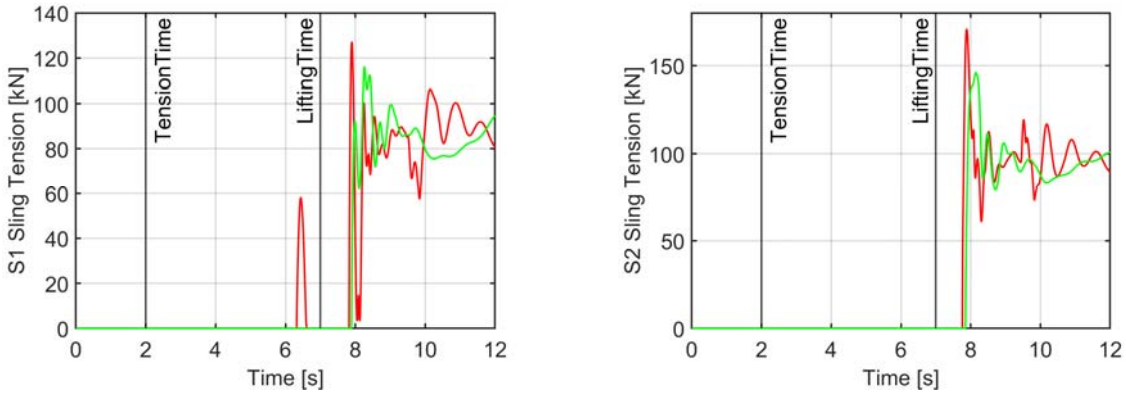

(b) Sling tensions

Figure 5-14: Coupling forces (Hs=1m, Tp=6s)

The allowable sea state analysis provides the overall view of the lift-off criteria for the operation. The same methodology is used while assessing the sea states. The figure involves the

results from the DeckFender. Using both criteria is the most compelling scenario as it is also shown in the results of Figure 5-14. Especially, the allowable sea states by using two criteria are the closest one among the other studies to the results of DeckFender model.

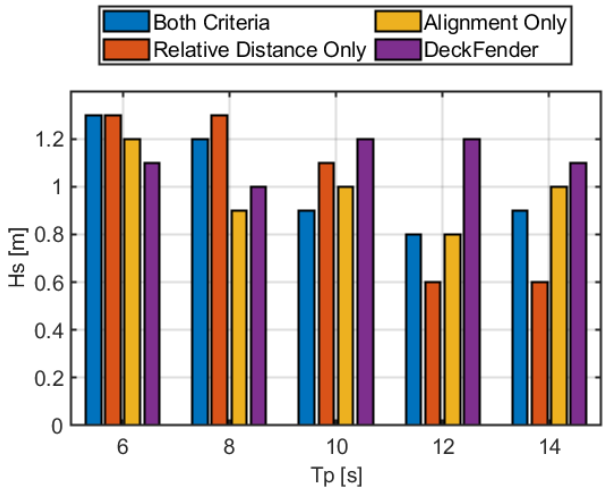

Figure 5-15: Allowable sea states for criteria study

As resulted from this study, two criteria have a positive impact on the lift-off operation in the same way of applied in the post-processing method. However, the outcoming results are more rigid in order to provide a more precise number of wave seeds. While the sea states are favourably increased, the confidence in this method has improved in a better way that the safe seeds and proper seed are significantly higher. The success rate in this analysis is more than 90% with an average of 85 safe seeds. Therefore, in further sensitivity studies, both criteria will be applied in the MCS in further analysis.

5.4.4 Winch speed study

In this chapter, the winch speed's effect on lifting operation will be studied. The winch speed corresponds to the hook velocity in the z-direction. Various winch speed's impact on the spool lifting operation will be discussed. Allowable sea states for each case will be shown.

Based on the manufacturer's instruction book, the hook speed can be increased up to 1.19m/s with the max load of 400tonnes. This capacity of the main crane gives us a wide variety

of winch speeds to conduct the lifting operation. It is quite expectable that higher winch speed allows the lift-off operation completes in a shorter time. That is to say; this would result in the dominant fact that the re-hit probability would be relatively less, and leads to higher sea states compared to the lifting models with lower winch speeds. In Chapter 3.4, the re-hit probability has calculated by using three hours of simulation for each sea state. The probability is calculated with the constant winch speed of 0.5m/s. The equation also can be applied with the variable as winch speed according to DNVGL regulations. DNVGL states that the probability of re-hit should be lower than 0.01 in 10 operations. Having this equation equal to the vital probability will result in the minimum winch speed required for the lifting operation. Subsequently, an insight into the winch speed is established by this equation. As it is seen from the following figure, the plot follows the same trend with the standard deviation (Figure 3-5), and 0.5m/s is the minimum speed required for this lift-off operation in the range of 0.8m-3m Hs and 4s-14s Tp.

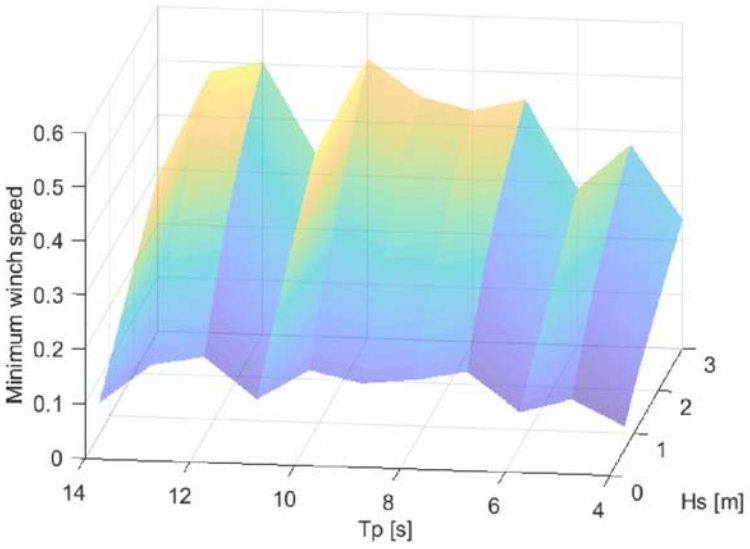

Figure 5-16: Winch speed according to DNVGL regulations [2]

The foremost challenge in the higher winch speed is the acceleration of the spool body at the initial moment of lifting. This acceleration combines with the dynamic relative acceleration between the crane tip—this coupled acceleration the transportation barge outcomes higher tensions in the slings and the lifting wire at the initial moment of the lifting. After the winch reached its

constant speed, the relative acceleration is valid on the tensions at the lift wire and the slings. Based on the availability of higher capacity slings, the lifting wire should be taken as the primary operational criterion in this study. Dynamic Amplification Factor (DAF) is taken in the maximum limits as 1.3.

Secondly, the challenge is to lift the spool while the crane tip is not aligned perpendicularly with the spool. Therefore, the high acceleration on the spool body with tilted lifting wire creates unstable lifting where there is a force being applied on horizontal directions. The misalignment criterion is used to minimize the unstable lifting for the spool together with the relative distance criterion.

The range of the winch speed tested in this model starts from 0.4m/s and goes up to 0.9m/s. These models are evaluated with the operational criteria explained in Chapter 3.3. Because, the different winch speed results in different timing for the lifted moment of the spool body. This issue is resolved with an update for the post-process method. "DT" is redefined dynamically as the time of the spool's position that begins to increase from the average z-position in the past time history.

Hence, the same seed used to illustrate the winch speed effect over the lift-off operation. The wave seed is taken from the model with 1.4m Hs and 6s Tp. Four different speed are used in this figure. The MCS system is using both criteria to define the initial time for the winch. Due to the dynamic winch controlling system, the lift-off operation is conducted on different time steps. Therefore, the tension time is referenced to plot the values on the y-axis. Time (s) does not refer to the actual time, but the relative time to the tension time as it is also applied in the previous study. In Figure 5-17, the relative distance is plotted, which shows the lifting vessel and the transportation barge’s motions which are quite similar before the winch starts. The plots do not follow each other tightly after winch starts, due to different moment applies to the crane tip that leads to vessel roll towards the port side where the transportation barge is aligned.

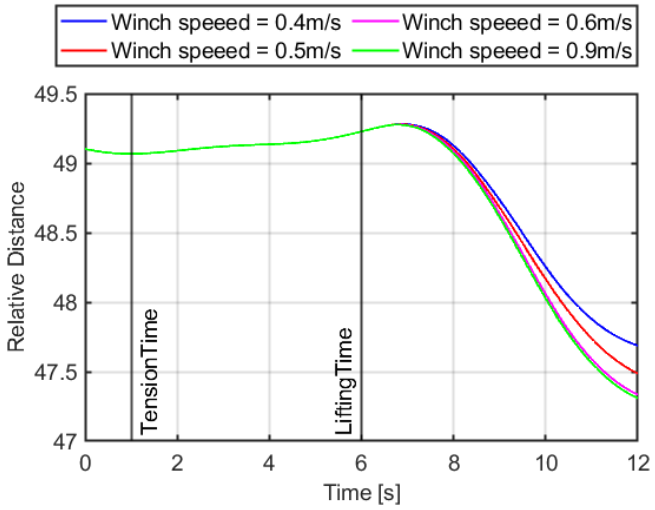

Figure 5-17: Relative distance figure for different winch speeds

The different winch speeds result in a variation in lift wire tension at the initial motion as mentioned previously as a foremost challenge. This phenomenon is observed in Figure 5-18 for lift wire tension and two sling tensions. The highest tension on the lift wire is caused by the winch speed of 0.9m/s at the first phase of the lifting operation. This high tension has induced the slings as seen in Figure 5-18 After the first phase, the tension in the rigging arrangements fluctuates until the lifting system stabilizes the operation.

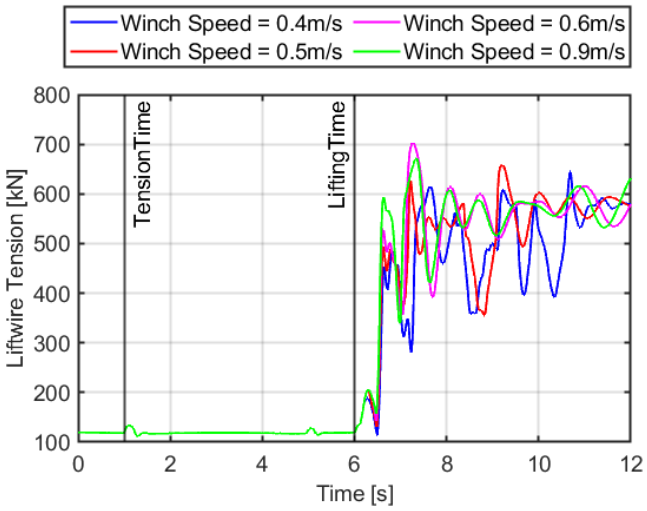

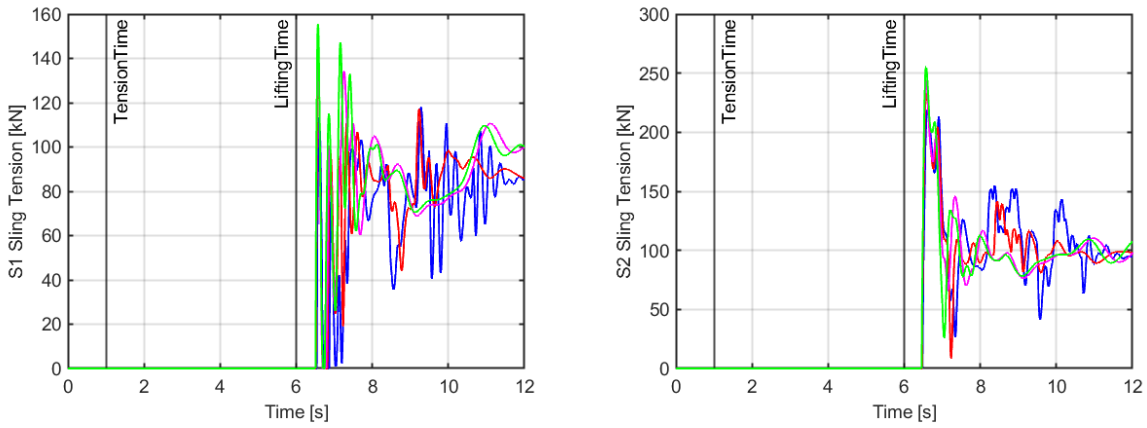

Figure 5-18: Lif wire, S1 & S2 sling tensions for different winch speeds (Hs=1.4m, Tp=6s)

Due to the higher winch speed, the spool is lifted from the transportation barge more quickly. That also helps the re-hit criterion being less effective in the operational limits. Figure 5-19 shows the spool position in the z-direction, together with the fender forces. In the first part of the figure, the winch with 0.9m/s speed lifts the spool almost 2 meters while the other winches lift the spool no more than 1 meter. This quick lift leads the lift-off operation complete without re-hit in the highest speed winch model as it is shown in the figure below. While the high impact forces occur in the fender points for the winch speed of 0.4m/s and 0.5m/s models, the models with winch speed of 0.9m/s and 0.6m/s experiences no re-hit forces. Even a small increase in the winch speed for 0.1m/s can influence the lift-off operation in broader aspects.

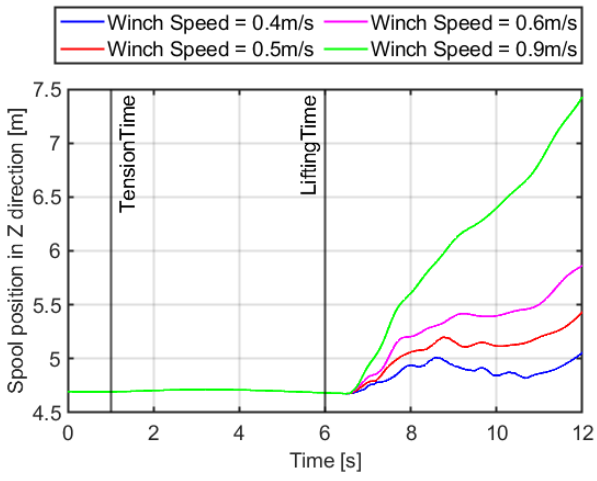

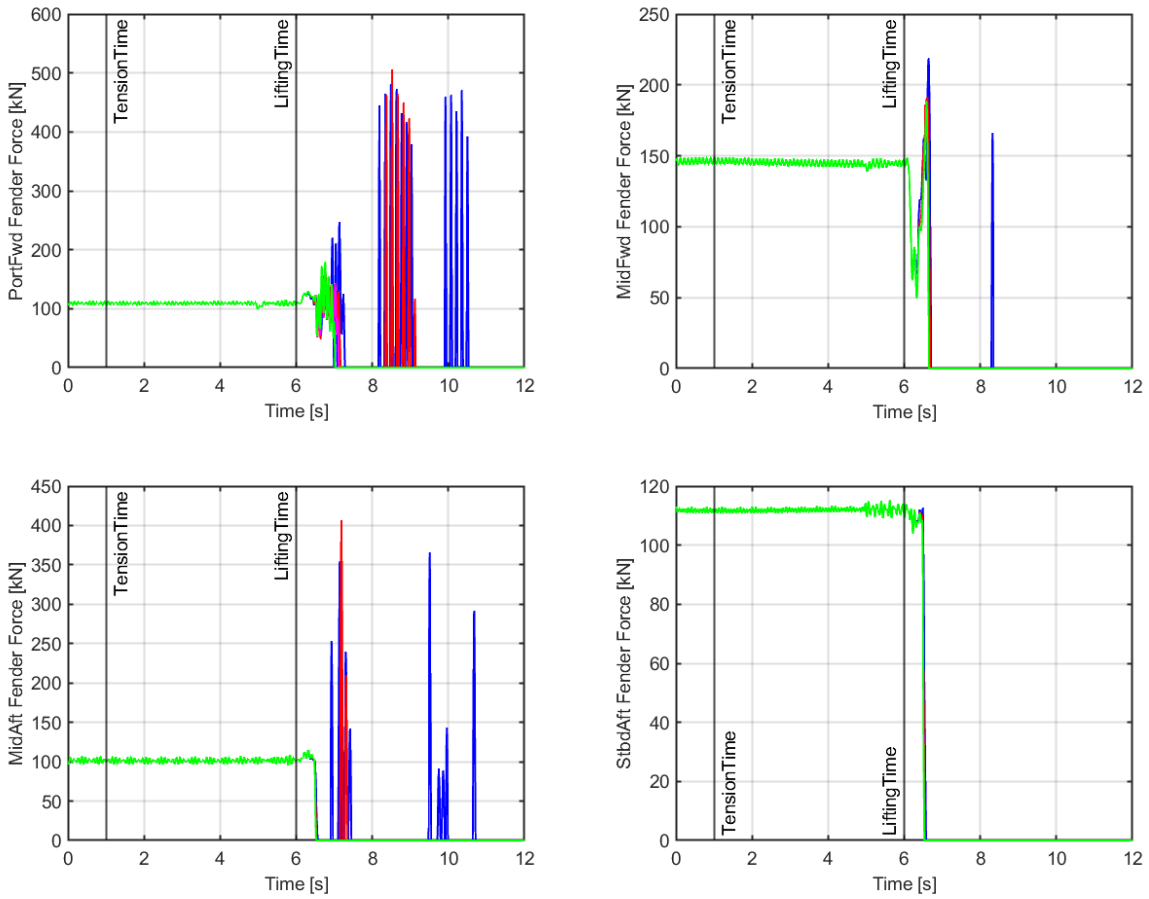

Figure 5-19: Spool position and coupling forces in different winch speeds (Hs=1.4, Tp=6s)

As it is shown in Figure 5-16, each Tp and Hs has a different winch speed of conducting the lift-off operation in the operational limits. In this figure, the allowable sea states of the winch speed of 0.7m/s are also included. By changing the winch speed with small amounts, it can increase the operational limits disproportional to the increment in the winch speed. The acceleration of the crane tip also plays a vital role in the higher sling tensions. This effect of the winch speed is presented below with an allowable sea state in Figure 5-20. The model with winch speed of 0.9m/s reaches the higher sea states compared to the other models. On the other hand, a small decrease in the winch speed for 0.1m/s worsens the operational conditions, so that the allowable sea states are remarkably low compared to the model with 0.6m/s winch speed.

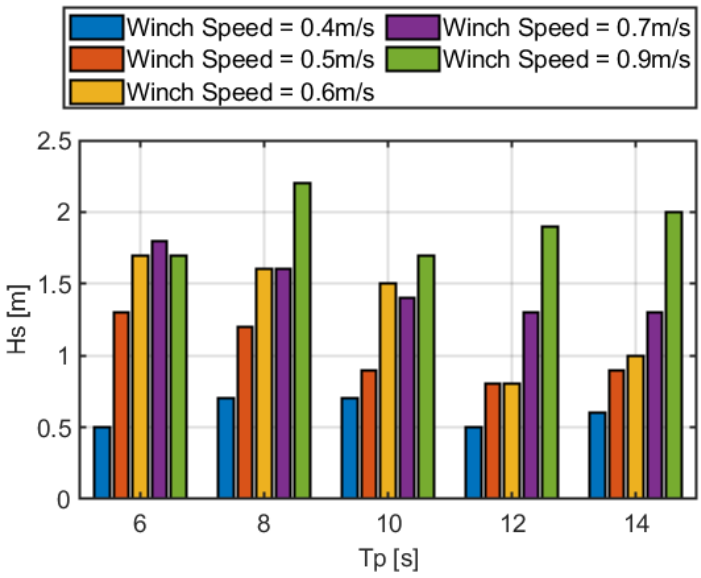

Figure 5-20: The allowable sea states for the winch speed study

Above all, the winch speed of 0.5m/s will be used in the different lift-off approaches study. The primary purpose is to define the operational limits with the highest probability. The winch speed of 0.5m/s complies with the DNVGL regulations for this operation and gives us the highest probability of re-hit among the other winch speeds. The winch speed of 0.4m/s is not considered in this following study because it is not approvable according to DNVGL rules.

5.4.5 Different lift-off timings respect to relative motion

Since the MCS provides control over the vessel motions, the different lifting instants in the relative motion is studied for the vessel motion. In Chapter 5.2, it is discussed that the operational criteria allow the lift-off operation to start while the relative distance is increasing. This criterion is elaborated with interest in consequences of the vessel motions at the start of the lifting operation. The central concept is the increasing relative motions; therefore, the preliminary estimation method is used in this study. So, the future estimation method is dependent on the preliminary estimation, where the most critical point is the wave trough analysis. Therefore, the instants are designated around the wave troughs as listed as follows,

- Lifting at the wave-trough

- Lifting before the wave-trough
- Lifting after the wave-trough
- Tensioning at the wave-trough

In this sensitivity study, another critical thing to remember is that the preliminary estimation gives 90% confidence in the increasing relative motion. Therefore, not all the seeds are the perfect representative of each designated studies. With this in mind, the proper seed methodology is updated with the winch control methods so that sensitivity study concepts are rechecked in the post-process phase. The interpretation of these approaches is implemented in the MCS system by defining manipulator parameters. These parameters are sent to the MCS Java code through the generic external control system explained in Chapter 5.4.1. These parameters are shifting the starting algorithm for tensioning speed and the lifting speed in the MCS Java code back and forward. These manipulator parameters; TensionTime, MinTension, MaxTension, LiftingTime are labelled as t1, t2, t3 and t3 respectively in the following figure. The process is shown in the figure below.

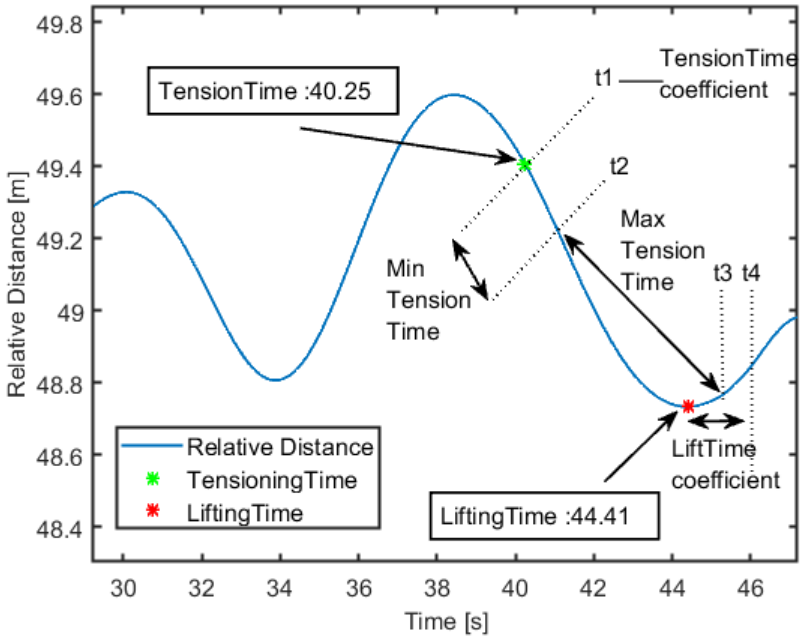

Figure 5-21: The MCS algorithm parameters

According to the figure, the TensionTime (t1) shows the start of tensioning speed after the suitable crest observed according to the method described in the previous chapter. The MinTension time (t2) addresses the minimum required time to tension the lifting wire. MaxTension (t3) implements the maximum tension time set for the winch. The trough is analyzed in the interval between t2 and t3. If the trough is found in the time history, the winch control system sets the winch speed as LiftingSpeed. This LiftingTime can be shifted by LiftTime (t4) so that lifting can be started after the trough as well. This coefficient will be used in further analysis to define. Since the starting mechanism is modelled within the intervals, it is necessary to use safety barriers to ensure that the algorithm does not exist the operational limits. Due to stochastic wave conditions can provoke the higher accelerations on the spool body, this may derail the algorithm methodology. For these safety concerns, the lifting wire tension and the spool position is taken into the algorithm as a stopping function not to tension more or not to lift more than structural limits.

The different approaches triggered a variance in the crane tip acceleration and also in the motion directions. This approach creates a requirement for the spool separation position. The spool position in z-direction fluctuates around 4.8m to 5.1m. Thus, another time definition is implemented as SpoolUp Time for further discussion of the re-hit. In this study, the lifting speed is taken in the same value of the lift-off criteria analysis, which is 0.5 m/s. Likewise, the condition of the transportation barge and the lifting vessel is judged within the relative motion and misalignment criteria. The comparative study will be held after these approaches explained.

Lifting at wave trough

In this lifting approach, the lifting initiates right at the moment of the wave trough. In order to achieve this approach, the parameters for the manipulators are given in the table below.

Table 5-5: Manipulator parameters for lifting at wave trough model

Manipulator Parameters	TensionTime	MinTension	MaxTension	LiftTime
Time (second)	1	2	7	0

These parameters enable the lift-off operation conducted in an approach depicted in Figure 5-22. The spool position plotted in the figure is a representative of the spool motion in the z-direction. It is not related to the values on the y-axis. In the static control model, the tensioning time was 5s. In this figure, the tensioning time is close to 5.2s. The increment in the relative motion is observed after lifting time more than 2s. Moreover, the time of the subsea spool is lifted is 2s after the winch runs with the lifting speed.

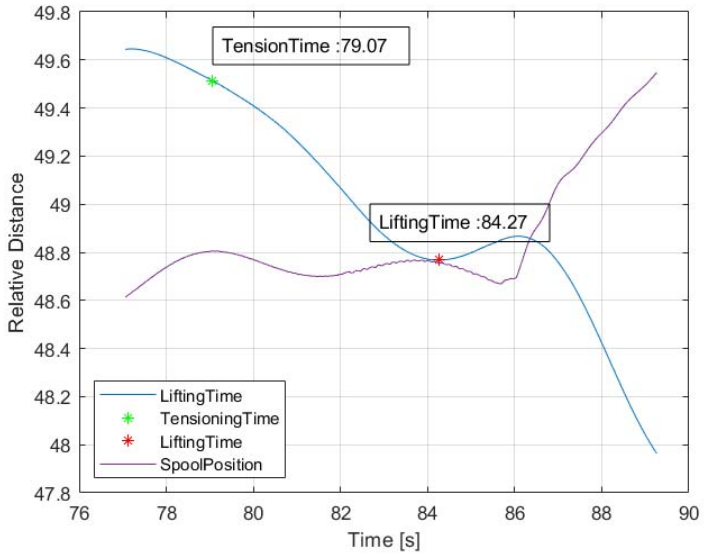

Figure 5-22: Relative distance and spool position (Hs=2m, Tp=6s)

This wave seed is also used in Figure 5-23 with the intension of demonstrating the sling and the fender force conditions while having relative motion in Figure 5-22. In the lift-off model, the most critical couplings are PortFwd and StbdAft Fender with corresponding sling locations in S1 and S2, as also discussed earlier in Chapter 4. These coupling models are used to show the response of lift-off in the lifting at wave trough approach. The noise is seen in the PortFwd Fender prior to the lift-off because the spool is not fastened to the transportation barge before the lift-off initiates as well as the deck fender is used in this analysis. DeckFender provides less stiffness and less damping behaviour between the spool and the deck of the transportation barge. With this in mind, while the spool is still on the transportation barge, these forces can be observed. However, the sling tensions are also increased for a second before the tensioning speed applies. So that, the

conditions in this seed is not favourable with the lift-off operations, especially with the 2m Hs and 6s Tp. Above all, the MCS system conducted a safe operation for the spool lifting where a smooth increase is observed in the sling tensions and no high re-hit forcers observed in this operation.

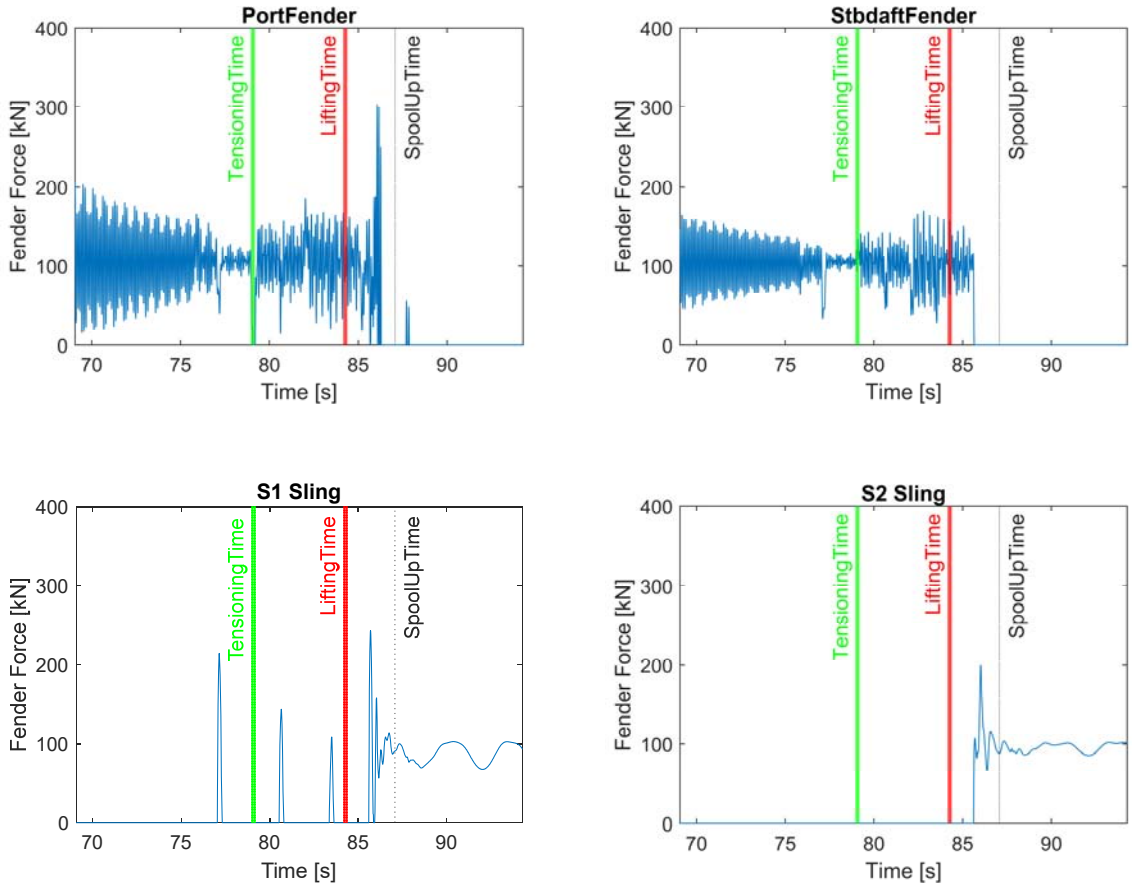

Figure 5-23: Coupling force in lifting after at trough instant (Hs=2m, Tp=6s)

Lifting before wave trough

In this method, the crane winch is ran with the lifting speed before the trough observed in the relative motion. In order to implement this method, the manipulator's parameters are defined as listed as follows.

Table 5-6: Manipulator parameters for lifting before the trough model

Manipulator Parameters	TensionTime	MinTension	MaxTension	LiftTime
Time (second)	0	2	3	0

The relatively smaller parameters induce the MCS algorithm to start earlier than when the relative motion changes its direction. Despite of the relative motion criterion for the lifting speed is avoided, and the MaxTension becomes the primary criterion for altering the speed. Another critical point to remember is that the peak periods are not long enough to have the whole tensioning period without turning point in the relative motion. These two facts are directing the lift-off operation in unfavourable conditions. These conditions will be compared further in this analysis. The relative motion and the spool position are shown in Figure 5-24.

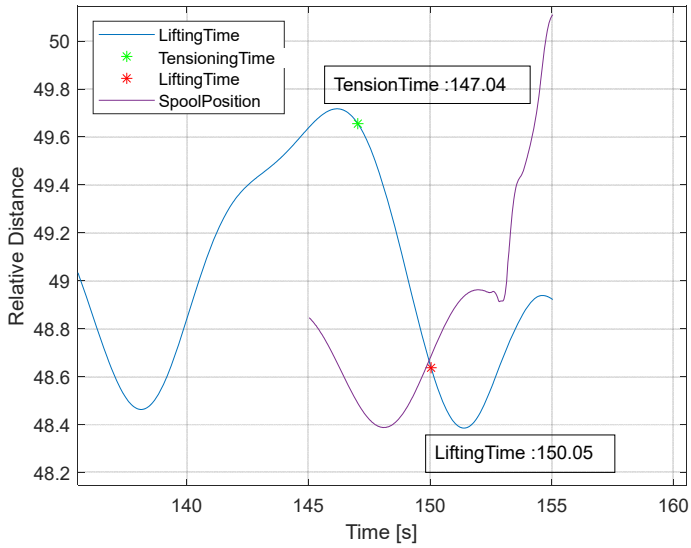

Figure 5-24: Relative distance and spool position (Hs=2m, Tp=6s)

In the following figures, the same coupling units are used to illustrate the forces using the lifting before the wave trough instant. As can be seen from the figures, the lifting of the subsea spool is started relatively later than the timing mentioned earlier. The winch increases the speed at 150.05 seconds, but the subsea spool is upheaved around 153 seconds. This value of the subsea spool position can be obtained from the decrement in the fender forces and the increment in the

sling forces. However, there is an increase in the fender force before the spool lifted utterly. This hit caused a fluctuation in the S2 sling tension. The time histories of the mentioned coupling units can be seen in Figure 5-25.

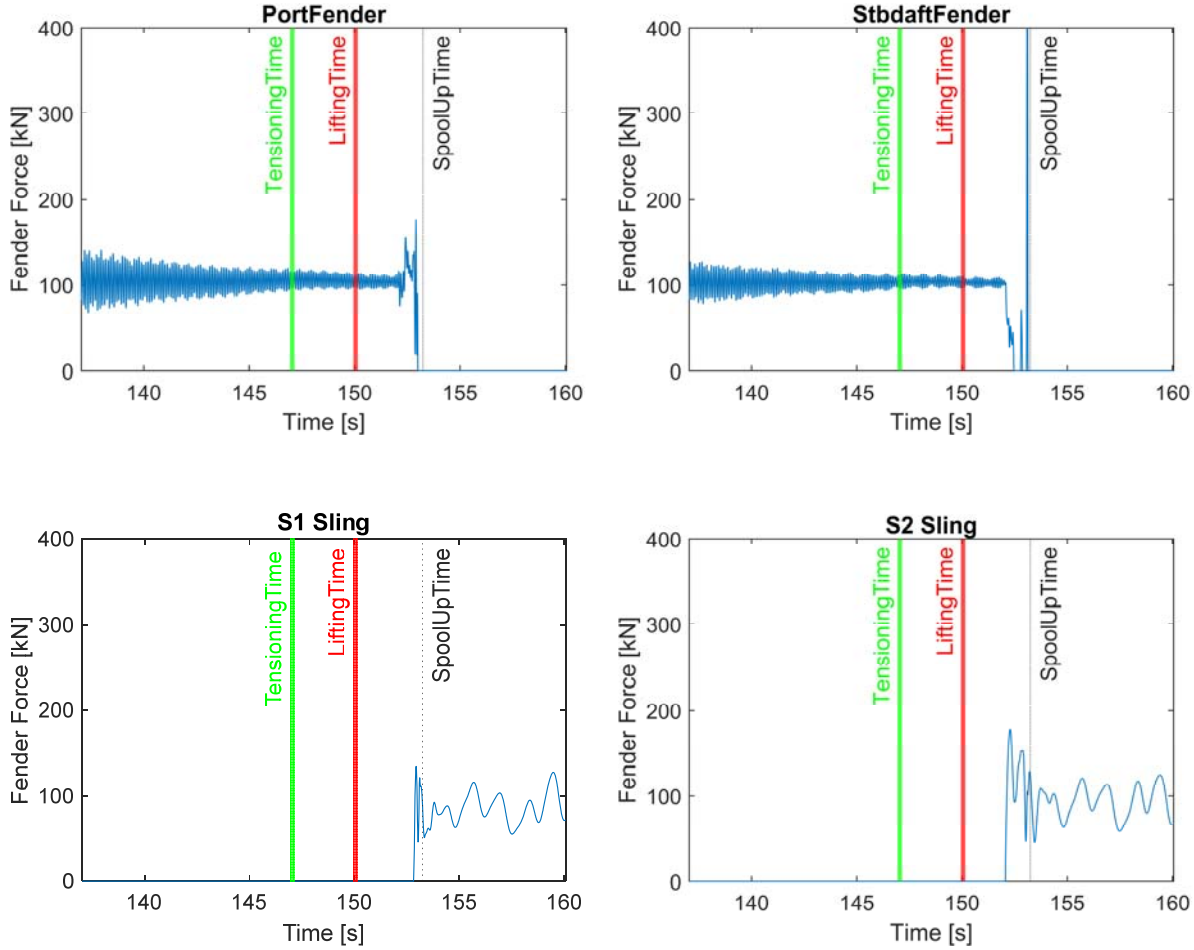

Figure 5-25: Coupling force in lifting before wave trough instant (Hs=2m, Tp=6s)

Lifting after wave trough

The MCS algorithm is interpreted further to shift winch speed to the lifting speed after the wave trough in the relative motion. The manipulator parameters are enhanced to obtain the wave trough in the analysis. The allowance interval for tensioning is increased to 8 seconds; however,

this criterion is less likely to be applied in the algorithm because the maximum Tp is 14s and tensioning starts 1 second after the crest. The parameters are listed as follows.

Table 5-7: Manipulator parameters for lifting after the trough model

Manipulator Parameters	TensionTime	MinTension	MaxTension	LiftTime
Time (second)	1	2	8	1

The lift-off scenario is depicted in Figure 5-26, together with the spool position in the z-direction. As mentioned earlier, the spool position in z-direction does not refer to its actual position, and it is truly shifted for 44.5m. The winch speed increases to lifting speed at one second after the trough is detected. This delayed start to the lifting tension may cause the increasing relative motion between the crane tip and the transportation barge. Still, the spool begins to be lifted after the winch speed is increased. As can be seen from Figure 5-26, the winch starts to influence the spool position in z-direction after the winch speed is moved up. Indeed, the difference between the LiftingTime and the time of the spool lifted is relatively shorter compared to other approaches mentioned.

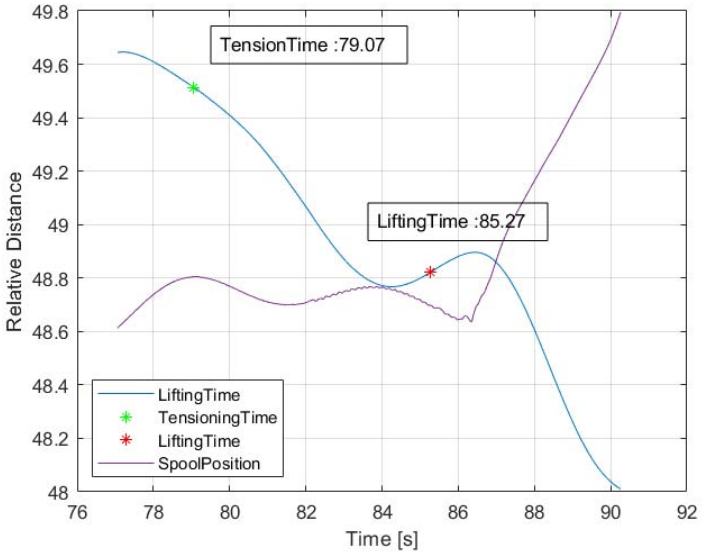

Figure 5-26: Relative distance and spool position (Hs=2m, Tp=6s)

The same wave realization is used in the following figure as well. The coupling models used in these figures are the same as the previous approaches.

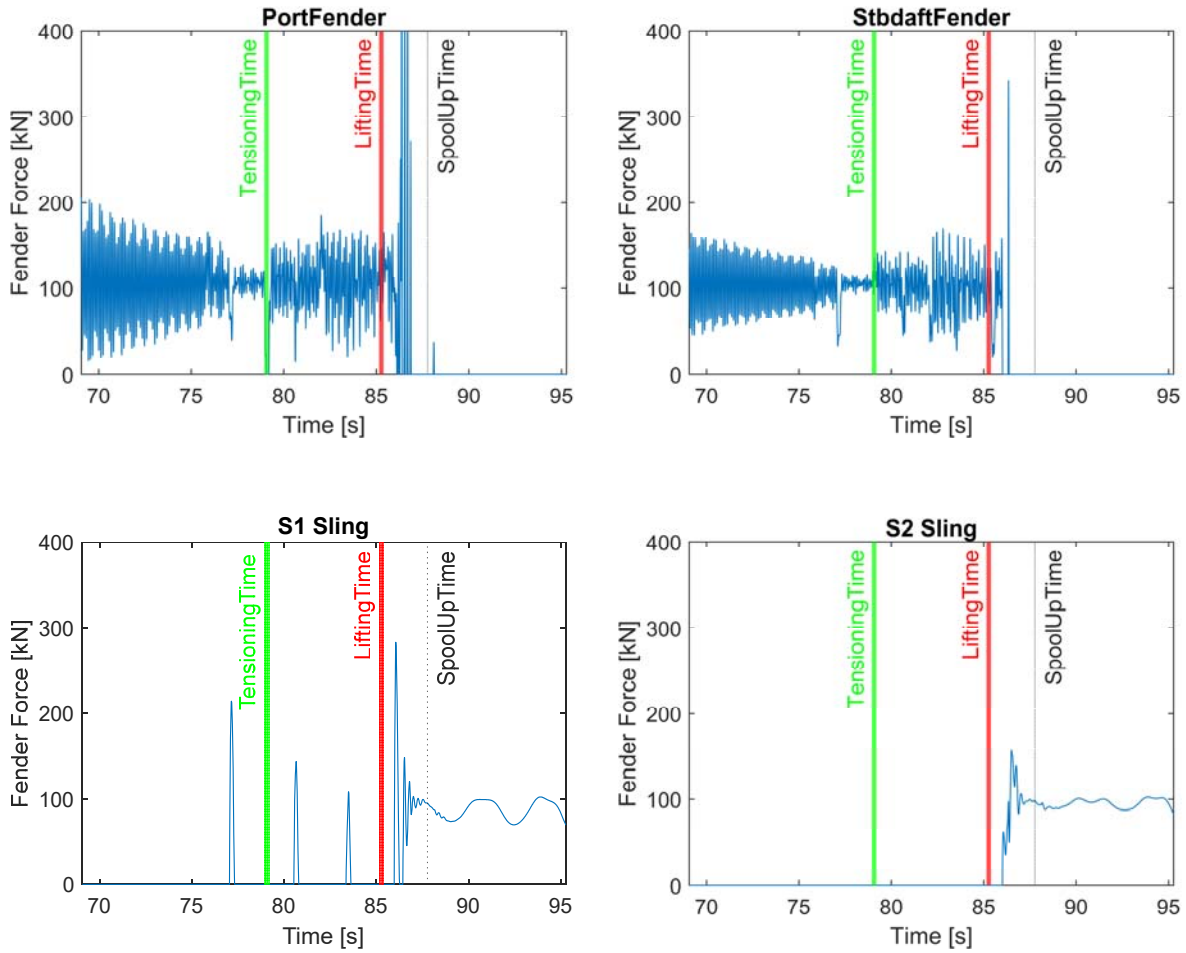

Figure 5-27: Coupling force in lifting after wave trough instant (Hs=2m, Tp=6s)

The noise in the fender force's time history does not represent favourable conditions for lift-off operation as it is also explained in the previous timing. There is a small magnitude re-hit that occurs after the SpoolUp time in the PortFwd fender. Moreover, there is a high fluctuation in the S1 sling corresponding to the times of high forces in the PortFwd fender. Since the lifting starting time is delayed, these noises in the fenders forces are expected to be observed in the time histories. These oscillations are related to the trough which comes before the LiftingTime. In an alternative way, because of the directional change in the relative motion. Besides, the sling tensions increases before the spool weight is applied to the slings.

Comparison of the lift-off instants

The lift-off instants are compared in Figure 5-28 by using the same seed. Due to the different lift-off times are experienced in each approach, the figure is illustrated by having the tensioning time as the reference point at 2s. Therefore, the x-axis does not reflect the actual time of the operation carried out in the simulations. The TensionTime line represents the reference point for each instance where the winch started with the tensioning speed. The marks on the relative distance plot show the times when the winch speed is increased to lifting speed. These wave seeds from each approach show the appropriate application of the MCS. Notably, the relative distance between the crane tip and the transportation barge increases for more than a second. Not to mention that the environmental conditions of 1.4m Hs and 12s Tp is not allowed for the DeckFender model, which is explained in the previous chapter.

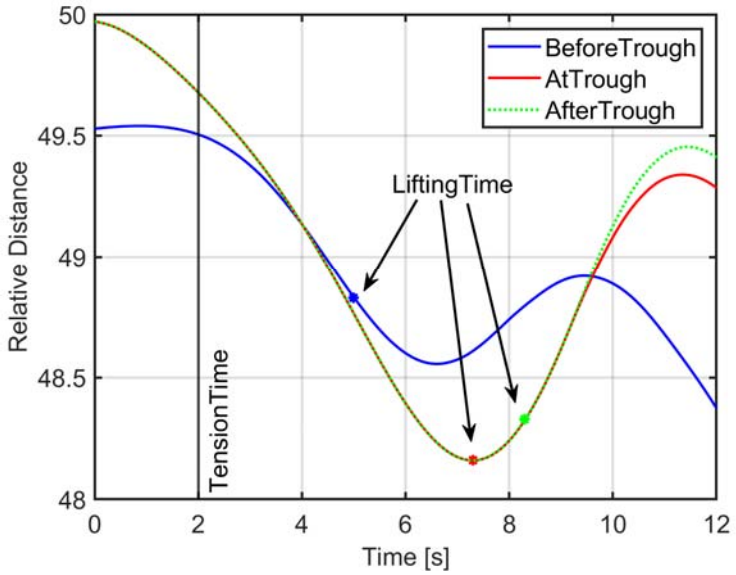

Figure 5-28: Relative distance (Hs=1.4m, Tp=12s)

The same seeds from each approach are used in the coupling force analysis in Figure 5-29. The four fender models are demonstrated in Figure 5-29. Re-hit force is observed for the BeforeTrough approach in all fender couplings other than the PortFwd fender. The tensioning duration is 5s which is the similar duration in the fender simulations. The early shift in the winch

speed without having the favourable relative motions result in the impact force in the fenders. Also, the fender forces have fluctuated before the separation point where the fender forces go down to zero. In the BeforeTrough approach, the winch speed changes at 5 second (referred to the figure timing). After 1 second of lifting speed used as winch speed, the fluctuation starts in fender forces while the relative motion still decreases. Thus, this fluctuation and the re-hits are related to the change in the direction of the relative motion.

Furthermore, there is another re-hit force occurs in the AfterTrough lift-off approach. Although the AfterTrough and AtTrough instants followed the least dissimilar motions among all approaches, there is an impact force occurs on the MidFwd fender point. This seed would not be considered as a safe seed because of this impact for AfterTrough approach.

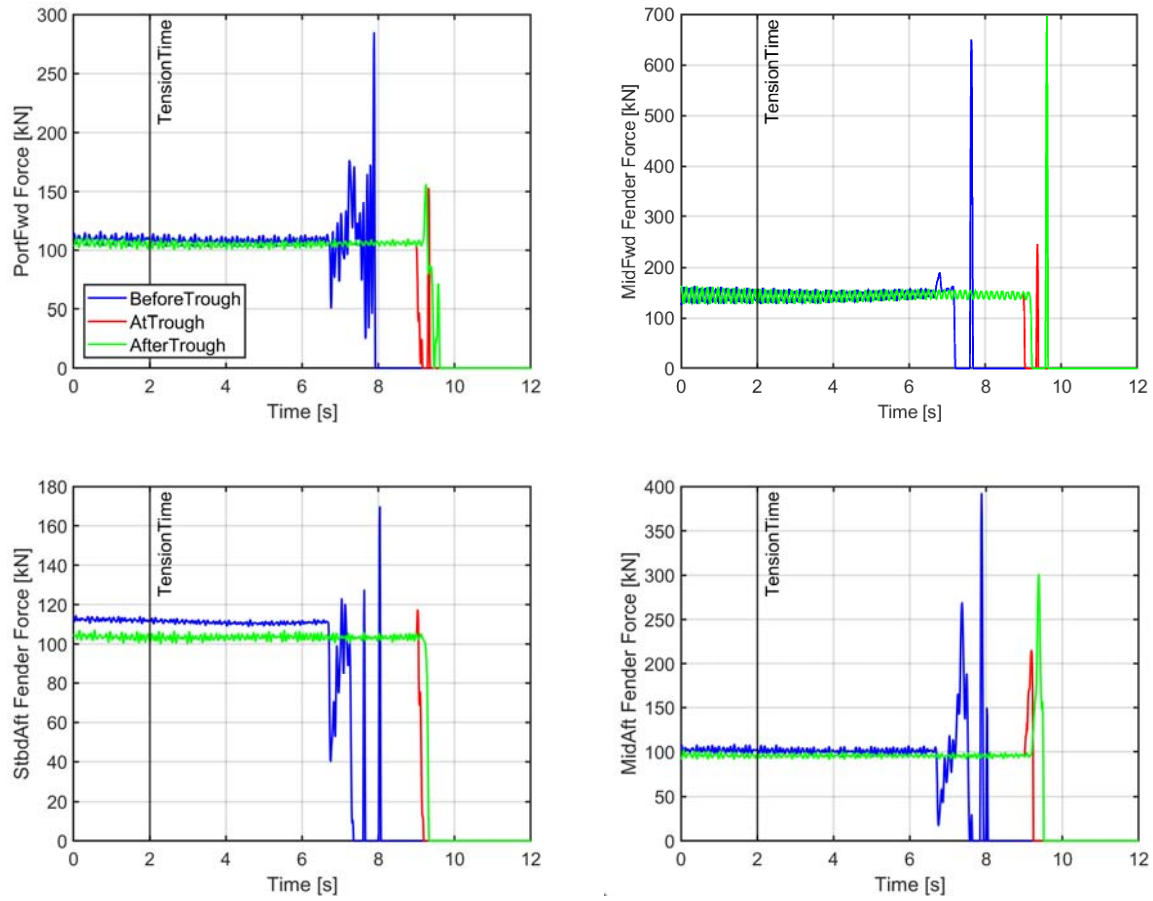

Figure 5-29: Fender forces and sling tensions (Hs=1.4m, Tp=12s)

The completion of the lift-off can be observed from the sling forces in Figure 5-30. Two slings will be used to illustrate the tension forces of the same wave seed used for the fender coupling analysis. The timing for the complete lift-off does not follow the same trend with the approaches. The first increase in the winch speed leads to complete the lift-off in a shorter time. As the slack sling condition can be observed from the sling tension plot, the BeforeTrough instant manages the lifting operation not in a safe scenario not only because the re-hit happens but also the slings slacks before the spool is lifted completely. As the conclusion of this seed comparison, the most compelling timing has resulted in AtTrough, and the results of allowable sea states will be presented as follows.

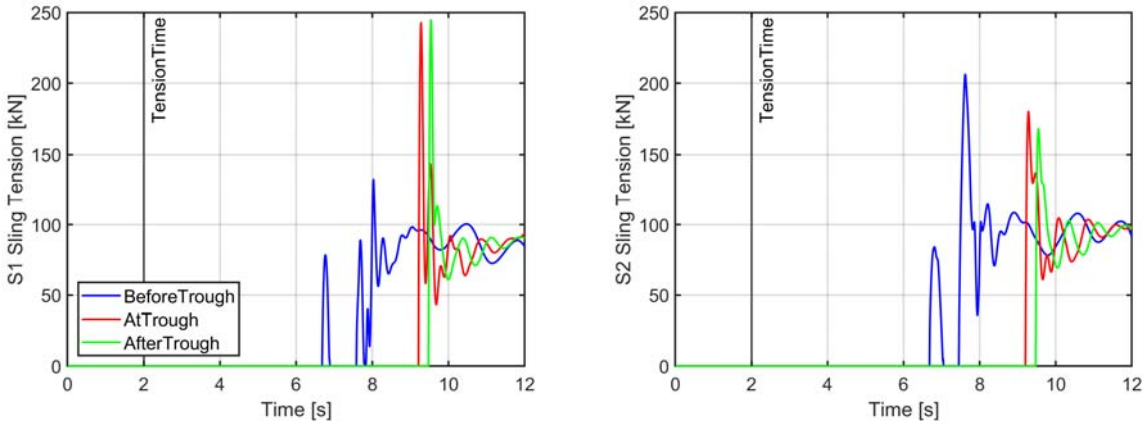

Figure 5-30: The sling tension plot (Hs=1.4m, Tp= 12s)

These approaches have been simulated for 100 times in each environmental sea states in order to describe allowable sea states. The same method mentioned in Chapter 3.3 is applied in this method; the allowable sea states is assessed by the 90% rule between the proper seeds and the safe seeds. The allowable sea states are shown in the following figure. The lifting AtTrough timing manages the lift-off operation in the most effective result, especially when it is compared to DeckFender Model in Chapter 3 since the only difference in these two models is the motion control system.

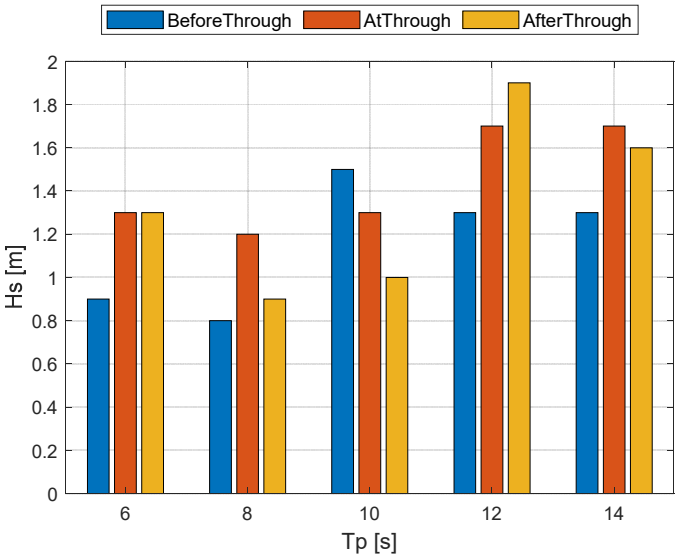

Figure 5-31: Allowable sea state for the MCS system

Although the sea states are increased more in the higher Tp's, the MCS does not show the same effect in the lower Tp values. As mentioned, the 90% rule is applied for the evaluation of the seeds. In addition to this, since the control algorithm checks the vessel motions, the only filtering criteria to define Proper Seeds is a check method to see if the MCS is worked or not in the wave seed. For instance, the evaluation of the wave seeds for Tp=6 second is shown below. Notably, the allowable sea states for 6s Tp is 1.3m.

Table 5-8: AtTrough model results in detail (Tp=6s)

Hs [m]	0.8	0.9	1	1.1	1.2	1.3	1.4	1.5	1.6
Safe Seeds	100	100	97	93	95	93	88	85	83
Proper Seeds	100	100	100	100	100	100	100	100	100

As a result of 90 % rule, 1.4m for Tp=6s is not considered as allowable because two seeds do not satisfy the operational conditions for the lift-off operation while 1.3m Hs was an allowable sea state. The 90% rule is interpreted from DNVGL-ST-N001 in the section of re-hit probability[1]. With this in mind, the extreme values are plotted in the following figure. The values are taken from a hundred wave seeds in the environmental condition of 1.4m Hs and 6s Tp. The

maximum values are considered from the time when the subsea spool is separated from the deck of transportation barge. These values are fit onto General Extreme Value Distribution (GEV). GEV distribution is used to find accurate limit distribution for minima and maxima, which is built on Gumbel, Weibull and Frechet standard extreme value distributions . General The first figure (a) represents the maximum sling tensions from each wave realization [45]. The maximum sling tensions slightly deviated from GEV. This deviation occurs because of different separation times in each part of the subsea spool, in alternatively, one of the main challenges in this lift-off operation.

On the other hand, the maximum fender forces (b) cannot fit onto a General Extreme Value distribution because of the zero values in the plot. The maximum values are only represented by the re-hits in the time history after the spool is lifted. So, there are a lot of zero values shown in the figure. That is why the maximum values of the fender force can not represent a suitable distribution. To summarize, more than 99% of sling tensions fits in the operational criteria, on the other side, the re-hits on the fender points lower the number of safe seeds which does not satisfy 90% rule by two seeds only. Then, this environmental condition is not considered as allowable.

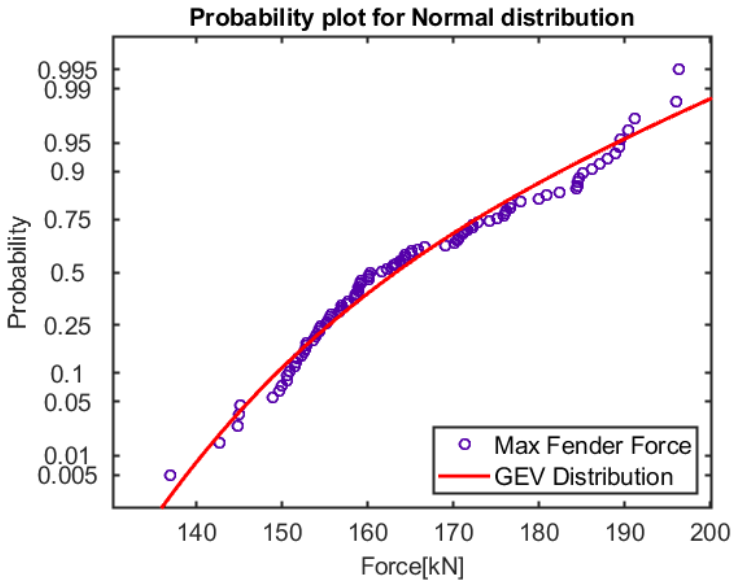

(a) Maximum sling tension fitting to General Extreme Value distribution

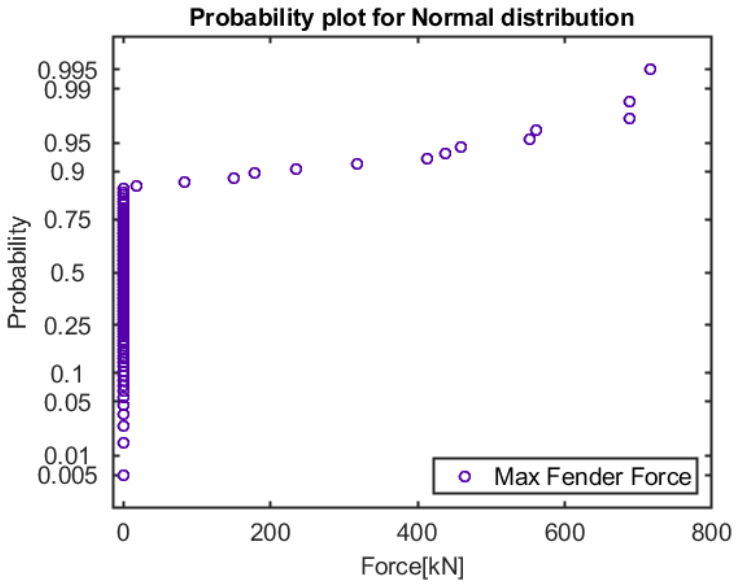

(b) Maximum fender force-fitting

Figure 5-32: General Extreme Value distribution fittings

Another critical point to take into account that the preliminary estimation only gave the confidence of 90% in future motion analysis. In light of this fact, although the MCS system has an average of 10% unreliability among Tp values between 6s to 14s. As well as this unreliability differs in each sea states. These fluctuations in the unreliability of the MCS system, have a negative impact on the results in an overall view.

Hence, the 90% rule is eased reasonably to define allowable sea states more suitably. The higher allowance (more than 10%) also helps diminish the effect of the unreliability of the estimation method. This allowance will only be used for Tp=6s and Tp=10s conditions. This allowance would not be applicable for Tp=8s, because the safe seeds number is much less compared to the other Tp. The allowable sea states are provided in detail in Table 5-9 for the AtTrough lift-off timing.

Table 5-9: Allowable sea states for AtTrough timing

Tp [s]	6	8	10	12	14
Hs [m]	1.3	1.2	1.3	1.9	1.7
Safe Seeds	93	92	93	90	82
Available Seeds	100	100	100	92	88

Tp=6s and Tp=10s will be examined with the numbers of safe and proper seeds in the higher Hs models in Table 5-10. There is a minor difference between the higher Hs and the allowable Hs as it is shown in Table 5-10. Based on this fact; the sea states will be considered as 1.5m for both Tp values.

Table 5-10: Safe and Proper seeds for the AtTrough lift-off timing (Tp=6s, 10s)

Tp [s]	Hs [m]	0.8	0.9	1	1.1	1.2	1.3	1.4	1.5	1.6
6s	Safe Seeds	100	100	97	93	95	93	88	**85**	83
	Proper Seeds	100	100	100	100	100	100	100	**100**	100
10s	Safe Seeds	96	95	94	95	93	88	87	**87**	82
	Proper Seeds	100	100	100	100	100	100	100	**100**	100

In conclusion, the allowable sea states of the MCS are shown in the following table. This sea states will be used in the operability analysis in order to see the effect of the MCS in the subsea spool installation.

Table 5-11: The allowable sea states for the MCS

Tp [s]	6	8	10	12	14
Hs [m]	1.5	1.2	1.5	1.9	1.7

The MCS can be improved by the automatically created manipulator parameters for any environmental condition. In this sensitivity study, manipulator parameters are used as static coefficients taken roughly calculated from linear wave theory. Only environmental condition implemented in these coefficients is the zero-up crossing period. Even in this approach, there are some wave realizations that the MCS could not define a suitable wave condition to initiate the lifting speed. If this approach is more strictly defined, it will create a requirement for longer simulation length and more massive computational power.

5.5 Summary of comparative results

In this chapter, the main objective is to define the most favourable time to start the lift-off operation. In light of the main objective, the first focus point is the lift-off instance analysis in order to tailor the conditions of two floating body motions in a promising way. Thus, the misalignment criterion is defined together with the relative motion criterion and impact on the lift-operation is studied. Since the lift-off criteria can be more precisely selected, the appearance of available intervals which are fit in these criteria are analysed in the time history of three hours. Due to the relative motion criterion requires the future estimation of the vessel motions; the estimation methods are reviewed in the time histories. The preliminary estimation method is taken into account for further analysis. The motion control system is created by using external control function in SIMO simulation, and the insights gained through these studies are implemented in the algorithm. In conclusion, the motion control system over two floating bodies is achieved, and sensitivity studies are conducted in three different concepts.

Since the control over the motion of the floating bodies is achieved, the sensitivity studies are applied to the MCS. Firstly, the lift-off criteria study is applied to see the difference between the decision methodology applied in the post-process and the continuous process. The allowable sea states from these methods were quite similar to each other, but the significant difference is the confidence given by the seed numbers supporting the evaluation. This sensitivity study followed with the crane speed analysis due to the higher speed capacity is available in the crane module. Both lift-off criteria are used in this sensitivity study. The only difference between the cases is the lifting speed. The outcome of the higher winch speed and acceleration is analyzed through this study with the variable speeds. In the last study, the lift-off criterion is expended into further

details. The dominant criterion is examined as the relative motion criterion. Therefore, this criterion is expended into a variety of lift-off approaches. The lift-off approach refers to the trend of the relative motion in the time history. In this sensitivity study, the same winch speed of 0.5m/s and both lift-off criteria are used, but the only variation is the trend of the relative motion. AtTrough lift-off timing is concluded to be the most effective method among the other methods. The allowable sea states assessed by this approach will be used as a conclusion of the MCS in the operability analysis.

Chapter 6
Operability analysis

6.1 Overview

In this chapter, the operability of the subsea spool installation operation will be studied for ın a reference offshore location. The operational limits have been assessed by using different approaches for the lift-off task in Chapter 4 and 5. The operational limits in terms of the allowable sea states will be used as input for this chapter to evaluate their effects of the fender models and motion control on operability for the spool installation. Besides, sensitivity studies on installation methods and different transportation time will also be presented.

6.2 General procedures of operability analysis

Commencing a marine operation requires complete fulfilment of the assumptions used in the design and the planning phase as per DNVGL recommendations. These assumptions are also practical in giving clear insights about whether to start the lifting operation or not. The decision for starting the operation relies on the operational limits and the conditions in the offshore site such as vessel responses, and weather forecast. Especially, DNVGL states that operational limits shall include wind speed, wave conditions and relative motions in the operational manual[1].

Generally, a marine operation is considered as a complex operation which requires a definition of the main task divided into several subtasks. These subtasks are operated by following a sequential procedure established in the planning phase. Establishment of this phase relies on the operational limits and the information from the installation area such as weather forecast. Therefore, a time frame with suitable weather conditions is required to complete the operation. Alternatively, this is called weather window analysis. The sequence, duration and continuity of each sub-operations are the vital parameters in the weather window analysis. The method demands an evaluation of the allowable sea states with the hindcast wave data of the available period for each sub-operation referenced. Fundamentally, the weather window provides continuous sea states merged within a period of appropriate duration to complete each sub-operation. If the weather windows comply with the allowable sea states, these weather windows are labelled as workable weather windows (WOWW) [3].

The marine operations have two phases, such as the planning phase and the execution phase. Prior to the execution phase, the planning phase is critical to define suitable conditions and operational periods. In this phase, the operational limits and rules will be defined, and the procedure and the schedule will be planned. Besides, different approaches and mitigation methods will be considered in the planning phase.

The execution of the lifting operation consists of two steps, including the monitoring and the execution. The monitoring phase before initiating the lift-off operation, monitoring of the critical responses is required. In this phase, vessel responses such as velocities, accelerations, and motions are examined and compared with the operational limits. The decision of starting the operation is based on checking the values received in the monitoring phase with the operational limits. In the monitoring phase, vessel responses are hydrodynamically linear as a result of time-invariant properties which is caused by no external force affecting the lifting system such as the spool weight at the crane tip [3]. Once the decision of starting the operation is made, the execution of the operation will be initiated.

6.2.1 Planning phase

In the planning phase, there are two methods to carry out the operability analysis. The first method, the operational limits of the lifting operation are directly compared with the characteristic

values of the hydrodynamic loads. These operational values are calculated via hindcast wave spectra. Although this method can be useful for the stationary processes, the lifting operation of the spool body is a non-stationary system. Therefore, this will require a high computational system in case of large hindcast wave data. The second method is a method of WOWW that requires measurement of the allowable sea states with hindcast wave data from the offshore site. Initiating this method requires a definition of WOWW of the operational procedures. This definition is provided by DNVGL and explained as follows[1].

The operation reference period is the duration required to use in WOWW analysis,

$$T_R = T_{POP} + T_C \quad \text{Eq. 6-1}$$

Where, T_{POP} is a short term of planned operation period (POP) and is defined as the foreseen time required to complete the operation as per the procedures. T_{POP} can be introduced from the experiences in similar operations. It is also suggested that 10-20% of exceedance of POP should be expected.

T_C stands for the estimated maximum contingency time. It provides additional time referenced from the below list.

- General uncertainty in T_{POP}
- Ineffective time throughout the operation
- Possible circumstances that entail additional time for completion

Furthermore, these circumstances should be frequently experienced in the history data (such as equipment malfunction). It is unnecessary to include rare situations in the calculation of T_C. Essentially, the T_C should not be lower than T_{POP} except for exceptional conditions. In the special conditions, half of the T_{POP} is acceptable as T_C but T_C should not be less than 6 hours for any operations. If it is less then 6 hours, the operation ought to documented thoroughly. The exception conditions are listed below as:

- Operations with vast experience from similar operations

- Towing operation with accurately evaluated towing speed
- Repetitive operations with full experience

When the reference period is less than 96 hours, and planned operation time is less than 72 hours, this operation categorized as “weather restricted operation” as per DNVGL regulations. Operation periods are depicted in Figure 6-1. In the weather restricted operations, the weather forecast is issued before the operation start and, is frequently updated every 6 to 24 hours [1].

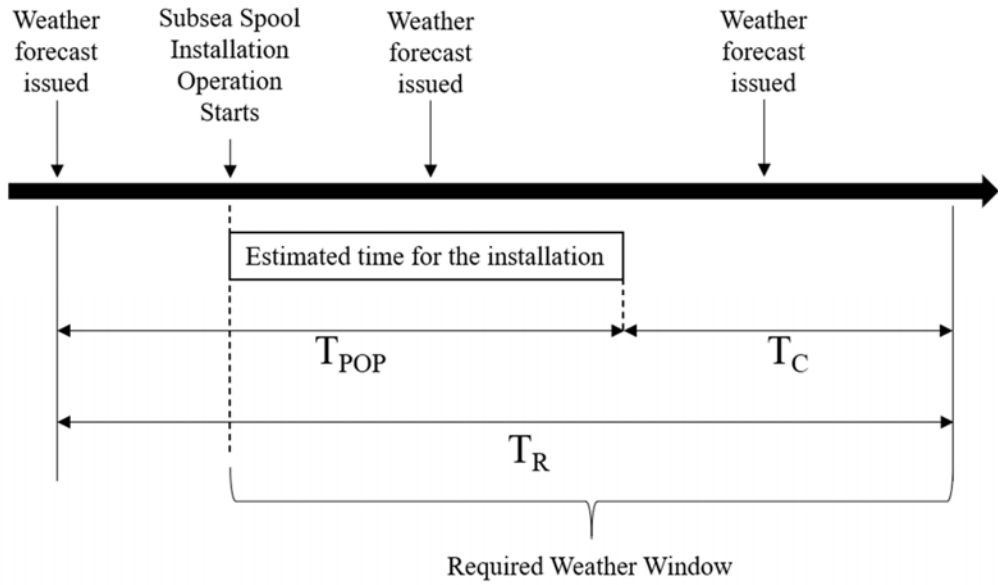

Figure 6-1: Operation periods

A limit of the Hs parameter is usually considered for the weather-restricted operations. This parameter is scaled by an alpha-factor that accounts for uncertainties in the weather forecast methods and the operation reference period T_R of the activities [3]. The alpha-factor increases with increasing Hs and decreases with increasing T_R. Reliable forecast sources entail to a higher alpha-factor[46]. Alpha-factor differs in time for each sub-operation, because of different T_{POP} and OP_{LIM}.

According to DNVGL[1], operability shall be calculated by using forecasted operational criteria – OP_{WF} defined as the equation below.

$$OP_{WF} = \alpha \text{ x } OP_{LIM} \quad \text{Eq. 6-2}$$

The alpha factor is selected based on the facts listed below:

- The recommended tables in criteria of weather forecast levels provided by DNVGL
- Operational limits in significant wave height, OP_{LIM}
- The planned operation period, T_{POP}

Furthermore, the weather forecast levels vary with operation sensitivity. There are three weather forecast levels labelled as A, B, C and refers to operational sensitivity of high, moderate, and low respectively. DNVGL-ST-N001 recommends the meteorologist availability and maximum weather forecast (WF) intervals. In this study, the scope of work is related to offshore lifting and subsea installation, therefore, it is suggested as level B [1].

6.2.2 Execution phase

The execution phase represents the actual performance in the marine operation. Unlike the planning phase, where the hindcast model is required, the weather forecast is issued in real-time in the offshore site. Based on this new forecast, the workable weather windows are established by the comparison with allowable sea states. Alternatively, the operation start decision is based on the weather forecast available on the site.

In the actual practice, this decision is supported by the on-board monitoring systems. The allowable sea states can be compared with the responses from monitoring systems and the uncertainties in the planning phase can be minimized. According to Guachamin Acero et al[3] , there are significant differences in the weather windows when the vessel motions are monitored with the monitoring systems.

Notably, this phase is implemented to SIMA-SIMO model by a winch control algorithm explained in Chapter 5.4. The response between the transportation barge and the crane tip of the lifting vessel is the focus in the control algorithm. The models in the SIMA-SIMO simulations are run with known environmental conditions. Therefore, the simulation completes the lift-off

operation in a relatively shorter period than the actual operation in the offshore sites. The motion control system is representative of the execution process in terms of having an algorithm to start/stop the winch during the lifting operation.

6.3 General procedures for subsea spool installation

The subsea spool installation operation is conducted under six subtasks. The categorization of these subtasks is established by similarity in the concept, which also has the same allowable sea states. The subsea spool lift-off operation is considered as irreversible operations. Therefore, after a subtask started, it shall not be suspended for any reason. This feature of the marine operations also needs to be bear in mind when categorizing the tasks.

General tasks of the subsea spool installation are listed below.

- Initial work
- Preparatory work
- ROV Survey
- Lift-off from transportation barge
- Lowering to the seabed
    - Lowering through the splash zone
    - Lowering through the water column
- Installation
- Voyage

Initial work starts with the loading of the subsea spool to the lifting vessel or the transportation barge. Then, the vessel transports the spool to the offshore site. During this period, initial checks are carried out, and vessel equipment/crew are prepared for the lift-off operation. The offshore site is 30 km away from the loading port. The maximum speed of the vessel is 16 knots. For the initial work, T_{POP} is assumed as 4 hrs. The Hs limit for the initial work is assured as 3.0m for all Tp variations based on the operational experience.

After the lifting vessel arrives at the offshore site, preparatory work is to be performed. The work includes rigging arrangement, crane positioning checks, removal of the subsea spool

fastenings and the last structural checks before the lifting operation commences. This duration of this subtask is estimated as 2hrs. The same Hs of 3.0m with the initial work phase for all Tp values.

Prior to lifting operation of the subsea spool, remotely operated underwater vehicle (ROV) is deployed to sea. ROV is used to ensure that the installation zone at the seabed is ready. Due to the dynamic environment in the subsea, the installation zone might be affected adversely in the meantime after installation location is prepared. The retrieving spool back to transportation barge is not possible, but it is possible to wet-store. Therefore, the operation must be managed with control over subsea, seabed and surface together. The ROV survey is carried out for 3hrs. The operational limit is estimated as the same as the preparatory work as 3.0m.

Furthermore, the lifting operation takes place. The lifting operation involves the lift-off of the spool and the lowering operation. Before the operation conducts, the monitoring of the environmental conditions is required. If the environmental conditions found satisfactory, the lifting operation can be performed. After the subsea spool is lifted off to a safe height, the transportation barge departures from its location. Besides, ballasting operations take place to keep the lifting vessel stable before the lowering operation. The duration of the subtask is estimated as a half-hour. The allowable sea states have been discussed in different methods. Due to the low sea states compared to lowering operation, the mitigation actions such as fender models and the motion control system are taken into account in the sensitivity study in Chapter 6.5.

The lift-off subtask is followed by lowering operation of the subsea spool. The lowering operation includes two phases resulting in two different operational limits. The first phase is lowering through the splash zone. As a result of highly dynamic hydrodynamic loads occurring on the subsea spool body, it is one of the challenging phases in this installation. After the splash zone, the hydrodynamic loads become insignificantly weak. The depth is presumed as 50m to consider the effects of hydrodynamic loads are weak. In the splash zone, the dynamic changes in the hydrodynamic loads induce critical responses in the subsea spool and the couplings. The winch speed is recommended to use as the lowest practical value in this phase. Therefore, the lowering operation through the splash zone is counted as 0.5 hrs. The operational limits were studied by Parra[17] . The same allowable limits will be used in this study. The allowable sea states are presented in Table 6-1. The second phase – lowering through the water column is conducted. In

this phase, Active Heave Compensator (AHC) is engaged. The AHC dissipates the impact of the heave motion at the spool in subsea in the lowering operation. Therefore, the sea states are higher than the splash zone. Furthermore, this operation goes until a safe distance above the seabed before the assembly starts. Since the operation is not assumed to be performed in ultra-deep waters, the reference period is assumed as 1 hour.

Table 6-1: Allowable sea states for the lowering of the spool in the splash zone[17].

Tp [s]	6	8	10	12	14
Hs [m]	2.3	1.8	1.7	1.7	1.4

The last subtask in the subsea spool installation is the assembly of the subsea spool to the designated place. Because of the shifted position of the lifting vessel, generally, the lifting vessel manoeuvres to get back in the exact position to the assembly zone. The main crane lands the subsea spool to the position. Once the position and condition of the subsea spool are acceptable, the rigging arrangement is retrieved back to the lifting vessel. This operation is estimated to take 4hrs in total, and the operational limit is as same as the initial phase. Hence, Hs is 3.0m for all Tp range.

As a summary, all the subtasks for the subsea spool installation are shown in Table 6-2 including the operational limits and the reference period. However, these specifications of subtasks will be interpreted corresponding to the sensitivity studies in the following chapters.

Table 6-2: General methodology for the subsea spool installation

The installation procedure		T_{POP} [hrs]	OP_{LIM} [m]
No.	**Subtasks**		
1	Initial work	4	3.0
2	Preparatory work	2	3.0
3	ROV survey	3	3.0
4	Lifting operation	1	0.9-2.4
5	Lowering operation	1	1.4-2.3
6	Installation of the subsea spool	3	3

After the subtask no 6, the return voyage is not presented in the table. This installation procedure is used as a reference for the different installation methods. This procedure will be interpreted according to the number of spool installations and method. Generally, the subsea installation operation is completed after the lifting vessel sails back to the port.

6.3.1 Installation Site

The metocean parameters in the offshore site play a significant part in the operability analysis in terms of schedule and the cost. The wave data of a reference site in the North sea is presented by Li et al. [47] as an ideal model of the North sea in order to apply in the operability analysis. The environmental conditions of the offshore site are imparted in Table 6-3.

Table 6-3: Meteocean data from the installation site

Site no	Area	Name	Water depth [m]	Distance to shore [km]	Average wave power density [kW/m]	50-year Hs [m]	Average Tp [s]
14	North Sea	Norway 5	202	30	46.43	10.96	11.06

The metocean data is produced from a hindcast model from 2001 to 2010. The wave data is sampled hourly, and the scatter diagram is presented in Appendix I.

6.4 The methodology of the operability analysis

The methodology of the identification of the WOW is an upfront process as per the approach suggested by Guamin Acero et al [9]. In this approach, the environmental parameters such as Hs, and Tp are required in time histories for the offshore site. The hindcast wave data is representative of weather conditions in the installation site. These time histories are categorized in the intervals of the time steps. By comparing the time steps of forecast Hs and Tp with the operational limits of sub-tasks for a defined period, the WOWW can be identified. The lift-off and lowering of the subsea spool lifting operation are categorized as an irreversible operation. Thus, these two subtasks cannot be stopped and reversed after the spool starts to be lifted-off. Therefore, these subtasks are linked to each other to provide continuity in the operability analysis.

Identification method of WOWW is illustrated in Figure 6-2. The hindcast wave data is shown in Figure 6-2 (a) and Tp_i is the peak period at the current time step. The operational limits for subtask 1 and 2, respectively shown in Figure 6-2 (b) as in Hs and Tp. Tp_i is used to identify corresponding Hs_i for each subtask as in Figure 6-2 (b). At the current time step, the Hs from the hindcast wave data is compared with the Hs_i (operational limit). If the Hs is lower than Hs_i for a particular period of each subtask, WOWW is defined as it is shown in Figure 6-2 (c). When the environmental conditions exceed the operational limits after the operation is initiated, the operation can behold for a 'waiting on weather' time if the subtasks are not irreversible. The period to suspend the operation for suitable weather conditions is called 'waiting on weather'. The waiting on weather interval is shown in Figure 6-2 (c) at the peak period of the hindcast wave data. The subtask two is started after the environmental conditions become suitable for the operation.

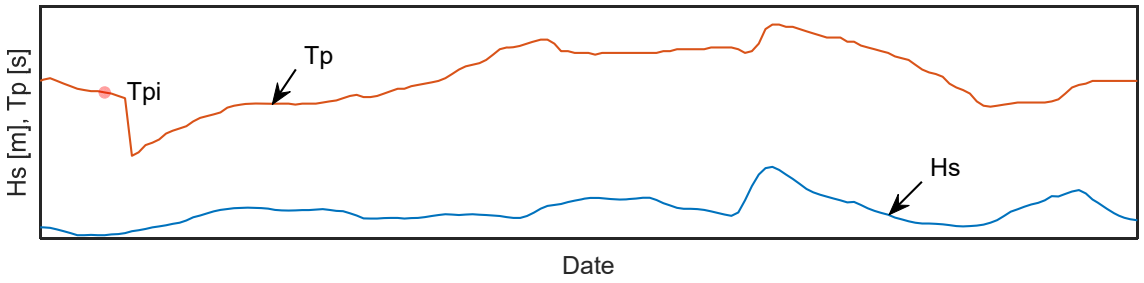

(a) Hindcast environmental parameters received from the offshore site

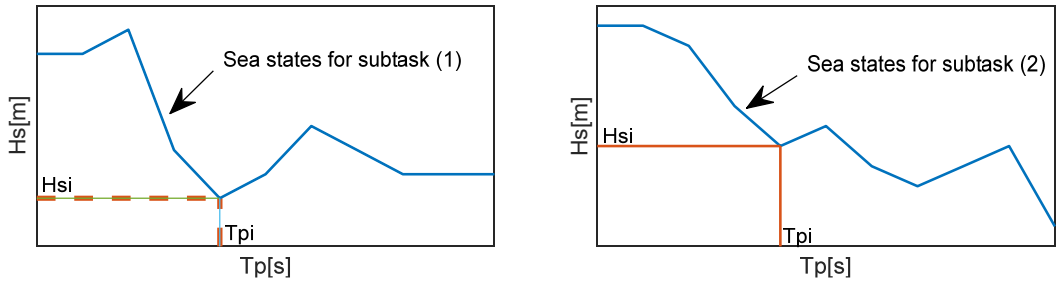

(b) Allowable sea states for the subtasks of the installation operation

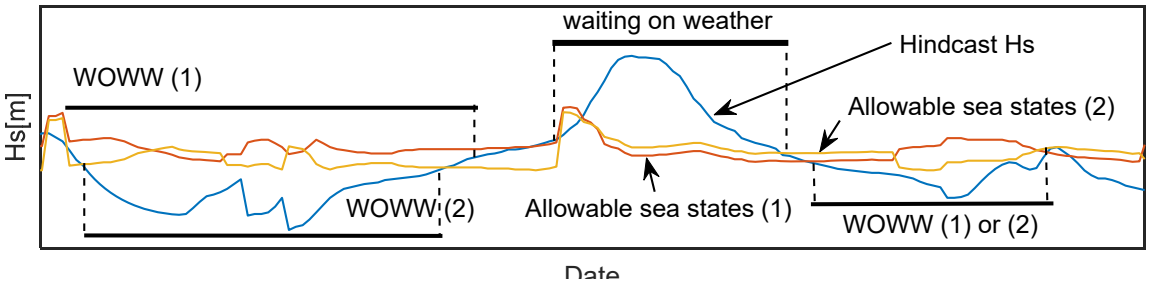

(c) Allowable sea states for the subtasks of the installation operation

Figure 6-2: Methodology for identification of WOWW

The operability analysis will be based on the total operation time (TOT) in this analysis. The total operation time (TOT) is the period from the start time of the first subtask to the completion time of the last subtask. In case of multiple spool installations, TOT ought to cover all the subsea spool installation; therefore; the subtask list will include the repetitive tasks until all subsea spools are installed. Nevertheless, not all the subtasks are irreversible in this operation as is illustrated in the below Figure 6-3 (a), WOWW's duration can be longer than the period of all

the subtasks of the installation task. In this type of WOWWs, all the subtasks will be performed in sequence without interruption. TOT will be equal to the sum of the T_R of each sub tasks. On the other hand, the weather conditions will not be suitable to conduct all the subtasks sequential as it is shown in Figure 6-2 (c). In these cases, operation holds for suitable weather conditions for a time period. In the case where the installation operation suspends for waiting on the weather window, as is shown in Figure 6-3 (b), the total operation time will be prolonged. The total operation time will vary not only on the weather condition but also on the number of spools, the installation location and the methods. These parameters will be elaborated in Chapter 6.5.1.

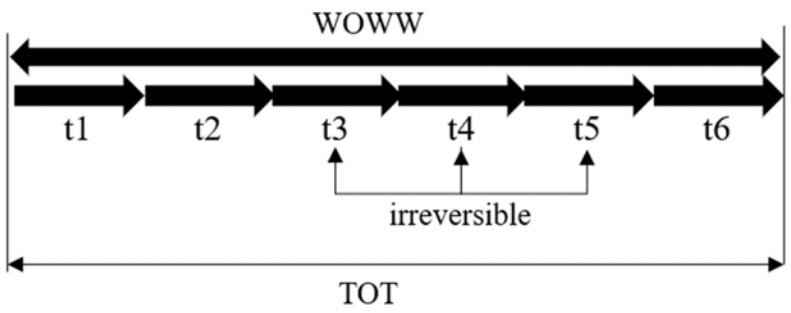

(a) TOT for a subsea spool installation without waiting on weather period.

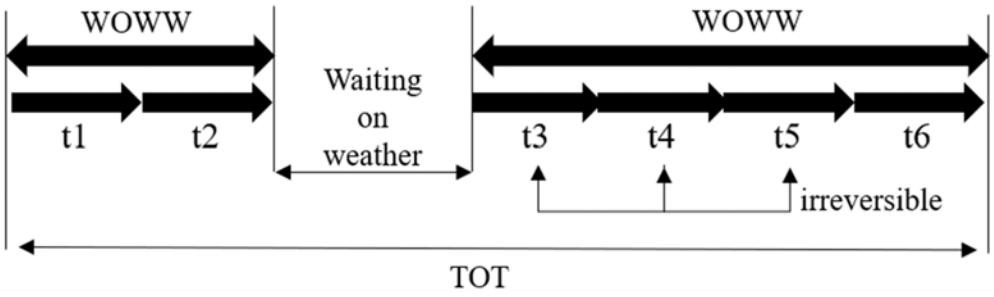

(b) TOT for a subsea spool installation with waiting on weather period

Figure 6-3: Total operational time illustration over WOWW

In the subsea spool installation, TOT's analysis in specific months will result in many variations. The waiting on weather windows triggers these variations due to high environmental conditions. The environmental conditions fluctuate widely over a year. Summer months have relatively more favourable weather conditions among a year. Because of that, generally, the installation operations are planned to be conducted in the summer times. Therefore, the operational

months are the time interval, starting from the first day of April and ending on the last day of August. These four months will be used in the statistical analysis in this study for every year. With the aim of a better view of the data and a proper comparison between the studies mentioned in Table 6-4, the statistical analyses will be conducted over the average value of TOT in 10 years and the P10, P50, P90 estimation using empirical distribution function. The most suitable estimation is used in the ratio with planned TOT to calculate the operability of subsea spool installation.

Mean TOT analysis

The first statistical analysis will be the meantime for TOT. Comparison of mean values is one of the ways to categorizing the data samples [48]. The TOT analysis will be performed for ten years taken from the hindcast wave data. The hindcast wave data will be presented in Chapter 6.3.1. The operations will be starting at any suitable time for the installation. From the overall operation time, the average TOT will be calculated.

$$\bar{x} = \frac{1}{n}\sum_{i=1}^{n} x_i \qquad \text{Eq. 6-3}$$

In EquationEq. 6-3, The mean TOT is addressed as $\bar{x}$, the number of possible operations in four months as n, and the TOT for each operation as x_i. This calculation is not only used for overall TOT mean value but also be calculated monthly to find out the most efficient time for this operation.

P10, P50, P90 estimation

In this analysis, P10, P50, P90 for the TOT will be estimated by using empirical distribution function. The non-exceedance confidence will be introduced to TOT values over the data samples. Furthermore, this value will be used to calculate the operability of this installation by taking the ratio to the planned TOT time. The empirical distribution function is presented in the below equation.

$$F_x(x_k) = \frac{k}{m+1} \qquad \text{Eq. 6-4}$$

Hence in this analysis, m will be the number of all suitable times in a specific period for the installation operation. The other term, k, stands for the number of observation equal or less to x_k. For instance, P50 estimation refers to 50% of the observed values exceed the value of x_k, which stands for TOT mean values. According to Borges, in the distributions which has the values skewed, P50 and the mean is the point where it begins to diverge [49]. Therefore, the median estimation becomes the most reasonable estimation to consider for further analysis.

Operability

The operability of the installation methods is calculated by the ratio of the planned time and the P50 estimation. When planned TOT is equal to P50 estimation, the operability is 100%. That means the environmental conditions in the offshore site is higher than the operational limits for a given period that allow the subsea spool installation to be carried out according to the plan. Therefore, the following formula is used.

$$operability = \frac{TOT_{plan}}{TOT_{P50}} \qquad \text{Eq. 6-5}$$

6.5 Subsea spool installation case study

The subsea spool installation procedures are explained in Chapter 6.3. The sea states resulted in the previous chapters will be referenced as operational limits and combined with these procedures of the subsea spool installation. The main objective is to present the effect of higher allowable sea states assessed by the methods used in the lift-off operation in the operability of the subsea spool installation.

In this section, firstly, the general procedures of the subsea installation will be elaborated onto two different installation methods. The main difference in these installation methods is the use of the transportation barge. These methods will be evaluated over the number of spools and the transportation time from the installation site distance to the loading port. In addition, different fender models are studied their effect in the lift-off operation in Chapter 4. Due to the different application cost and allowable sea states assessed by using different fender models in the lift-off operation, the effect in the operability will be examined. Furthermore, the model using the Motion

Control System has relatively better sea states compared to the conventional model. Thus, the effect of higher sea states achieved with MCS is studied in terms of the operability of the installation in Chapter 6.5.3. All the sensitivity cases are summarized in Table 6-4 with the allowable sea states.

Sensitivity study	Fender model	Installation method	The Motion control system	Transportation time to the offshore site	The allowable Hs for lift-off operation				
					Tp 6s	*Tp 8s*	*Tp 10s*	*Tp 12s*	*Tp 14s*
Installation method	DeckFender	IM1	No	3hrs 12hrs	1.1m	1.0m	1.2m	1.2m	1.1m
Installation method	DeckFender	IM2	No	3hrs 12hrs	2.3m	1.8m	1.7m	1.7m	1.4m
Fender models	SoftFender1	IM1	No	3hrs	2.4m	1.7m	2.0m	1.8m	1.8m
Fender models	SoftFender3	IM1	No	3hrs	1.6m	1.6m	1.5m	1.5m	1.3m
The motion control system	DeckFender	IM1	Yes	3hrs	1.5m	1.2m	1.5m	1.9m	1.7m

Table 6-4: General view over the sensitivity studies

6.5.1 Installation methods study

The spool installation can be carried by following two different installation methods. The operability of these installation methods will be discussed in this study. The main difference in these installation methods is the usage of transportation barge and therefore, the procedures. The motivation of this study is to evaluate the barge usage due to multiple numbers of subsea spools and variety in the distance from the installation site to shore. Two installation methods are introduced in the following way.

Installation Method 1 (IM1) includes the transportation barge and the lifting vessel together in this operation. The transportation barge allows the lifting vessel to work with the structures that have larger dimensions than the lifting vessel can secure on deck. Besides, transportation barge can create a logistical advantage in this operation, where the logistical advantage refers to reduced operational costs by having less cargo/load weight and maybe a shorter voyage time. The primary purpose of this installation method is to avoid voyages between the offshore site and the loading port in the case of multiple subsea spool installations. Thus, the installation operation is managed by one lifting vessel and the transportation barge, which the number varies with the number of spools to be installed. The daily rate of the lifting vessel compared to the transportation barge is significantly high. Therefore, usage of the transportation barge at the optimum level will lead to a reduced operational cost at most.

The general installation methods described for spool installation in Chapter 6.3. will be interpreted for N spools in the best possible way. In this installation method, the subtasks for the first spool installation will be the same with Table 6-2. However, for installation of the following spool; the subtask list is presented in Table 6-5. In the repetitive tasks, the subtask number one is avoided because the lifting vessel stays at the offshore site. The transportation barge is assumed to be in standby mode in the installation site while the last subtask is carried out by the lifting vessel. Therefore, the duration for the preparatory work is reduced from two hours to one hour. After all the spool installations finished, the lifting vessel will return to the port.

Table 6-5: Subtask list for Installation Method 1

The Installation Method 1				
The number of repetition	**No.**	**Subtasks**	T_R **[hrs]**	OP_{LIM} **[m]**
1	1	Initial work	4	3.0
	2	Preparatory work	2	3.0
	3	ROV survey	3	3.0
	4	Lift-off operation	1	0.9-2.4
	5	Lowering operation	1	1.4-2.3
	6	Installation of the subsea spool	3	3
(N -1)	2	Preparatory Work	1	3.0
	3	ROV survey	3	3.0
	4	Lift-off operation	1	0.9-2.4
	5	Lowering operation	1	1.4-2.3
	6	Installation of the subsea spool	3	3
1	7	Return voyage	3	3

In **Installation Method 2**, (IM2) the operation is handled by only the lifting vessel. Therefore, the lifting vessel needs to return to port to load another subsea spool between the installations. The subtask number 7 (return voyage) is added to the subtask list in Table 6-2. In case of N spools, complete tasks for installation of N spools using IM2 are shown in Table 6-6.

Table 6-6: Subtask list for Installation Method 2

The Installation Method 2				
The number of repetition	**No.**	**Subtasks**	T_R **[hrs]**	OP_{LIM} **[m]**
N	1	Initial work	4	3.0
	2	Preparatory work	2	3.0
	3	ROV survey	3	3.0
	4	Lift-off operation	1	0.9-2.4
	5	Lowering operation	1	1.4-2.3
	6	Installation of the subsea spool	3	3.0
	7	Return voyage	3	3.0

In this method, the installation operation is limited by the lowering operation, according to DNVGL-RP-N103 [2]. Due to the most critical criterion, the relative motion between the crane tip and the deck of the lifting vessel is insignificant. Because of the crane tip and the deck is rigidly connected to the lifting vessel, the motions follow the same trend with the lifting vessel and the difference between two points is negligible. As a result, the allowable sea states for the lowering operation becomes dominant in this installation method. The operability analysis will be conducted by using the sea states shown in Table 6-1 for the lift-off and lowering subtasks.

The mean TOT (TOT_{mean}) is calculated based on ten years of wave data, as mentioned in Chapter 6.4. In Figure 6-5, the TOT_{mean} for three months by using two installation methods are present for two spools, eight spools, and fifteen spools, respectively. Although IM1 does not include the return voyage, the TOT is much higher than the IM2 where the transportation barges are used in operation. The low allowable sea states in the lift-off operation from transportation barge limits the operation and causes waiting on weather windows. For instance, in the case of two spools, the mean TOT required for the subsea spool installation can be more than 200hrs by using IM1.On the other hand, the TOT_{mean} stays below 100hrs for two subsea spool installations. These

figures are created by using the wave data in the interval between May to the end of June. As it is observed from the figure, the TOT times follows a decreasing trend starting from the first of May. Therefore, the weather conditions become more suitable in the summertime.

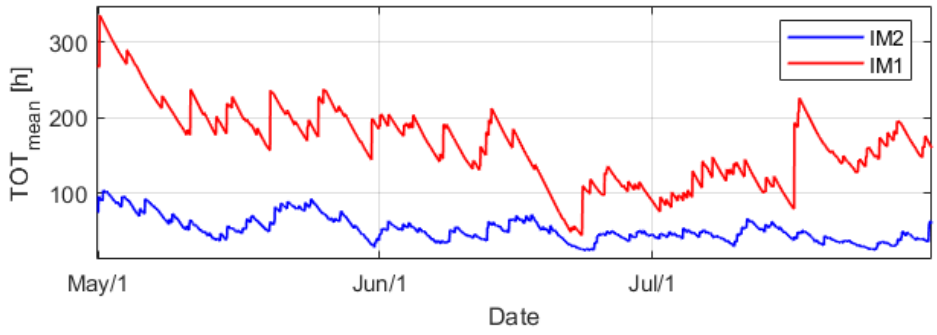

(a) 2 subsea spools installation

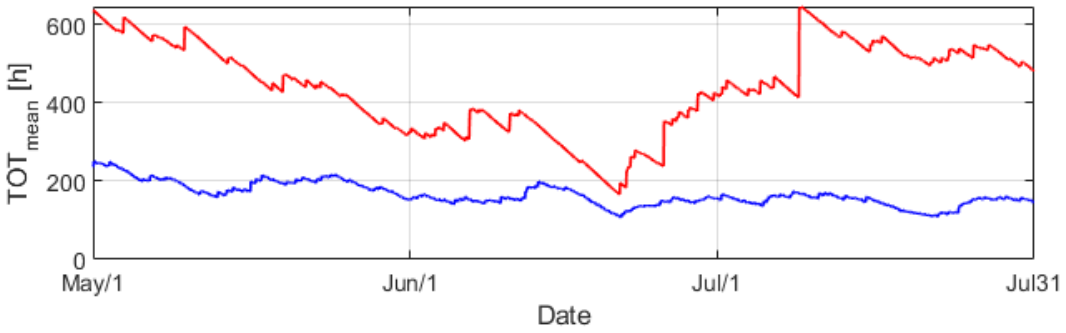

(b) 8 subsea spool installations

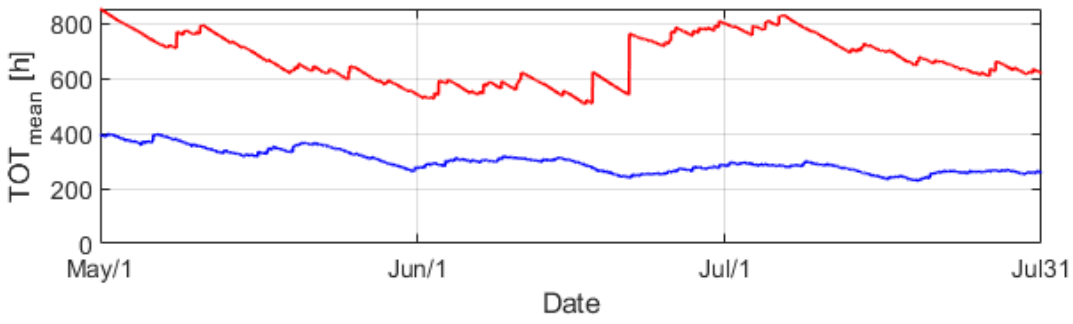

(c) 15 subsea spool installations

Figure 6-4: The mean total operation time comparison among the spool number

In Figure 6-6, the TOT_{mean} values of both installation methods are compared over the number of spools together with the planned operation time. The planned time refers to the total time required to complete the operation without any suspension. As shown in Figure 6-5, the operations held in August have the highest TOT compared to other months. Indeed, by using only lifting vessel (IM2), spool installation is completed in lower operation time because of the higher allowable sea states in the lift-off operation. For instance, while fourteen subsea spools installed in 800hrs by using IM1, the operation of the same number of spools is completed in 400hrs by using IM2.

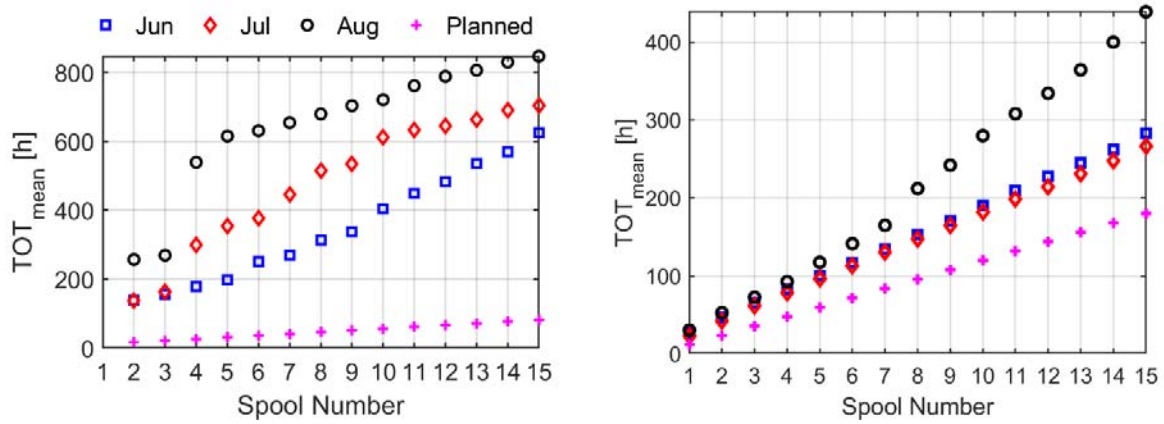

(a) Installation Method 1 (b) Installation Method 2

Figure 6-5: TOT_{mean} of each month over the spool numbers

In the next step, the P10, P50, P90 estimates are calculated by using the empirical distribution function. These values will be plotted for different number of spools in three months (April, July, and August) in the below figure. As the same methodology applied in the mean value for TOT, the subsea spool installation can start at any instant during this period. Three subsea spools are considered in the results for Figure 6-6.

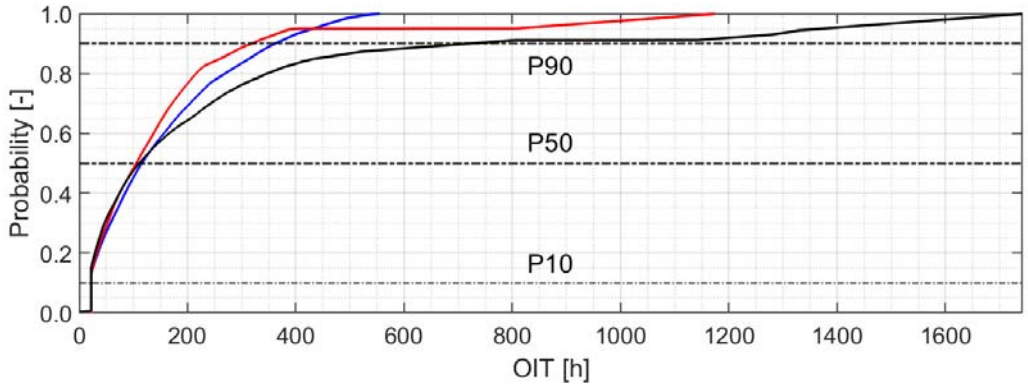

(a) The installation method one

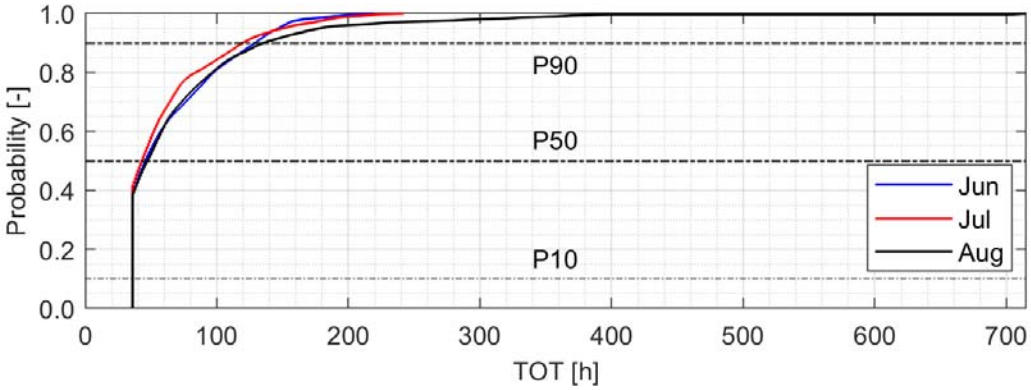

(b) The installation method two

Figure 6-6: P10, P50, P90 estimates for TOT of three subsea spools installation

The separation point of the plots is quite close to P50 estimate as depicted in Figure 6-6. It is also mentioned in the methodology that P50 estimate is the median estimation for the TOT values, in an alternative way, the mean begins the diverge. In the below table, the estimate values are listed. The environmental conditions for the offshore installations are more favourable in July than other months. This statement can also be understood from the lowest total operation time is in July. In the overall view, the operation is completed using the installation method two with significantly lower TOT.

Table 6-7: P10, P50, P90 estimate values for three subsea spools installation

	The Installation Method 1			**The Installation Method 2**		
ESTIMATES	TOT_{mean}					
	Jun	July	Aug	Jun	July	Aug
P10		22hrs			36hrs	
P50	46hrs	43hrs	47hrs	105hrs	111hrs	116hrs
P90	129hrs	119hrs	135hrs	363hrs	321hrs	727hrs

In Figure 6-8, the operability of the two installation method is presented with a different spool number in three months. The IM2 is showed better operability results when it compared to IM1. The operability of IM2 lies between 60% to 100%, whereas the operability of IM1 is in the range of 16% to 23%. The highest operability is achieved in July where the environmental conditions are more favourable than the other months.

On the other hand, the operations held in August experienced lower operability compared to June and July. In operation started in August, there are less waiting on weather windows due to the lower environmental conditions. Although the subsea spool installation number increases the voyage duration of the lifting vessel in IM2, still, IM2 provides better operability than the IM1. The reasons that lead to lower operability for IM2 are

- Lower allowable sea states due to the lift-off operation compared to lowering operation in IM1,
- Location of the offshore site is only 30km away from the loading port; the time used to load another spool on the lifting vessel does not affect the whole operation as much as the lower sea states achieved in the lift-off analysis.

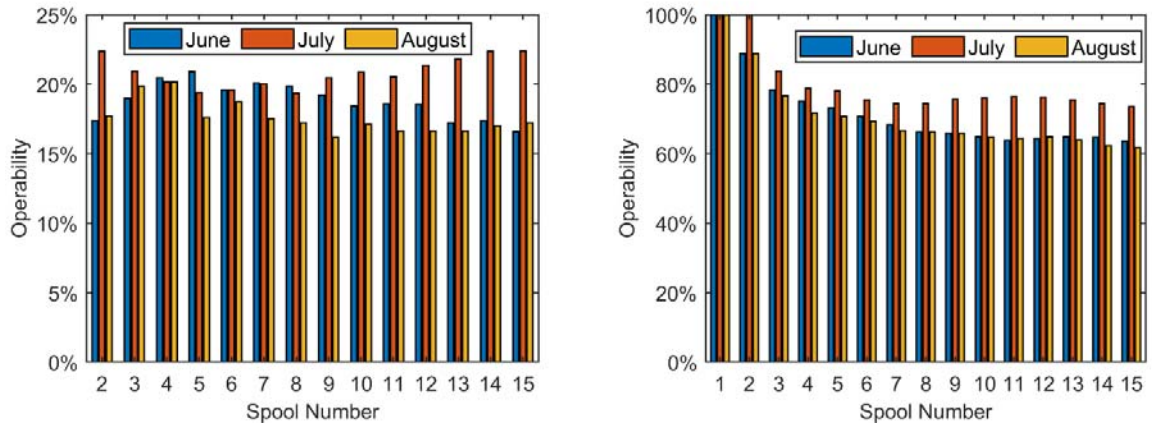

(a) Installation Method 1 (b) Installation Method 2

Figure 6-7: Operability of the installation methods

The location of the offshore site determines the transportation time and may influence the TOT for spool installation. Two distances of the offshore site, i.e., 30 km and 120km are compared to study the influences on the installation time. When the distance is increased from 30km to 120km, the voyage duration increases from 3hrs to 12hrs. The TOT planned is calculated as 29hrs for a spool installation. In the below figure, the TOT_{mean} times are displayed.

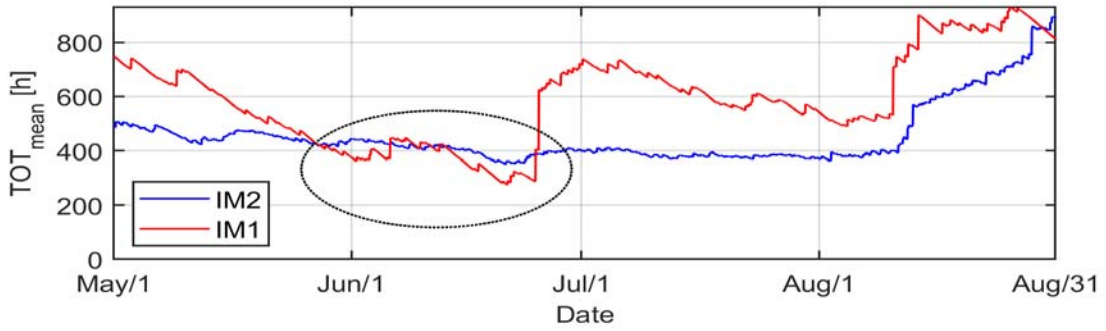

Figure 6-8: TOTmean for ten subsea spool installations in different location site

Still, the installation method two has lower total operation times compared to IM1. In early June, the total operation time coincides for both installation method; even IM1 can manage the

operation in a shorter time. The operability of installation methods with the transportation time of 12 hrs is compared in Figure 6-9.

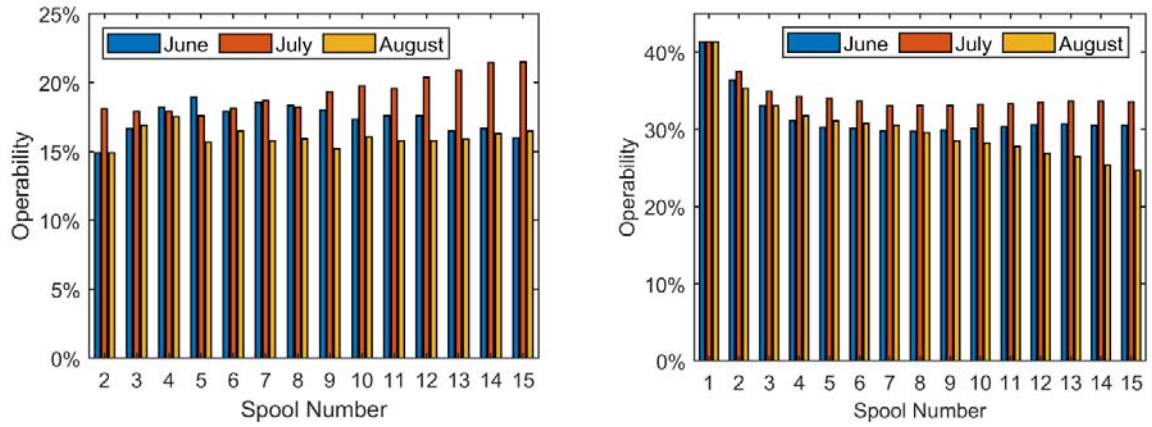

(a) Installation Method 1 (b) Installation Method 2

Figure 6-9: Operability of IM1 and IM2 with transportation time of 12hrs

In comparison with the previous case, which has 3hrs of transportation time, the same operability percentages are resulted by the IM1 because the transportation time is not a dominant criterion. The operability of the IM2 is between 40% to 30%, which is roughly half of operability calculated for the IM2 with the transportation time of 3hrs. Nevertheless, IM2 still has higher operability for the subsea spool installation. The allowable sea states and waiting on weather windows are the dominant factor in this operability analysis.

6.5.2 Influence of the fender models in the lift-off operation

The fender models influence in the lift-ff operation is studied in Chapter 4. The allowable sea states for each model are presented. In the conclusion of the fender study, SoftFender1 model has the most promising results as allowable sea states among the other models. This model followed by the SofFender3 where the traditional model is used in the lift-off operation. However, the cost of implementation of these fender models is significantly unique. While the SoftFender1 has the most expensive application module since it is used primarily in the production industry, the SoftFender3 module is relatively cheaper and is easily found around the world, and it is

conventionally used in the marine industry. Although, the higher sea states will result in lower TOT; alternatively, refers to higher operability for the subsea spool installation, the application cost might induce the feasibility of this operation adversely. The application of these models will be examined and discussed in the operability of the subsea spool installation in the same specific period with the installation method study. Firstly, the SoftFender1 model is studied in the aspects of operability. In Figure 6-10, the TOT_{mean} is plotted for the SoftFender1 model using IM1 and IM2 to compare how the higher sea states assessed with SoftFender1 model, and installation method affects TOT. The higher allowable sea states enable the lower operation time by using IM1 than the IM2. The lowest period is also observed in July. Moreover, while the operation times differ between 200hrs to 600hrs in the DeckFender model as in Figure 6-4 (b), the operation time remains in the lower limit of 200hr in the SoftFender1 model. This is because of higher allowable sea states assessed by SoftFender1.

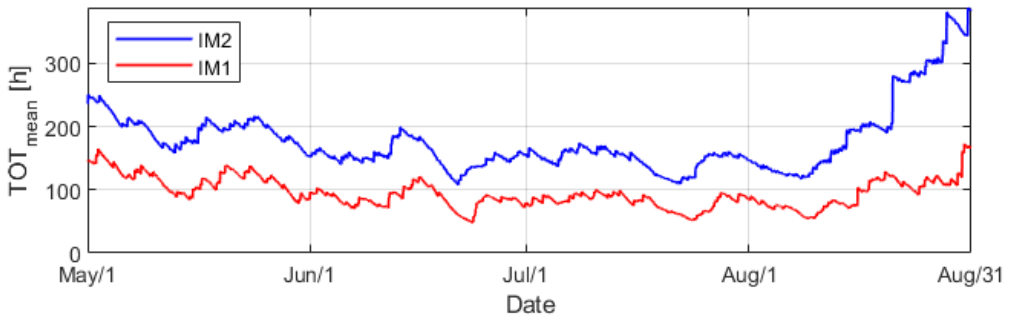

Figure 6-10: TOT_{mean} for eight subsea spools by using SoftFender1 model

Secondly, the TOT_{mean} figure is created for the SoftFender3 model. Due to higher sea states of the SoftFender3 model than the DeckFender model, the lift-off operation is more resilient to environmental conditions in the offshore site. Therefore, the total operation times are lower than the installation method 2 with DeckFender model. However, in Figure 6-11, TOT_{mean} values of IM1 with SoftFender3 model might exceed TOT_{mean} values of IM1 with DeckFender. This finding occurs in operation starting on 12^{th} August, which is highlighted with the circle in the below figure.

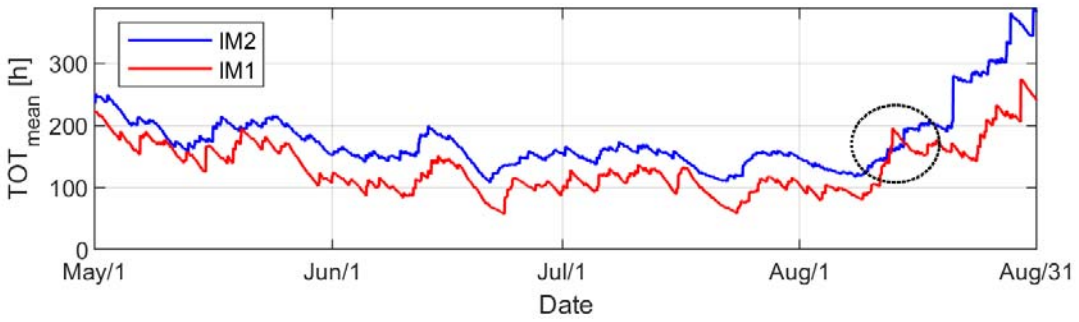

Figure 6-11: TOT_{mean} for eight subsea spools by using SoftFender3 model

TOT estimates for SoftFender1 and SoftFender3 are compared in the next figure of P10, P50 and P90 estimates. In the case of three subsea spool installations, the estimated mean TOT is relatively lower than the values resulted by DeckFender model, such as respectively 69hrs and 88-95hrs for the fender models when it is in the range of 105-116hrs for DeckFender model. This P50 estimate values for TOT will be used in the operability of the subsea spool installation.

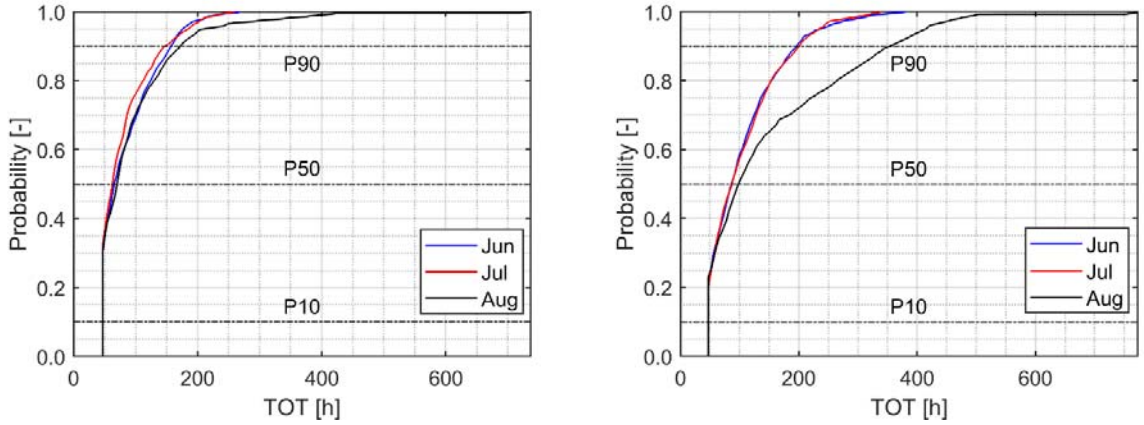

(a) SoftFender1 Model (b) SoftFender3 Model

Figure 6-12: P10, P50, P90 estimates for a total operation time of fender models

In the following figure, the operability percentage is plotted for a different number of subsea spool installations.

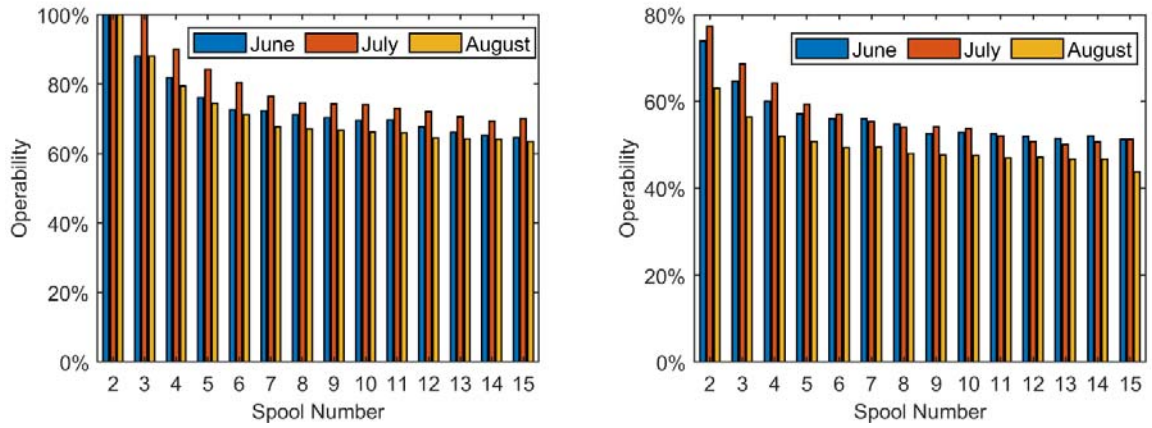

(a) SoftFender1 Model (b) SoftFender3 Model

Figure 6-13: Operability of fender models in IM2

The operability using installation method 1 with SoftFender1 model is in the range between 65% to 100% for a various number of spools. On the other hand, the operability for the SoftFender3 model lies between 56% to 78%. For a small number of spool installations, SoftFender1 model gives higher operability for the installation. However, for more than seven subsea spools, the difference in the operability between the two models is smaller.

Above all, the application costs of the fender models should be considered in the result of this study. Between two models, roughly a maximum of 20% operability difference is observed. Operability of 20% can be avoided or improved with proper scheduling for the installation. Besides, according to market research, the SofFender1 fender module is more than three times expensive than the SoftFender3 module. The size of the modules is not the same either. Conversely, when this cost is compared to the daily cost of the lifting vessel, the cost of using the expensive model would not be negligible. Therefore, the decision on usage of the fender models relies mostly on the scenario of the number of spools, operation month. As a result, both fender models increased the operability of the installation method one to the level that is now comparable to Installation method 2.

6.5.3 Influence of the MCS in the lift-off operation

The allowable sea states assessed by using the motion control system will be evaluated in operability analysis together and compared to the installation method 1. The MCS has provided more suitable lift-off instants for the multi-vessel operations, and consequently, relatively higher allowable sea states achieved. These sea states are compared to the regular model. The increased allowable sea states will be resulting in better operability in the subsea spool installation. The effect size of the allowable sea states achieved with MCS system on the operability of the subsea spool installation is the primary motivation in this study. In Figure 6-14, TOT_{mean} values are plotted by using IM2 with the MCS and IM1 without MCS.

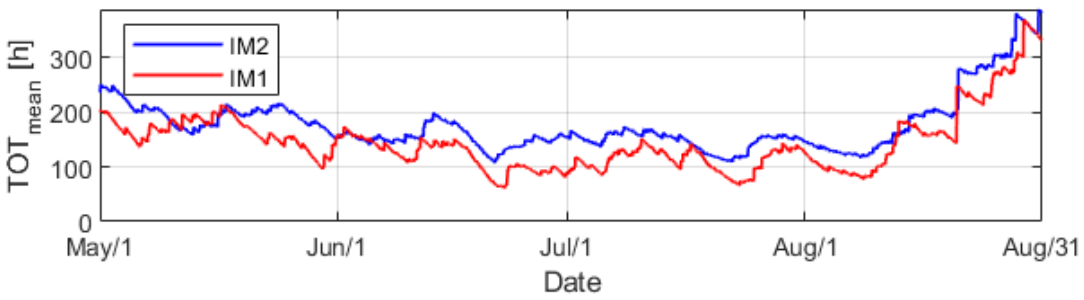

Figure 6-14: The mean TOT of eight spools for MCS results

In the Installation Method1, higher allowable see states are achieved with the help of Motion Control System that provides quite close TOT_{mean} values to IM2, as shown in Figure 6-14. The lower TOTmean values will also influence the operability of these operations. In Figure 6-15, the P10, P50, P90 estimates are shown.

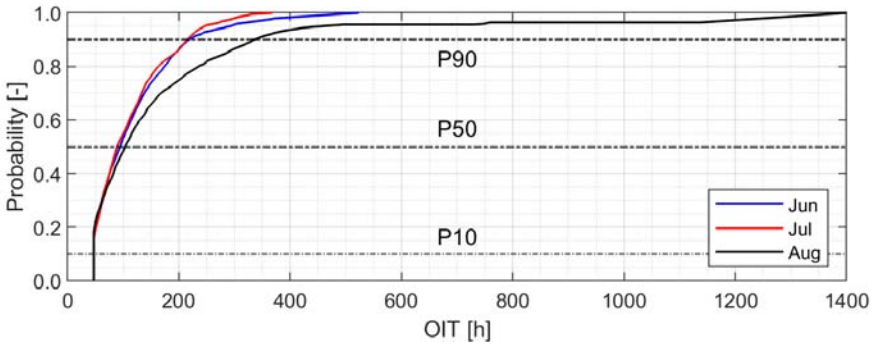

Figure 6-15: P10, P50, P90 Estimates for a total operation time of MCS

P50 estimates rely on between 87hrs to 98hrs for eight subsea spool installations which are relatively lower than the estimated value for IM2 without MCS. This lower operation time also reflects on the operability of this operation. The operability of the MCS is illustrated against the number of the subsea spool in Figure 6-16.

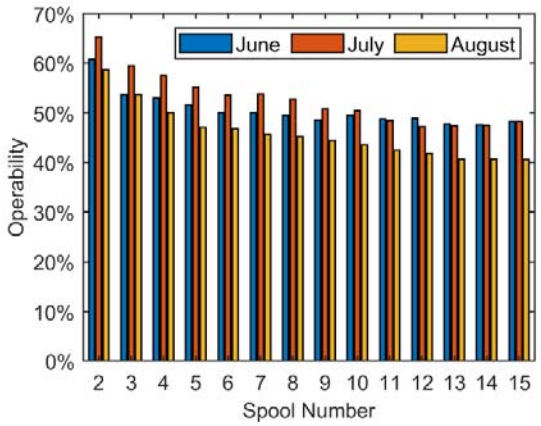

Figure 6-16: Operability of subsea spool installation with the motion control system

The figure shows the operability percentages in 3 months for a different number of spools to be installed. The operability lies between 68% to 45%, which is relatively high for the operability results of IM2 for the DeckFender model. Besides, in a comparison of two installation methods, the operability of the IM1 with MCS is relatively low in comparison with the IM2 without control system.

In conclusion, The Motion Control System provides the functionality of monitoring over the waves and control the winch in a suitable instant. This functionality leads to a higher allowable sea state for the lift-off operation. For the operability, these sea states give a boost in the installation to be completed in a shorter time. Therefore, the MCS improved Installation Method 2 by approximately 40%. However, there is still roughly 20% difference in operability between the two methods. This difference should be evaluated with the operation costs of the vessels and the implementation costs of the motion control system. After evaluating the costs, a clear statement can be made for choosing the installation methods for the subsea spool installation correctly.

Chapter 7
Conclusion

7.1 Conclusion

This thesis addresses the numerical analysis of the lift-off operation of a large subsea spool from a transportation barge. The numerical model includes the transportation barge, the spool, and the lifting vessel, with the coupling arrangement and hydrodynamic interactions. The numerical model of this lifting system is conducted in SIMA-SIMO software. Allowable sea states are assessed by using two different methods inthe lift-off operation, i.e., the fender modelsand winch control system. The influence of the different fender supports and the winch control system on the operability of the subsea spool installation are compared.

Firstly, four fender models are used in the numerical simulations, and the material of the fenders is selected based on the commonly used materials in the industry. 100 wave realizations are simulated for each Hs and Tp for the four different fender models. The responses of the system are evaluated first and only the seeds corresponding to the proper lift-off scenarios are selected. Then, the lift-off criteria are established, in which the re-hit between the spool and the deck of the barge is the dominant criterion. The allowable sea states are obtained by comparing the responses from the proper seeds with the criteria. The effects of different fender characteristics are examined in detail. It is concluded that all the three soft fender models have a positive influence on the

allowable sea states compared to the deck fender model, Among them, the SoftFender1 model has increased the allowable sea states remarkably because of the relative high damping and low stiffness characteristics.

Secondly, a winch controller method is developed to define favourable lift-off instance for the subsea spool. A favourable lift-off instance is introduced as lift-off criteria. Lift-off criteria are analyzed in responses of the DeckFender model in terms of the appearance in 3 hours and also the effect on the allowable sea states. It is concluded that the relative distance and misalignment criterion defines the optimum conditions for the lift-off operation. These criteria are used as a method in Java code. The estimation of the future motions is required to use the relative distance criterion in Java code. The preliminary estimation method is introduced and compared with well-known methods. The control in the spool operation is established by using these methods with the winch controller. The effects of lift-off criteria andvariable winch speeds arestudied. It is concluded that relative distance and the misalignment criteria are the most effective with the highest winch speed. These criteria are elaborated on the lift-off timing respect to the relative distance between the crane tip and the barge. Lifting at wave trough is concluded to be the most effective method among the other methods with higher allowable sea states.

An installation method is defined to account for the use of the transportation barge and the lifting vessel (IM1). IM1 is compared with a different installation method using only the lifting vessel (IM2). Operability analysis is carried out in a selected offshore site. Sensitivity studies are performed out in terms number of spools and transportation time. Because of the low allowable sea states assessed in lift-off operation from the barge, IM1 results in 40%-60% less operability in comparison with IM2. The difference in the operability decreases with a higher number of spools and transportation time; overall, IM2 results with higher operability then IM1. Besides, the allowable sea states of fender models and the motion control system are assessed. Therefore, the influences of these methods are compared and quantified when assessing operability. In the fender model method, SoftFender1 and SoftFender 3 are compared by using IM1. The operability of SoftFender1 is quite close to the operability of IM2, and SoftFender3 is 20% less. Alternatively, the operability of IM1 using the motion control system is assessed. For IM1, the increased sea

states by winch controller leads to higher operability by 40% than the conventional model without winch controller.

7.2 Further work

This thesis provides the study of efficiency in using different methods to increase the sea states for the spool liftin operation from the transportation barge. Based on this thesis, the following aspects are proposed to improve numerical models, which can be studied in future work.

- Improve the damping coefficient for the fender models. The fender models are used in the elastic phase, where it can return as its normal conditions after stress applied. Alternatively, these fenders can be used until the ultimate tensile stress level, in other words, until its cracks — for instance, sacrificial elements used in rigid body structures. The detailed properties of the fender models can be tested in the lab for the ultimate stress level in the mean of dissipated energy. The damping coefficients obtained from the lab tests can be used to improve the fender models in the lift-off operation.
- Increased height of the fender modules. The distance between the deck and the spool increases because of the fender modules. Consequently, the re-hit probability decreases. On the other hand, a higher position in the z-direction of the spool will create higher motions acting on the spool, and therefore, there will be higher tension occurred in the slings.
- Improvement of the motion control system. In the current version of the code, the environmental conditions are known inputs for the control algorithm. By having this input, the control code can alter the winch speed, the lift-off timing to achieve better responses. The new updated code can be used with random environmental conditions for different periods. So, the offshore site can be represented in the simulation, and operability analysis can be conducted accordingly.

References

1. DNVGL, *DNVGL-ST-N001: Marine Operations and Marine Warranty.* June 2016.
2. DNVGL, *DNVGL-RP-N103: Modelling and Analysis of Marine Operations.* April 2017.
3. Acero, W.G., L. Li, Z. Gao, and T. Moan, *Methodology for assessment of the operational limits and operability of marine operations.* Ocean Engineering, 2016. 125: p. 308-327.
4. Gao, Z., W. Guachamin Acero, L. Li, Y. Zhao, C. Li, and T. Moan. *Numerical simulation of marine operations and prediction of operability using response-based criteria with an application to installation of offshore wind turbine support structures*. in *Proceedings of the Third Marine Operations Specialty Symposium (MOSS2016), Singapore*. 2016.
5. Li, L., *Dynamic analysis of the installation of monopiles for offshore wind turbines.* 2016.
6. Li, L., Z. Gao, and T. Moan. *Operability analysis of monopile lowering operation using different numerical approaches*. 2016. ISOPE.
7. Acero, W.G., Z. Gao, and T. Moan, *Numerical study of a novel procedure for installing the tower and rotor nacelle assembly of offshore wind turbines based on the inverted pendulum principle.* Journal of Marine Science and Application, 2017. 16(3): p. 243-260.
8. Verma, A.S., Z. Jiang, N.P. Vedvik, Z. Gao, and Z. Ren, *Impact assessment of a wind turbine blade root during an offshore mating process.* Engineering Structures, 2019. 180: p. 205-222.
9. Guachamin-Acero, W. and L. Li, *Methodology for assessment of operational limits including uncertainties in wave spectral energy distribution for safe execution of marine operations.* Ocean Engineering, 2018. 165: p. 184-193.
10. Bai, Y. and Q. Bai, *Subsea engineering handbook*. 2018: Gulf Professional Publishing.
11. MEF Marine Engineering Services. *Technical Services Announcement*. 2019 [cited 2019 05 Dec]; Available from: http://www.mes-indonesia.com/.

12. Sarkar, A. and O.T. Gudmestad, *Study on a new method for installing a monopile and a fully integrated offshore wind turbine structure.* Marine structures, 2013. 33: p. 160-187.

13. Gordon, R.B., G. Grytøyr, and M. Dhaigude. *Modeling suction pile lowering through the splash zone*. in *International Conference on Offshore Mechanics and Arctic Engineering*. 2013. American Society of Mechanical Engineers.

14. Verma, A.S., Z. Jiang, Z. Ren, Z. Gao, and N.P. Vedvik, *Response-Based Assessment of Operational Limits for Mating Blades on Monopile-Type Offshore Wind Turbines.* Energies, 2019. 12(10): p. 1867.

15. Li, L., C. Parra, X. Zhu, and M.C. Ong, *Splash zone lowering analysis of a large subsea spool piece.* Marine Structures, 2020. 70: p. 102664.

16. Dreng, Å.V., *Limiting operational wave criterion for spool installation lift-with emphasis on analysis and wind-wave modeling*. 2015, University of Stavanger, Norway.

17. Parra, C.A., *Numerical Study on Offshore Lifting Operations of a Subsea Spool*. 2018, University of Stavanger, Norway.

18. MARINTEK, *SIMO - Theory Manual Version 4.6.* MARINTEK, Trondheim, Norway., 2015.

19. Reinholdtsen, S.-A., K. Mo, and P.C. Sandvik. *Useful force models for simulation of multibody offshore marine operations*. in *The Thirteenth International Offshore and Polar Engineering Conference*. 2003. International Society of Offshore and Polar Engineers.

20. Chen, H., T. Moan, S. Haver, and K. Larsen, *Prediction of relative motion and probability of contact between FPSO and shuttle tanker in tandem offloading operation.* J. Offshore Mech. Arct. Eng., 2004. 126(3): p. 235-242.

21. Valen, M., *Launch and recovery of ROV: Investigation of operational limit from DNV Recommended Practices and time domain simulations in SIMO*. 2010, Norges teknisk-naturvitenskapelige universitet, Fakultet for ….

22. Næss, T., J. Havn, and F. Solaas, *On the importance of slamming during installation of structures with large suction anchors.* Ocean engineering, 2014. 89: p. 99-112.

23. Wu, X., G.R.S. Gunnu, and T. Moan, *Positioning capability of anchor handling vessels in deep water during anchor deployment.* Journal of Marine Science and Technology, 2015. 20(3): p. 487-504.

24. Newmark, N.M., *A method of computation for structural dynamics.* Journal of the engineering mechanics division, 1959. 85(3): p. 67-94.

25. Higham, D.J. and N.J. Higham, *MATLAB guide*. 2016: SIAM.

26. Kawakami, H., *The Use of Marine Fenders as Energy Absorbing Damper Units in Mooring Systems*, in *Advances in Berthing and Mooring of Ships and Offshore Structures*. 1988, Springer. p. 474-490.

27. Metzger, A.T., J. Hutchinson, and J. Kwiatkowski, *Measurement of marine vessel berthing parameters.* Marine Structures, 2014. 39: p. 350-372.

28. Aboshio, A. and J. Ye, *Numerical study of the dynamic response of Inflatable Offshore Fender Barrier Structures using the Coupled Eulerian–Lagrangian discretization technique.* Ocean Engineering, 2016. 112: p. 265-276.

29. König, M., D.F. González, M. Abdel-Maksoud, and A. Düster, *Numerical investigation of the landing manoeuvre of a crew transfer vessel to an offshore wind turbine.* Ships and Offshore Structures, 2017. 12(sup1): p. S115-S133.

30. Fan, W., W. Guo, Y. Sun, B. Chen, and X. Shao, *Experimental and numerical investigations of a novel steel-UHPFRC composite fender for bridge protection in vessel collisions.* Ocean engineering, 2018. 165: p. 1-21.

31. El-Sawy, M., V. Shagin, and M. Elmorsi. *Vessel Collision Analysis and Design of a Pile Support Fender System*. in *Structures Congress 2020*. 2020. American Society of Civil Engineers Reston, VA.

32. BAGHERI, H., M. Ghassemian, and S.A. Hosseini, *FEASIBILITY OF OPTIMIZING THE GEOMETRY AND ENERGY ABSORPTION OF MARINE FENDERS.* 2014.

33. Alghamdi, A., *Collapsible impact energy absorbers: an overview.* Thin-walled structures, 2001. 39(2): p. 189-213.

34. Gómez, S., A. Metrikine, B. Carboni, and W. Lacarbonara, *Identification of energy dissipation in structural joints by means of the energy flow analysis.* Journal of Vibration and Acoustics, 2018. 140(1).

35. Getzner. *Sylodamp SP1000 data-sheet*. 2019 [cited 2019 15 Dec]; Available from: http://www.getzner.com/.

36. Pisarenko, G.S., *THE OSCILLATIONS OF ELASTIC SYSTEMS IN THE PRESENCE OF DISSIPATION OF ENERGY IN THE MATERIAL* 1955(Kiev, Izd-vo. Akad. Nauk SSSR, 1955, Z39 pp.).

37. Sundolitt. *XPS plateprodukter*. [cited 2020 Jan. 05]; Available from: http://www.sundolitt.com/.

38. L.Lin, L.W., *EPS Lightweight Filling Work Methods, Research Report.* 2000.

39. Trelleborg. *Fender systems, Product Brochure*. [cited 2020 Jan. 05]; Available from: https://www.trelleborg.com/en.

40. Mostofi, A. and K. Bargi, *New concept in analysis of floating piers for ship berthing impact.* Marine structures, 2012. 25(1): p. 58-70.

41. Alujević, N., I. Ćatipović, Š. Malenica, I. Senjanović, and N. Vladimir, *Ship roll control and power absorption using a U-tube anti-roll tank.* Ocean Engineering, 2019. 172: p. 857-870.

42. M. Beale, M.H., H. Demuth *Deep Learning Toolbox.* March 2020.

43. Brooks, S., A. Gelman, G. Jones, and X.-L. Meng, *Handbook of markov chain monte carlo*. 2011: CRC press.

44. Levold, P., *Use of SIMO Generic External Control System for Winch Control.* SINTEF Ocean AS, 2018.

45. Bali, T.G., *The generalized extreme value distribution.* Economics letters, 2003. 79(3): p. 423-427.

46. Wilcken, S., *Alpha factors for the calculation of forecasted operational limits for marine operations in the Barents Sea*. 2012, University of Stavanger, Norway.

47. Li, L., Z. Gao, and T. Moan, *Joint distribution of environmental condition at five european offshore sites for design of combined wind and wave energy devices.* Journal of Offshore Mechanics and Arctic Engineering, 2015. 137(3).

48. Haver, S., *Metocean modelling and prediction of extremes.* Lecture notes in TMR4195-Design of Offshore Structures. Department of Marine Technology, Norwegian University of Science and Technology, 2017.

49. Borges, V. *Terminology Explained : P10, P50, P90.* [cited 2020 May 15]; Available from: https://blogs.dnvgl.com/.

Appendices

Appendix A

		Tp											
		4	**5**	**6**	**7**	**8**	**9**	**10**	**11**	**12**	**13**	**14**	
Hs	**0.60**	34.4	33.9	33.7	33.9	33.9	34.6	34.6	36.3	34.9	34.7	37.3	
	0.70	34.7	33.9	33.7	34.0	34.0	34.6	34.6	36.3	34.9	34.7	37.3	
	0.80	35.0	33.9	33.7	34.0	34.0	34.6	34.6	36.3	34.9	34.7	37.3	
	0.90	35.2	34.0	33.7	33.9	34.0	34.6	34.7	36.3	34.9	34.7	37.3	
	1.00	35.4	34.0	33.8	34.0	34.0	34.6	34.7	36.4	34.9	34.7	37.4	
	1.10	35.5	34.0	33.8	34.0	34.0	34.6	34.7	36.4	34.9	34.7	37.5	
	1.20	35.6	34.0	33.8	34.0	34.0	34.6	34.7	36.4	35.0	34.7	37.5	
	1.30	35.7	34.0	33.9	34.0	34.0	34.6	34.7	36.4	35.0	34.8	37.5	
	1.40	35.8	34.1	34.0	34.0	34.0	34.6	34.7	36.4	35.0	34.8	37.6	
	1.50	35.9	34.1	34.0	34.0	34.0	34.6	34.7	36.4	35.0	34.8	37.7	
	1.60	36.0	34.2	34.1	34.0	34.0	34.6	34.8	36.4	35.0	34.8	37.7	
	1.70	36.1	34.3	34.2	34.1	34.0	34.6	34.8	36.4	35.0	34.8	37.8	
	1.80	36.2	34.3	34.2	34.1	34.0	34.6	34.8	36.4	35.1	34.8	37.9	
	1.90	36.3	34.3	34.3	34.1	34.1	34.6	34.8	36.4	35.1	34.9	37.9	
	2.00	36.4	34.4	34.4	34.1	34.0	34.6	34.8	36.4	35.1	34.9	38.0	
	2.10	36.4	34.4	34.4	34.2	34.1	34.6	34.8	36.4	35.1	34.9	38.0	
	2.20	36.6	34.5	34.5	34.2	34.1	34.6	34.8	36.4	35.2	34.9	38.1	
	2.30	36.6	34.5	34.5	34.2	34.0	34.6	34.8	36.4	35.2	35.0	38.1	
	2.40	36.7	34.6	34.6	34.3	34.1	34.6	34.8	36.4	35.2	35.0	38.2	
	2.50	36.8	34.6	34.6	34.3	34.1	34.6	34.8	36.4	35.2	35.0	38.4	
	2.60	36.9	34.7	34.6	34.3	34.1	34.6	34.8	36.4	35.3	35.0	38.4	
	2.70	36.9	34.7	34.6	34.4	34.1	34.6	34.8	36.5	35.3	35.1	38.6	
	2.80	37.0	34.8	34.6	34.4	34.1	34.6	34.8	36.5	35.3	35.1	38.6	
	2.90	37.0	34.8	34.7	34.5	34.1	34.6	34.8	36.5	35.3	35.1	38.8	
	3.00	37.0	34.8	34.7	34.5	34.1	34.6	34.9	36.5	35.4	35.2	38.9	**Avg**
	Average	**36.1**	**34.3**	**34.2**	**34.1**	**34.0**	**34.6**	**34.8**	**36.4**	**35.1**	**34.9**	**37.9**	**35.17**

Appendix B

		Tp [s]											
		4	**5**	**6**	**7**	**8**	**9**	**10**	**11**	**12**	**13**	**14**	
Hs [m]	**0.60**	25.82	12.40	18.26	8.64	5.29	9.29	6.16	12.38	3.97	3.44	7.61	
	0.70	22.32	9.29	15.94	6.57	3.72	7.06	4.67	9.55	2.87	2.54	5.86	
	0.80	19.18	7.16	13.71	5.12	2.88	5.57	3.73	7.63	2.19	2.01	4.65	
	0.90	16.12	5.73	11.78	4.06	2.17	4.41	2.97	6.13	1.75	1.64	3.73	
	1.00	13.56	4.54	10.10	3.22	1.74	3.56	2.48	5.11	1.40	1.33	3.05	
	1.10	11.35	3.66	8.47	2.63	1.37	2.91	2.14	4.31	1.15	1.10	2.55	
	1.20	9.48	3.01	6.96	2.19	1.12	2.45	1.86	3.62	0.94	0.88	2.14	
	1.30	8.08	2.51	5.82	1.88	0.93	2.01	1.64	3.05	0.81	0.76	1.84	
	1.40	6.81	2.18	4.93	1.59	0.81	1.70	1.41	2.68	0.68	0.66	1.60	
	1.50	5.75	1.84	4.23	1.46	0.70	1.45	1.25	2.26	0.59	0.55	1.40	
	1.60	4.86	1.59	3.70	1.30	0.61	1.25	1.07	1.96	0.53	0.48	1.24	
	1.70	4.16	1.41	3.19	1.14	0.55	1.10	0.98	1.73	0.48	0.43	1.10	
	1.80	3.58	1.22	2.75	0.98	0.46	0.98	0.91	1.48	0.44	0.38	0.99	
	1.90	3.21	1.11	2.45	0.90	0.43	0.83	0.84	1.26	0.43	0.36	0.88	
	2.00	2.80	1.01	2.14	0.79	0.35	0.71	0.75	1.14	0.42	0.33	0.80	
	2.10	2.51	0.91	1.84	0.72	0.30	0.65	0.71	1.01	0.38	0.31	0.69	
	2.20	2.17	0.83	1.65	0.63	0.25	0.60	0.62	0.89	0.35	0.30	0.60	
	2.30	1.95	0.73	1.53	0.56	0.21	0.53	0.56	0.81	0.32	0.27	0.54	
	2.40	1.76	0.65	1.39	0.50	0.18	0.48	0.52	0.73	0.31	0.27	0.47	
	2.50	1.55	0.60	1.26	0.46	0.18	0.43	0.48	0.69	0.29	0.28	0.42	
	2.60	1.42	0.53	1.14	0.44	0.16	0.41	0.42	0.64	0.27	0.27	0.37	
	2.70	1.29	0.49	1.04	0.43	0.21	0.39	0.38	0.59	0.25	0.26	0.32	
	2.80	1.20	0.48	0.89	0.40	0.23	0.39	0.34	0.55	0.23	0.24	0.29	
	2.90	1.10	0.46	0.83	0.38	0.24	0.38	0.31	0.51	0.22	0.22	0.27	**Overall Average**
	3.00	1.00	0.44	0.73	0.36	0.26	0.38	0.27	0.46	0.19	0.18	0.24	
	Average	**6.92**	**2.59**	**5.07**	**1.89**	**1.01**	**2.00**	**1.50**	**2.85**	**0.86**	**0.78**	**1.75**	**2.47**

Appendix C

		Tp [s]										
		4	**5**	**6**	**7**	**8**	**9**	**10**	**11**	**12**	**13**	**14**	
Hs [m]	**0.60**	33.92	26.11	30.84	18.66	18.44	22.09	16.76	27.02	11.68	12.04	19.61	
	0.70	32.31	23.02	28.76	16.36	14.09	18.65	13.44	23.03	8.89	9.19	16.32	
	0.80	30.47	19.60	26.53	14.28	10.89	15.77	10.80	19.58	7.08	7.07	13.53	
	0.90	28.60	16.51	24.17	12.49	8.50	13.32	8.90	16.74	5.88	5.75	11.48	
	1.00	26.73	14.05	22.03	10.82	6.75	11.24	7.60	14.46	4.98	4.75	9.76	
	1.10	24.41	11.95	20.01	9.41	5.53	9.67	6.48	12.50	4.25	3.92	8.32	
	1.20	21.96	10.18	18.23	8.21	4.54	8.29	5.58	10.94	3.57	3.36	7.20	
	1.30	19.69	8.75	16.57	7.12	3.88	7.07	4.92	9.60	3.11	2.97	6.28	
	1.40	17.55	7.48	14.79	6.22	3.34	6.13	4.31	8.49	2.69	2.61	5.52	
	1.50	15.56	6.51	13.17	5.46	2.92	5.34	3.83	7.48	2.39	2.30	4.86	
	1.60	13.81	5.78	11.70	4.84	2.53	4.71	3.46	6.68	2.15	2.06	4.36	
	1.70	12.30	5.20	10.47	4.30	2.24	4.17	3.14	5.94	1.92	1.85	3.94	
	1.80	11.03	4.65	9.25	3.88	1.98	3.67	2.86	5.32	1.72	1.68	3.56	
	1.90	9.77	4.19	8.29	3.53	1.82	3.28	2.60	4.84	1.54	1.54	3.23	
	2.00	8.77	3.72	7.35	3.21	1.69	2.93	2.41	4.37	1.38	1.43	2.94	
	2.10	7.91	3.40	6.46	2.84	1.59	2.62	2.23	3.96	1.28	1.37	2.69	
	2.20	7.21	3.11	5.78	2.55	1.48	2.37	2.07	3.60	1.16	1.30	2.46	
	2.30	6.57	2.87	5.11	2.33	1.42	2.17	1.93	3.31	1.09	1.24	2.28	
	2.40	5.99	2.66	4.59	2.16	1.35	2.01	1.80	3.05	0.99	1.14	2.09	
	2.50	5.41	2.47	4.18	2.02	1.30	1.86	1.67	2.80	0.92	1.09	1.88	
	2.60	4.94	2.30	3.82	1.90	1.24	1.71	1.55	2.57	0.86	1.04	1.72	
	2.70	4.52	2.15	3.46	1.76	1.21	1.62	1.44	2.38	0.80	1.01	1.60	
	2.80	4.17	2.00	3.14	1.65	1.18	1.52	1.36	2.19	0.76	0.97	1.45	
	2.90	3.82	1.90	2.89	1.59	1.21	1.42	1.25	2.01	0.72	0.92	1.34	
	3.00	3.54	1.78	2.64	1.54	1.13	1.37	1.18	1.86	0.70	0.86	1.24	**Avg**
	Average	**14.44**	**7.69**	**12.17**	**5.96**	**4.09**	**6.20**	**4.54**	**8.19**	**2.90**	**2.94**	**5.59**	**6.79**

Appendix D

		Tp [s]											
		4	**5**	**6**	**7**	**8**	**9**	**10**	**11**	**12**	**13**	**14**	
Hs [m]	**0.60**	34.49	33.90	33.74	32.39	33.79	33.94	33.51	36.30	31.38	31.55	36.08	
	0.70	34.76	33.86	33.75	30.10	32.97	32.90	31.72	36.03	28.62	28.57	34.37	
	0.80	34.99	32.96	33.75	27.95	31.50	31.48	29.65	35.51	25.77	25.53	32.50	
	0.90	35.19	31.56	33.77	26.19	29.49	30.01	27.48	34.54	23.02	22.75	30.13	
	1.00	35.26	30.26	33.70	24.86	27.33	28.53	25.18	33.19	20.64	20.12	28.04	
	1.10	35.18	29.08	33.43	23.71	25.02	26.81	23.08	31.56	18.36	17.95	25.70	
	1.20	34.80	27.85	32.92	22.61	22.90	25.20	21.20	29.86	16.46	16.25	23.71	
	1.30	34.23	26.50	32.36	21.52	20.96	23.66	19.55	28.06	14.77	14.68	21.99	
	1.40	33.61	25.19	31.56	20.43	18.86	22.04	17.79	26.35	13.41	13.38	20.32	
	1.50	32.92	23.91	30.77	19.36	17.17	20.36	16.38	24.64	12.15	12.18	18.84	
	1.60	32.03	22.45	29.78	18.35	15.69	18.89	15.12	22.96	11.08	11.09	17.51	
	1.70	30.97	21.06	28.60	17.27	14.45	17.58	13.97	21.55	10.20	10.16	16.17	
	1.80	29.68	19.74	27.42	16.20	13.42	16.24	12.84	20.12	9.46	9.36	15.09	
	1.90	28.32	18.48	26.08	15.24	12.53	14.96	11.83	18.89	8.79	8.70	14.02	
	2.00	26.93	17.31	24.67	14.26	11.76	13.89	10.88	17.76	8.25	8.15	13.08	
	2.10	25.47	16.23	23.36	13.37	11.01	12.98	10.14	16.60	7.74	7.66	12.25	
	2.20	24.04	15.20	21.97	12.44	10.39	12.20	9.47	15.68	7.33	7.21	11.45	
	2.30	22.62	14.20	20.60	11.64	9.83	11.38	8.85	14.78	6.92	6.75	10.75	
	2.40	21.47	13.42	19.24	10.95	9.34	10.70	8.33	13.77	6.50	6.39	10.03	
	2.50	20.25	12.70	18.11	10.34	8.91	10.04	7.80	13.03	6.14	6.06	9.37	
	2.60	19.10	12.03	17.05	9.64	8.51	9.50	7.24	12.31	5.76	5.68	8.78	
	2.70	18.02	11.39	15.87	9.07	8.16	8.98	6.83	11.67	5.44	5.37	8.31	
	2.80	16.97	10.78	14.75	8.55	7.94	8.47	6.42	11.03	5.17	5.13	7.79	
	2.90	16.01	10.19	13.67	8.00	7.63	8.04	6.08	10.47	4.95	4.91	7.31	
	3.00	15.17	9.69	12.78	7.53	7.34	7.65	5.74	9.94	4.73	4.72	6.90	**Avg**
	Average	**27.70**	**20.80**	**25.75**	**17.28**	**16.68**	**18.26**	**15.48**	**21.86**	**12.52**	**12.41**	**17.62**	**18.76**

Appendix E

		Tp [s]											
		4	**5**	**6**	**7**	**8**	**9**	**10**	**11**	**12**	**13**	**14**	
Hs [m]	**0.60**	89,4	93,6	93,9	95,5	95,7	95,0	95,2	92,2	95,6	95,7	91,6	
	0.70	92,7	95,6	95,0	95,9	96,1	95,1	95,5	92,9	95,2	95,9	92,7	
	0.80	91,9	95,6	95,4	96,1	96,4	95,6	95,6	93,4	95,7	96,2	92,0	
	0.90	94,0	95,3	95,6	95,4	96,2	95,5	95,6	94,2	96,0	96,4	93,4	
	1.00	94,3	95,9	95,7	94,8	96,5	95,5	95,7	94,8	96,3	96,4	93,0	
	1.10	94,4	94,9	96,0	96,2	96,4	95,7	95,6	94,8	95,8	96,3	93,0	
	1.20	94,3	96,0	96,2	96,4	96,4	95,7	95,9	94,8	96,1	96,4	93,1	
	1.30	94,6	96,2	95,5	96,3	96,3	96,0	95,6	94,6	96,1	96,6	93,1	
	1.40	95,1	95,7	95,6	96,5	96,1	95,8	96,2	94,5	95,7	96,3	93,5	
	1.50	94,5	96,0	96,1	96,6	96,8	96,2	96,0	94,7	95,9	96,3	93,3	
	1.60	94,9	96,1	95,6	96,8	96,6	96,1	96,0	95,2	96,3	96,1	94,0	
	1.70	95,5	96,3	95,8	96,6	96,4	96,0	96,2	95,1	96,4	96,7	94,0	
	1.80	95,6	96,1	96,2	96,6	96,4	95,9	95,7	94,9	96,3	96,5	93,6	
	1.90	95,3	96,1	96,1	96,5	96,4	96,2	96,2	94,9	96,1	96,3	93,9	
	2.00	95,1	96,1	95,9	96,5	96,4	96,5	96,0	95,0	96,0	96,6	93,9	
	2.10	94,7	96,4	95,9	96,4	96,7	96,8	96,3	95,4	96,2	96,4	93,7	
	2.20	94,4	96,3	95,8	96,8	96,6	96,5	96,3	95,0	96,3	96,3	93,5	
	2.30	94,6	96,6	96,1	96,7	96,3	96,7	96,1	95,7	96,3	96,1	93,8	
	2.40	94,4	96,4	96,0	96,6	96,6	96,4	96,2	95,3	96,1	95,9	93,9	
	2.50	94,5	96,3	95,7	96,6	96,6	96,3	96,3	95,5	96,2	95,8	94,2	
	2.60	95,0	96,3	95,6	96,5	96,0	96,6	95,9	95,2	96,2	95,9	94,0	
	2.70	95,3	96,3	95,1	96,7	96,5	96,5	96,2	95,0	96,2	96,2	94,1	
	2.80	94,7	96,5	95,1	96,5	96,4	96,6	96,4	95,0	96,0	95,9	94,1	
	2.90	94,6	96,3	94,8	96,2	96,1	96,3	96,3	94,7	96,1	95,7	93,4	
	3.00	94,7	96,7	95,5	96,1	96,6	96,4	96,3	94,9	96,1	95,6	94,0	**Avg**
	Average	**94,40**	**96,03**	**95,65**	**96,36**	**96,43**	**96,12**	**96,02**	**94,76**	**96,10**	**96,22**	**93,52**	**95,60**

Appendix F

Time Step	2000	2001	2002	2003	2004	2005	2006	2007	2008	2009
Second	40.00	40.02	40.04	40.06	40.08	40.10	40.12	40.14	40.16	40.18
Error	0.02	0.10	0.07	0.19	0.03	0.02	0.06	0.05	NaN	0.06
Time Step	2010	2011	2012	2013	2014	2015	2016	2017	2018	2019
Second	40.20	40.22	40.24	40.26	40.28	40.30	40.32	40.34	40.36	40.38
Error	-0.02	0.02	0.01	0.01	0.01	NaN	0.03	0.02	0.07	0.02
Time Step	2020	2021	2022	2023	2024	2025	2026	2027	2028	2029
Second	40.40	40.42	40.44	40.46	40.48	40.50	40.52	40.54	40.56	40.58
Error	0.09	-0.03	0.06	0.17	-0.03	NaN	-0.03	NaN	0.05	0.10
Time Step	2030	2031	2032	2033	2034	2035	2036	2037	2038	2039
Second	40.60	40.62	40.64	40.66	40.68	40.70	40.72	40.74	40.76	40.78
Error	0.01	NaN	0.12	0.00	-0.05	-0.06	0.00	0.07	-0.03	-0.03
Time Step	2040	2041	2042	2043	2044	2045	2046	2047	2048	2049
Second	40.80	40.82	40.84	40.86	40.88	40.90	40.92	40.94	40.96	40.98
Error	-0.02	-0.02	-0.02	0.12	0.00	0.02	-0.08	NaN	-0.01	NaN

Appendix G

		Tp [s]											
		4	**5**	**6**	**7**	**8**	**9**	**10**	**11**	**12**	**13**	**14**	
Hs [m]	**0.60**	46.8	50.7	50.5	52.5	50.2	41.9	52.0	51.7	57.4	59.9	54.2	
	0.70	47.7	50.3	50.1	52.5	50.1	42.1	52.1	51.6	57.4	59.6	54.5	
	0.80	48.9	48.3	50.2	52.3	50.2	42.0	52.1	51.4	57.4	59.3	54.5	
	0.90	50.0	44.3	49.7	52.4	50.2	42.1	52.1	51.7	57.3	59.3	54.7	
	1.00	51.6	45.0	48.7	52.3	50.1	42.1	52.2	51.4	57.3	59.1	54.8	
	1.10	53.6	45.5	47.8	52.5	50.1	42.0	52.1	51.7	57.2	59.0	54.9	
	1.20	56.5	46.0	46.5	52.5	50.3	42.0	52.2	51.4	57.0	58.9	54.9	
	1.30	60.7	46.1	44.7	52.5	50.3	42.0	52.1	51.5	57.0	58.9	54.8	
	1.40	65.5	46.2	42.2	52.5	50.2	41.9	52.2	51.3	57.2	58.8	54.7	
	1.50	65.0	45.8	37.4	52.4	50.1	41.9	52.1	51.5	57.1	58.8	54.9	
	1.60	64.5	45.2	37.4	52.5	50.1	42.0	52.0	51.4	57.1	58.8	54.8	
	1.70	64.1	43.5	37.6	52.6	50.2	42.0	52.0	51.2	57.0	58.8	54.8	
	1.80	63.7	44.3	37.7	52.5	50.1	41.8	52.1	51.1	57.0	58.7	54.7	
	1.90	63.3	45.1	37.8	52.6	50.1	41.8	52.1	51.1	57.1	58.7	54.7	
	2.00	63.1	45.8	37.7	52.6	50.1	41.8	52.0	51.0	56.8	58.8	54.6	
	2.10	62.7	46.4	37.7	52.7	50.2	41.8	52.0	50.9	56.8	58.8	54.7	
	2.20	62.4	47.0	37.9	52.9	50.2	41.8	51.9	50.9	56.8	58.8	54.4	
	2.30	62.2	47.6	37.7	53.0	50.2	41.7	51.7	50.6	56.8	58.8	54.6	
	2.40	61.9	48.0	37.8	53.3	50.2	41.7	51.9	50.7	56.8	58.8	54.5	
	2.50	61.7	48.4	37.8	53.3	50.3	41.8	51.8	50.6	56.6	58.8	54.4	
	2.60	61.4	48.9	37.7	53.5	50.4	41.8	49.3	50.4	56.5	58.9	54.3	
	2.70	61.2	49.2	37.8	53.7	50.4	41.8	47.7	50.0	56.7	58.9	54.2	
	2.80	60.9	49.5	37.7	53.9	50.4	41.8	46.4	50.3	56.6	59.0	54.4	
	2.90	60.7	49.8	37.6	54.3	50.6	41.9	45.5	50.3	56.6	58.9	54.2	
	3.00	60.6	50.0	37.6	54.3	50.7	42.0	44.6	50.1	56.6	59.1	54.1	**Avg**
	Average	**59.2**	**47.1**	**41.3**	**52.8**	**50.2**	**41.9**	**50.9**	**51.0**	**56.9**	**58.9**	**54.5**	**51.4**

Appendix H

WinchController_UpdateLowTpTension.java

```
1 package no.marintek.control;
2
3 import java.io.FileNotFoundException;
14
15 public class WinchController_UpdateLowTpTension implements IController {
16
17     private double dt,average;
18     private double x,y,xy,xb,yb,xyb;
19     private double err, previousErr;
20     private double barge_z, rdistance;
21     private double z, ms, rd, dts,liftwire,tension;
22     private int ts, ts2, ts3;
23     private int K = 0;
24     private int L = 0;
25     private int J = 0;
26
27     private boolean logValues= false;
28     private PrintStream stream;
29     private int logInterval = 1;
30     private int stepsSinceLog= 0;
31
32     // private boolean hasCrossedZero = false;
33     private double x0,y0,z0,u1,u2,xy_diff,TensionSet;
34     private int t1,t2,t3,t4;
35     // private String bodyID;
36     private String vesselID; //Only used for logging
37     private String bargeID;
38     private String hookID;
39     private String wireID;
40     private String bodyID = null;
41
42     private double[] runSpeed_arr = new double[50000];
43     // private Map<Double , Signal> measureMap;
44     private double[] rdistance_arr = new double[50000];
45     private double[] min_arr =  new double[8001];
46     private double[] max_arr =  new double[8001];
47     private double[] time_arr = new double[8001];
48     private double[] misalignment_arr= new double[1];
49     private double[] runSpeed_feedback= new double [1];
50     private boolean liftcriteria=false;
51     private boolean ok2lift=false;
52
53     @Override
54     public void init(double dt, Parameters parameters) {
55         this.dt=dt;
56
57         //If string parameter `filename` exists, print log to this file
58
59         if(parameters.getStringNames().contains("filename")) {
60             String filename = parameters.getString("filename");
61             if(parameters.getIntNames().contains("logValues")) {
62                 if(parameters.getInt("logInterval") == 0) {
63                     logValues = false;
64                 } else {
65                     logValues = true;
66                     try {
67                         FileOutputStream fos = new FileOutputStream(filename);
68                         stream = new PrintStream(fos);
69                         System.out.println("Echoing to file: "+filename);
70                     } catch (FileNotFoundException e) {
71                         e.printStackTrace();
72                     }
73                 }
74             }
```

WinchController_UpdateLowTpTension.java

```
75        }
76
77        if(parameters.getIntNames().contains("logInterval")) {
78            logInterval = parameters.getInt("logInterval");
79        }
80        if(parameters.getStringNames().contains("vesselID")) {
81            vesselID = parameters.getString("vesselID");
82        }
83        if(parameters.getStringNames().contains("bargeID")) {
84            bargeID = parameters.getString("bargeID");
85        }
86        if(parameters.getStringNames().contains("bodyID")) {
87            bodyID = parameters.getString("bodyID");
88        }
89        if(parameters.getStringNames().contains("hookID")) {
90            hookID = parameters.getString("hookID");
91        }
92        if(parameters.getStringNames().contains("wireID")) {
93            wireID = parameters.getString("wireID");
94        }
95
96        x0 = parameters.getReal("x0");
97        y0 = parameters.getReal("y0");
98        z0 = parameters.getReal("z0");
99        barge_z=parameters.getReal("Barge_z");
100       u1 = parameters.getReal("u1");
101       u2 = parameters.getReal("u2");
102       xy_diff = parameters.getReal("xy_diff");
103       if(parameters.getRealNames().contains("LiftwireTension")) {
104           TensionSet = parameters.getReal("LiftwireTension");
105       }
106
107       if(parameters.getIntNames().contains("TensionTime")) {
108           t1 = parameters.getInt("TensionTime")*100;
109       }
110       if(parameters.getIntNames().contains("MinTension")) {
111           t2 = parameters.getInt("MinTension")*100;
112       }
113       if(parameters.getIntNames().contains("MaxTension")) {
114           t3 = parameters.getInt("MaxTension")*100;
115       }
116       if(parameters.getIntNames().contains("LiftTime")) {
117           t4 = parameters.getInt("LiftTime")*100;
118       }
119
120       err=0.0;
121       previousErr=0.0;
122       z = 0.0;
123       ts = 0;
124
125       if(logValues) {
126           stream.println("RunSpeed;");
127       }
128   }//end of initial
129
130   /**
131    * Method for calculating error
132    *
133    * @param measurements  Measurements from SIMO
134    */
135   private double getLt(Signal measurements) {
136       double [] LiftwireTension = measurements.getEntity(wireID).get("end1force");
137       liftwire = LiftwireTension[2];
138       return liftwire;
```

WinchController_UpdateLowTpTension.java

```
139     }
140
141     private double getErr(Signal measurements) {
142         double[] T = measurements.getEntity(vesselID).get("T");
143         double[] vesselPosition = measurements.getEntity(vesselID).get("position");
144         double[] bargePosition = measurements.getEntity(bargeID).get("position");
145         x = vesselPosition[0] + T[0]*x0 + T[3]*y0 + T[6]*z0;
146         y = vesselPosition[1] + T[1]*x0 + T[4]*y0 + T[7]*z0;
147         xb = bargePosition[0];
148         yb = bargePosition[1];
149         xy = Math.sqrt(Math.pow(x, 2) + Math.pow(y,2));
150         xyb = Math.sqrt(Math.pow(xb, 2) + Math.pow(yb, 2));
151         ms = xy - xyb;
152         return ms;
153     }
154
155     private double getRd(Signal measurements) {
156         double [] T=measurements.getEntity(vesselID).get("T");
157         double [] cranetip = measurements.getEntity(vesselID).get("position");
158         double [] bargePosition = measurements.getEntity(bargeID).get("position");
159         z = cranetip[2] + T[2]*x0 + T[5]*y0 + T[8]*z0;
160         barge_z = bargePosition[2];
161         rd = z - barge_z;
162         return rd;
163     }
164
165     @Override
166     public void step(double t, Signal measurements, Signal feedback) {
167         // TODO Auto-generated method stub
168         ts = (int) (t/dt);
169         dts = 1.0*ts;
170         //stepsSinceLog++;
171         if (liftcriteria == false) {
172             if(ts==0) {
173                 previousErr = getErr(measurements);
174                 runSpeed_arr[ts]=0;
175                 rdistance_arr[ts]=0;
176                 liftcriteria = false;
177                 stepsSinceLog++;
178                 return;}
179             if (0<ts && ts<2001) {
180                 runSpeed_arr[ts]=0;
181                 rdistance_arr[ts]=0;
182                 liftcriteria = false;
183                 return;}
184             if (ts>=2001 && ts<2003) {
185                 rdistance = getRd(measurements);
186                 rdistance_arr[ts] = rdistance;
187             return;}
188             if (ts>2002 && ts<10003) {
189                 rdistance = getRd(measurements);
190                 rdistance_arr[ts] = rdistance;
191                 if (rdistance_arr[ts-2]>rdistance_arr[ts-1] &&
    rdistance_arr[ts]>rdistance_arr[ts-1])
192                 {
193                     min_arr[ts-2003]=ts;
194                 }
195                 else if (rdistance_arr[ts-2]<rdistance_arr[ts-1] &&
    rdistance_arr[ts]<rdistance_arr[ts-1])
196                 {
197                     max_arr[ts-2003]=ts;
198                 }
199                 else {
200                     min_arr[ts-2003]=0;
```

WinchController_UpdateLowTpTension.java

```
201                 max_arr[ts-2003]=0;
202             }
203             runSpeed_arr[ts]=0;
204             liftcriteria = false;
205             return; }
206         if (ts==10003) {
207             rdistance = getRd(measurements);
208             rdistance_arr[ts] = rdistance;
209             int targetIndex = 0;
210             for( int sourceIndex = 0;  sourceIndex < min_arr.length;  sourceIndex++ )
211             {
212                 if( min_arr[sourceIndex] != 0 )
213                     min_arr[targetIndex++] = min_arr[sourceIndex];
214             }
215             double[] min_arr2 = new double[targetIndex];
216             System.arraycopy( min_arr, 0, min_arr2, 0, targetIndex );
217 
218             int tIndex = 0;
219             for( int sourceIndex = 0;  sourceIndex < max_arr.length;  sourceIndex++ )
220             {
221                 if( max_arr[sourceIndex] != 0 )
222                     max_arr[tIndex++] = max_arr[sourceIndex];
223             }
224             double[] max_arr2 = new double[tIndex];
225             System.arraycopy( max_arr, 0, max_arr2, 0, tIndex );
226             double sum = 0;
227             for( int n = 0; n<(min_arr2.length-1); n++)
228             {
229                 time_arr[n]=Math.abs(max_arr2[n]-min_arr2[n]);
230                 sum = sum + time_arr[n];
231             }
232             average = sum / min_arr2.length;
233         }
234         if (ts>=10004) {
235             err = getErr(measurements);
236             misalignment_arr[0] = err;
237             rdistance = getRd(measurements);
238             rdistance_arr[ts] = rdistance;
239             ts2 = (int) (ts - average/2 - t1);
240             int u = ts2+1;
241             int check = 0;
242             for (; u<=ts;u++) {
243                 if (rdistance_arr[u-1]<rdistance_arr[u]) {check = check + 1;} else
    {check = 0;}
244                 }
245             ts3 = (int) (ts2 - average/2);
246             int a = ts3;
247             int check2 = 0;
248             for (; a<ts2;a++) {
249                 if (rdistance_arr[a-1]>rdistance_arr[a]) { check2 = check2 + 1;} else
    {check2 = 0;}
250             }
251             if  (rdistance_arr[ts2-2]>rdistance_arr[ts2-1] &&
    rdistance_arr[ts2]>rdistance_arr[ts2-1] && check2==(ts2-ts3) &&
    Math.abs(misalignment_arr[0]-previousErr)<xy_diff)
252             {
253                 liftcriteria = true;
254                 int i = ts;
255                 for (; i<(ts+501); i++) {
256                     runSpeed_arr[i]=u1; //TO DO: Change the variable with U
257                 }
258                 L=ts+t2;
259                 J=ts+t3;
260                 K = i;
```

WinchController_UpdateLowTpTension.java

```
261                 /*for (; i<(ts+1501);i++) {
262                     runSpeed_arr[i]=-0.5; //TO DO: Change the variable with U
263                 }*/
264             } else {
265                 runSpeed_arr[ts]=0;
266                 liftcriteria = false;
267             }
268         }
269     }
270     else {
271         double[] bodyPos = {-1., -1., -1., -1., -1., -1.};
272         bodyPos = measurements.getEntity(bodyID).get("position");
273         double[] vesselVel = {-1., -1., -1., -1., -1., -1.};
274         vesselVel = measurements.getEntity(vesselID).get("velocity");
275         rdistance = getRd(measurements);
276         rdistance_arr[ts] = rdistance;
277         misalignment_arr[0] = getErr(measurements);
278         tension=getLt(measurements);
279         if (ts<K || tension<TensionSet) {
280         if(rdistance_arr[ts-2]>rdistance_arr[ts-1] &&
    rdistance_arr[ts]>rdistance_arr[ts-1]) {
281             ok2lift = true;
282         }
283         }
284         if(bodyPos[2]>11) {
285             runSpeed_arr[ts]=0;
286         } else {
287             int ts3 = ts - t4;
288             if (ts>K||tension>TensionSet) {
289             if ((rdistance_arr[ts3-2]>rdistance_arr[ts3-1] &&
    rdistance_arr[ts3]>rdistance_arr[ts3-1])|| ok2lift == true)
290             {
291                 int i = ts;
292                 for (; i<(ts+1001); i++) {
293                     runSpeed_arr[i]=u2; //TO DO: Change the variable with U
294                 }
295                 K = i;
296             }
297             else {
298             }
299             }
300         }
301         }
302
303     runSpeed_feedback[0]= runSpeed_arr[ts];
304     Set<String> winches = feedback.getAvaliableEntities();
305     for (String id : winches) {
306         SignalEntity winch = feedback.getEntity(id);
307         if(winch.getAvailableComponents().contains("runSpeed")) {
308             winch.set("runSpeed", runSpeed_feedback);
309         }
310     }
311
312     //check if set point is crossed for the first time
313     //if(err*previousErr < 0 && !hasCrossedZero) {
314     //  hasCrossedZero = true;
315     //}
316
317     //Store error for next step;
318     //previousErr=err;
319
320     //Print log
321     if (logValues) {
322         if(stepsSinceLog >= logInterval) {
```

WinchController_UpdateLowTpTension.java

```
323                 stepsSinceLog = 0;
324                 String f = "%f;";
325                 double[] bodyPos = {-1., -1., -1., -1., -1., -1.};
326                 if (bodyID != null) {
327                     bodyPos = measurements.getEntity(bodyID).get("position");
328                 }
329                 stream.format(Locale.ENGLISH, f + "\n",
330                         runSpeed_feedback[0]);
331             }
332             stepsSinceLog++;
333         }
334     }
335
336     private double rdistance_arr(int i) {
337         // TODO Auto-generated method stub
338         return 0;
339     }
340
341     @Override
342     public void finish()
343     {
344         // TODO Auto-generated method stub
345         //Close logfile
346         if (logValues) {
347             stream.close();
348         }
349     }
350 }
```

Appendix I

Hs [m]	Tp[s]								
	2	**4**	**6**	**8**	**10**	**12**	**14**	**16**	**Sum**
0.5	16	40	96	190	289	70	10	3	714
1.0	599	697	870	1094	1433	1741	927	377	7738
1.5	1565	2207	820	2345	2009	1720	1367	984	15017
2.0	1934	2543	3023	2489	2070	1328	969	692	15048
2.5	1612	2143	2676	2320	1798	1044	621	278	12492
3.0	1143	1536	2009	1913	1531	876	465	180	9653
3.5	706	934	1325	1305	1124	859	556	316	7125
4.0	355	679	783	851	833	744	480	270	4995
4.5	292	458	630	528	645	574	443	190	3760
5.0	303	364	498	478	510	360	232	158	2903
5.5	233	316	363	300	301	177	97	43	1830
6.0	122	173	238	214	156	126	97	47	1173
6.5	62	79	142	128	116	113	75	36	751
7.0	57	76	88	84	74	58	35	20	492
8.0	67	88	152	111	127	87	34	29	695
9.0	26	30	23	16	11	1	0	0	107
10.0	22	42	45	13	14	18	1	0	155
SUM	9114	12405	15781	14379	13041	9896	6409	3623	84648